PHOTORESPONSIVE POLYMERIZED CRYSTALLINE COLLOIDAL ARRAYS AND CHEMICAL SENSORS

by

Marta Kamenjicki Maurer

B.A., Wittenberg University, Springfield, OH, 1997

Submitted to the Graduate Faculty of

Arts and Sciences in partial fulfillment

of the requirements for the degree of

Doctor of Philosophy

University of Pittsburgh

2004

UNIVERSITY OF PITTSBURGH

FACULTY OF ARTS AND SCIENCES

This dissertation was presented

by

Marta Kamenjicki Maurer

It was defended on

April 22, 2004

and approved by

Professor David Waldeck

Professor Christian E. Schafmeister

David Finegold, M.D.

Professor Sanford A. Asher
Committee Chairperson

PHOTORESPONSIVE POLYMERIZED CRYSTALLINE COLLOIDAL ARRAYS AND CHEMICAL SENSORS

Marta Kamenjicki Maurer, Ph.D.

University of Pittsburgh, 2004

The focus of this thesis is the development of novel materials based upon a self-assembled array of highly charged, monodisperse colloidal particles, called a crystalline colloidal array (CCA). We have developed a method to permanently lock the order of the CCA by embedding the CCA into a polymer network (PCCA). The polymer around the CCA can be functionalized with some recognition element, making these materials useful as optical sensors.

This thesis describes a novel method for functionalizing PCCAs. We have successfully incorporated crown ethers and enzymes into PCCAs. The described method opens up the possibility of easy attachment of molecules containing amine, thiol and hydroxyl groups to PCCAs. The work includes incorporation of glycidyl methacrylate to the hydrogel network, and reacting the epoxide groups to develop sensing materials.

This thesis also describes the fabrication of a new photochemically controlled PCCA. This photoswitchable device shows a photoreversible shift in diffracted light, and acts as a novel recordable and erasable memory device. The photoresponsive PCCA was created by functionalizing a PCCA with an azobenzene-type molecule. Gradual red-shifting of the diffraction peak upon UV illumination is accompanied by a decrease in $\pi \rightarrow \pi^*$ absorption, and an increase in $n \rightarrow \pi^*$ absorption, due to the trans $\rightarrow$ cis isomerization of azobenzene. Excitation with visible light results in the reverse cis $\rightarrow$ trans isomerization and a diffraction peak blue-shift

to the original position. Information can be written using UV light and stored until visible light is used for erasing.

An additional route for developing a photoresponsive PCCA is to introduce photochemical crosslinks inside the hydrogel network around the CCA. For this purpose we have used azophenyl-p-N,N'-dimaleimide. In contrast to the previously described photoresponsive PCCA, in which the hydrogel volume increases under UV irradiation, the azobenzene-crosslinked PCCA's volume decreases under UV light. Both systems are controlled by free energy of mixing.

Different photochemically responsive PCCAs were created using a spiropyran derivative and different methods of attachment. These photochromic films are able to respond to UV and visible light by shifting the diffracted wavelength from the photosensitive film. The photochromic systems based on azobenzene and spiropyran described in this work could find wide technological applications in the future.

ACKNOWLEDGEMENTS

I would like to express gratitude to my research advisor, Professor Sanford A. Asher, for the opportunities, support, encouragement, and patience that he generously provided during my graduate studies at the University of Pittsburgh.

I would also like to thank Dr. Igor Lednev for his scientific insight and encouragement. He greatly contributed to my growth and success as a scientist. Also, I would like to thank all of the past and present members of the Asher research group for their support and friendship.

I would like to thank Prof. Craig Wilcox for mentoring my proposal and broadening my scientific knowledge.

The assistance of the librarians, machinists, electricians, glass blowers and support staff here at the University of Pittsburgh is gratefully acknowledged. This work was financially supported by the Office of Naval Research, DARPA, NSF and NIH. I gratefully acknowledge Viktor Meier for synthesizing the water soluble azobenzene derivative which made the work described in Chapter 3 possible.

I would especially like to thank all the teachers and professors who have guided me along my educational career, especially Professor Ferenc Gall for giving me the opportunity to use the resources at the University of Novi Sad (Yugoslavia) when I was 16. To him I owe my early success in Petnica Science Center (Yugoslavia) and in Frankfurt on Main (Germany). Mrs. Ruza Okljesa was my material science teacher in high school and deserves special thanks. Her energy and courage has been an example to me throughout my life.

I would also like to thank my professors at Wittenberg University, especially my advisor Prof. Sartoris, Prof. Sanders (who introduced me for the first time to the wonderful world of lasers) and Prof. Chatfield for their kindness and support. They were my mentors and have stayed my friends to this day. Without their input, I would not have achieved as much as I have.

My friends and family have supported me throughout my life. Special thanks go to Mr. Paul Stefanik for his encouragement and tremendous impact in my life. His goodness will never be forgotten, and my legacy is to continue his example throughout my life. It is a debt I can not repay, but an example I must pass on. It is a real privilege to have known him. I would also like to thank Mr. Michael Orth for his courage and support for the past ten years. His understanding is greatly appreciated.

I would like to express special thanks to my parents, Elena and Julijan. To them I owe my thirst for knowledge and love of truth. I owe much of my success to you. Thank you for your encouragement and love.

Finally, I would like to thank my husband, Bryan, for his love, understanding and support over the past three years. I am looking forward to many more wonderful years together.

"The larger the searchlight, the larger the circumference of the unknown"

Dick Taylor (from "The Tesseract" by Alex Garland)

TABLE OF CONTENTS

LIST OF TABLES

LIST OF FIGURES

Chapter 1.

Chapter 2.

Chapter 3.

Chapter 4.

Chapter 5.

Chapter 6.

Chapter 1

Introduction

1. INTRODUCTION

This thesis describes the synthesis and application of novel optical materials that contain mesoscopically periodic arrays of colloidal particles, called crystalline colloidal arrays (CCAs).[1-3] The CCAs diffract visible light according to Bragg's law, and the wavelength of diffraction depends upon the interparticle spacing. These materials make a thin, diffracting film and have applications as tunable filters, sensors, optical switches, and nonlinear optical devices.[4-9]

Crystalline colloidal arrays are three-dimensional periodic structures (Figure 1a), which self-assemble from suspensions of highly charged, monodisperse colloidal particles in low ionic strength solution. The surface charge on the colloidal particles derives from the dissociation of strong acid groups, introduced during the sphere synthesis, resulting in a negatively charged surface surrounded by a diffuse counterion cloud which extends into the medium.[10-14] When the suspending medium is free from ionic impurities, the diffuse counterion cloud does not completely screen the surface charge, and a net interparticle electrostatic repulsive interaction occurs. The repulsive interaction hinders free particle diffusion. At low ionic strength (< 1μM NaCl) and high particle concentration (~10^{13} cm^{-3}), the system assumes a minimum energy configuration and the colloidal particles self-assemble into a macroscopic crystal, which is either body-centered cubic (bcc) or face-centered cubic (fcc) depending on the interparticle spacing. CCA usually self-assemble with the highest particle density planes (the bcc(110) or fcc(111)) parallel to the container walls.[15-17]

The crystalline phases of colloidal dispersions are manifested by brilliant iridescent colors. These iridescent colors derive from Bragg diffraction from ordered layers of spheres (Figure 1).[17,18]

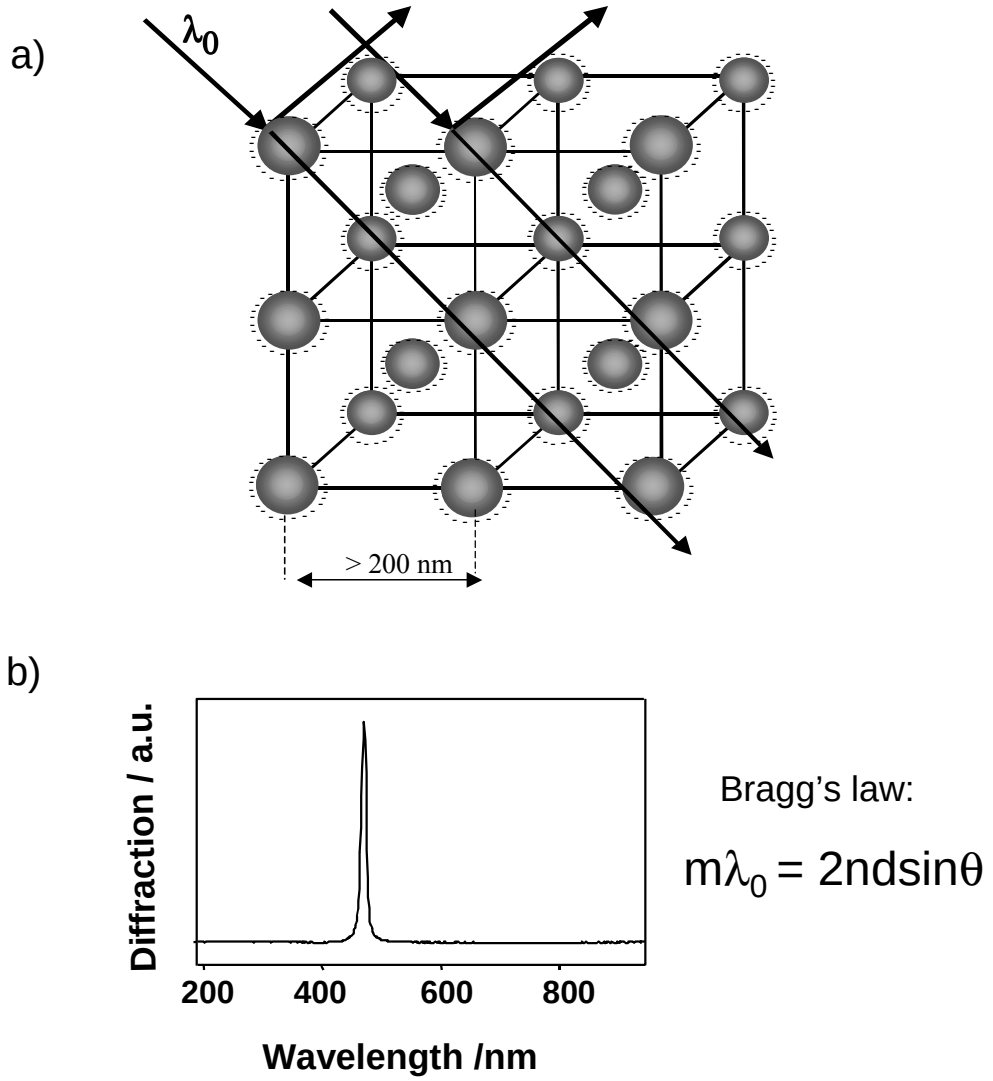

Figure 1.1. a) Self-assembly of a body-centered cubic CCA. At low ionic strengths, repulsion between monodisperse, highly charged colloidal particles forces the colloidal spheres into a minimum energy configuration, which is either a body- or face-centered cubic lattice. b) CCA diffracts visible light. The spectrum is measured with CCD spectrophotometer using reflectance probe. The diffraction obeys Bragg's law.

The Asher group has developed CCA materials which diffract light in the visible spectral region, generally using colloidal particles of ~120 nm diameter.[3] The colloidal particles may be composed of inorganic materials such as silica, or organic polymers such as polystyrene, poly(methyl methacrylate) or poly(N-isopropyl acrylamide). Since the periodicity of the CCA is on the order of 50 to 500 nm, the CCA diffracts ultraviolet, visible or near infrared light, depending on the lattice spacing and in agreement with Bragg's law:

$$m\lambda_0 = 2nd \sin\theta$$

where **m** is the order of diffraction, $\boldsymbol{\lambda_0}$ is the diffracted wavelength in a vacuum, **n** is the refractive index of the system (solvent, hydrogel and colloids), **d** is the spacing between the diffracting planes, and $\boldsymbol{\theta}$ is the glancing angle between the incident light propagation direction and the diffracting planes (Figure 1a). The interparticle spacing can be varied from a close-packed system to a system where the interparticle spacings are many times the particle diameter.[19-24]

The Bragg diffraction of light from these colloidal crystals is very efficient, and is analogous to the diffraction of X-rays from atomic crystals. Colloidal crystals can be prepared to diffract near the UV, visible, and near IR regions merely by diluting a concentrated suspension. The diffraction bands are narrow (< 10 nm), and light which is not diffracted transmits through the crystals. The Asher group has developed optical rejection filters based on these colloidal crystals.[3,6,7,25] Earlier work established that the diffraction of light from these colloidal crystals falls within the so-called Dynamical Diffraction limit.[10]

Ionic impurities inside the colloidal suspension (> 1 μM) screen the electrostatic repulsive interaction, causing disordering of the CCA. To make the system more robust, the

Asher group has developed methods to permanently lock the order of the CCA by embedding the CCA into a polymer network making polymerized colloidal arrays (PCCAs) (Figure 2a).[26]

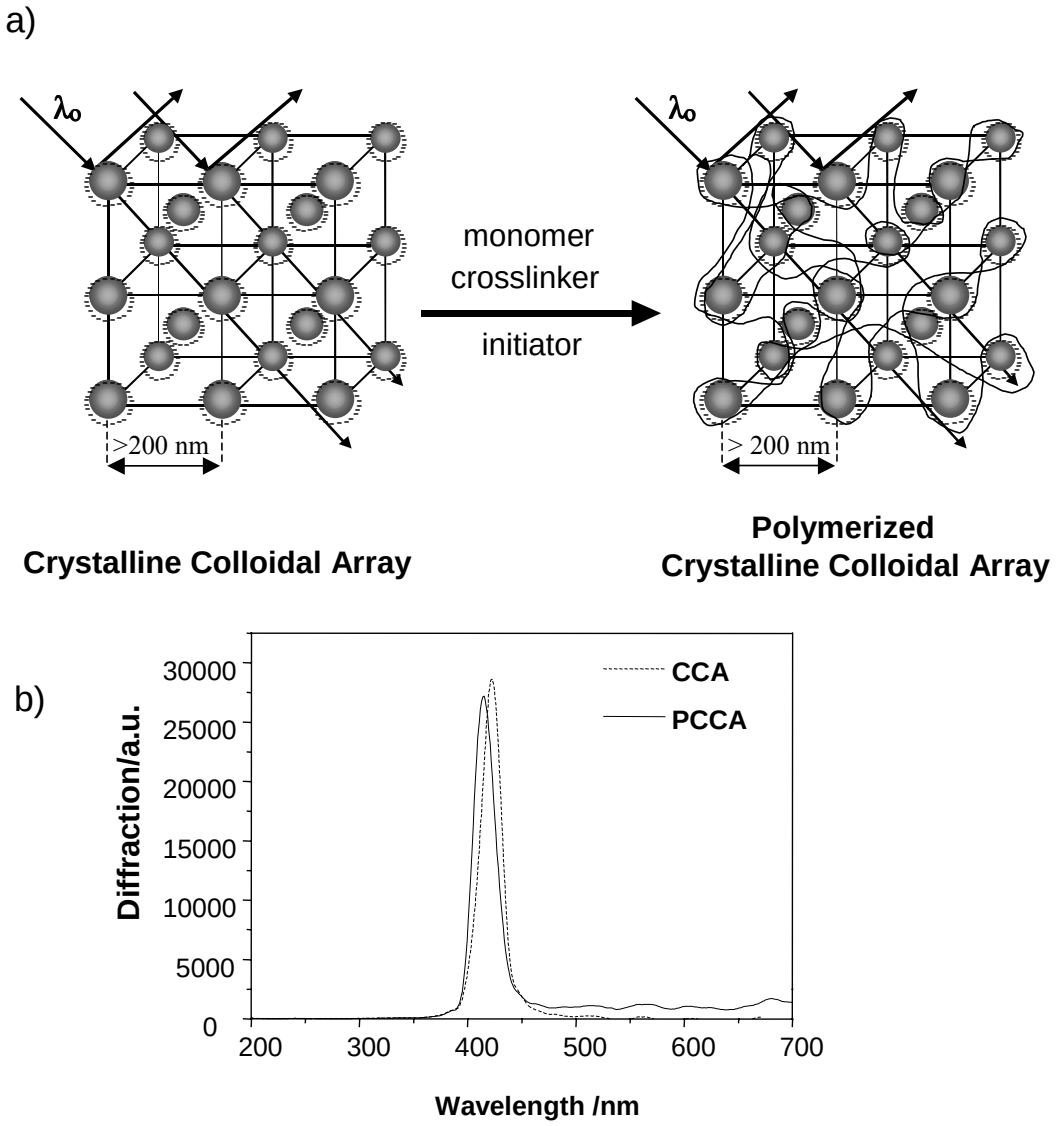

Figure 1.2. a) Polymerized crystalline colloidal array is developed by introducing a monomer (for example, acrylamide) and crosslinker (for example, N,N'-methylenebisacrylamide) inside the CCA liquid solution. CCA is made from 120 nm polystyrene colloidal particles. Schematically shown is the hydrogel polymerized around the CCA. b) The diffraction spectrum from CCA and PCCA is measured with CCD spectrophotometer using reflectance probe.

Photopolymerization of the mixture is completed in a quartz cell in order to make a thin, diffracting PCCA film. This cell consists of two quartz plates separated by a parafilm (125 μm thickness) or Duraseal (38 μm thickness). The diffraction of this hydrogel is approximately at the same wavelength as it was in the liquid CCA (Figure 2b).[27-29]

The spacing between the colloidal particles is now dependent on the properties of the surrounding polymer. This material is well suited for a wide range of applications due to the ease with which we can directly measure volume changes of the hydrogel by monitoring the CCA diffracted wavelength. The hydrogel network around the CCA is usually acrylamide crosslinked with N,N'-methylenebisacrylamide. The free-radical polymerization is initiated with diethoxyacetophenone (DEAP). The CCA periodic structure is "locked" inside this hydrogel matrix without affecting the CCA diffraction. The PCCA films are brightly colored due to the Bragg diffracted light from the CCA.[28,30,31]

The volume of a hydrogel depends on the polymer network, the composition of the solvent, and other environmental factors. A few forces determine the volume of a given gel (Figure 3).[32] Changing solvent composition results in a new hydrogel equilibrium volume due to change in the free energy of mixing (ΔG_{mix}) of the gel with the solvent. The gel volume changes, until the crosslinks that keep the polymer network together begin to resist the movement of the polymer in the bulk solvent. This restoring force is reflected in the free energy of elasticity, ΔG_{elas}, which can be changed only if some or all of the crosslinks inside the network are broken. If immobilized ions are attached to the hydrogel network, the change in osmotic pressure inside and outside the gel causes a change in Donnan potential, which will swell the hydrogel due to an alteration in ionic free energy, ΔG_{ion}. By increasing the ionic strength of the solution outside the hydrogel, the osmotic pressure will decrease, causing the gel to shrink. In

$$G_{tot} = G_{mix} + G_{ion} + G_{elas}$$

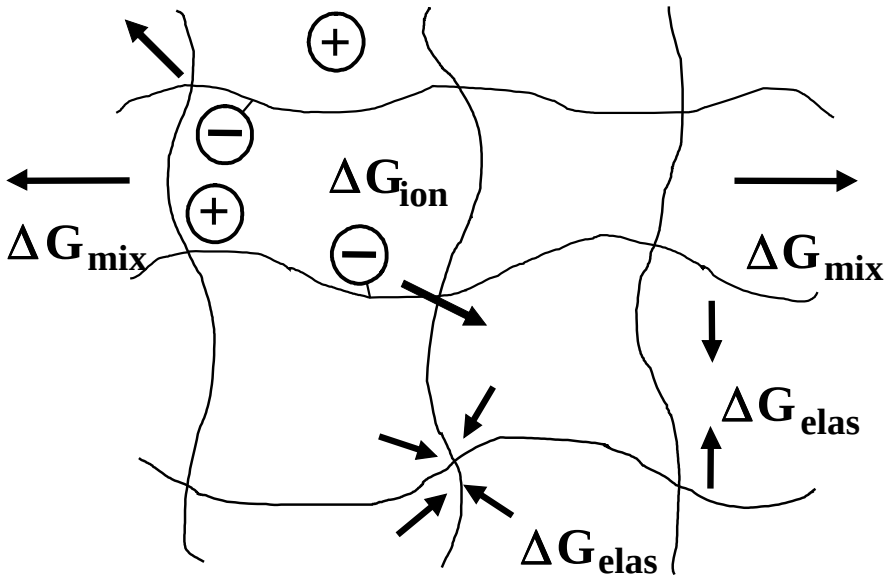

Figure 1.3. The forces that determine the equilibrium volume of a hydrogel can be expressed as a sum of free energies: the free energy of polymer/solvent mixing, the free energy due to ionic interactions, and the free energy of elasticity.

summary, the equilibrium volume of the gel depends on the balance of free energy of mixing, elastic free energy and free energy due to ionic interactions.[32-34]

The volume response to one particular chemical species makes PCCAs useful as sensing materials. The utility of this unique characteristic is limited only by the availability of suitable molecular recognition agents. Arrays of these types of sensors could test for multiple analytes within the same sample. The Asher group has already developed pH, ionic strength, lead, copper, arsenic, glucose, and oxygen sensors.[18-24,35-39] Other molecular recognition elements such as antibodies can be bound to the gels, making intelligent biosensing materials for viruses and bacteria.

PCCAs have the great advantage of having a response which is easily detectable by the human eye. The sensitivity and detection range of these sensors can be adjusted by controlling the gel composition, as well as the molecular recognition agents used. Applications in medicine, environmental chemistry, process control and remote sensing for these unique materials can be envisioned.

Chapter 2 describes a new method for synthesizing intelligent PCCAs as a class of materials that can be used for chemical sensing. Glycidyl methacrylate, together with acrylamide and N,N'-methylenebisacrylamide, was used in a free-radical polymerization to produce PCCA functionalized with epoxide groups. Glycidyl methacrylate has good balance of hydrolytic stability and reactivity with amine groups, and does not destroy the order of CCA. This method was used to create sensing materials that report on analyte concentrations via diffraction of visible light from a PCCA. This new procedure enables incorporation of molecular recognition agents into the PCCA to produce an intelligent PCCA without hydrolyzing the hydrogel network. Epoxide groups are available for further reaction immediately after the PCCA

is formed. The surface epoxide groups will readily react with thiol, amine or hydroxyl groups. Using this procedure, a lead sensor was created by exposing the epoxide-functionalized PCCA to 4-aminobenzo-18-crown-6. In addition, a glucose sensor was developed by covalently attaching glucose oxidase to the functionalized PCCA.

The work described in Chapter 3 focuses on development of a photoresponsive diffracting film which could be used for development of a memory storage device, or optical displays and optical switching**.** Photochromism is a process that involves a rapid and reversible change of color, and has many potential applications,[40-42] such as photochromic glasses that darken in the sunlight and bleach in dim light. In this work, a photoswitchable device was created by functionalizing a PCCA with an azobenzene-type molecule. A gradual red-shift of the diffraction peak upon UV illumination is accompanied by a decrease in $\pi \rightarrow \pi^*$ absorption, and an increase in $n \rightarrow \pi^*$ absorption, due to the trans $\rightarrow$ cis isomerization of azobenzene. Excitation with visible light results in the reverse cis $\rightarrow$ trans isomerization and a gradual diffraction peak blue-shift to the original position. Information can be written using UV light and stored until visible light is used for erasing. Optimization of the photoresponse can be achieved by varying the thickness of the hydrogel, the concentration of the azobenzene derivative, and the polymer crosslinking density. In addition, different azobenzene derivatives are studied and different synthesis routes are explored (Chapter 4).

Chapter 5 includes an additional route for developing a photoresponsive PCCA by introducing photochemical crosslinks inside the hydrogel network around the CCA. For this purpose we have used azophenyl-p-N,N'-dimaleimide. In contrast to the previously described PCCA (based on pendant azobenzene molecules), this PCCA shows the opposite photochemical switching behavior. UV light induces a blue-shift of the PCCA, and visible light induces a red-

shift. For all photoresponsive PCCAs, the volume change was controlled by free energy of mixing.

Chapter 6 describes the synthesis and properties of a photoresponsive material based on another photochromic family, spiropyrans. A spirobenzopyran derivative was attached to a hydrogel network via maleimide-sulfhydryl reaction. UV irradiation results in formation of a merocyanine form, which causes spiropyran-modified PCCA to swell. This process can be reversed with visible light. The photochemical response of this hydrogel was studied in dimethylsulfoxide. We also attached spiropyran derivative directly to the modified polystyrene colloids which constitute the CCA. Chlorine introduced on the surface of the polystyrene colloids reacts with the hydroxyl group on the spiropyran derivative. Spiropyran-functionalized colloids were then embedded in the polymer network. We describe the synthesis and behavior of this material under irradiation.

1.1. REFERENCES

1. Krieger, I. M.; O'Neill, F. M. *J. Am. Chem. Soc.* **1968**, *90*, 3114.

2. Hiltner, P. A.; Krieger, I. M., *J. Phys. Chem.* **1969**, *73*, 2386.

3. a) Asher, S. A. *U.S. Patents 4,627,689 and 4,632,517,* **1986**; b) Kesavamorthy, R.; Jagannathan, P.; Rundquist, P. A.; Asher, S. A. *J. Chem. Phys.* **1991**, *94*, 5172; c) Kesavamorthy, R.; Tandon, S.; Xu, S.; Jagannathan, S.; Asher, A. S., *J. Coll. Int. Sci.* **1992**, *153*, 188; d) Rundquist, P. A.; Jagannathan, P.; Kesavamorthy, R.; Brnadic, C.; Xu, S.; Asher, S. A. *J. Chem. Phys.* **1990**, *94*, 711.

4. Flaugh, P. L.; O'Donneell, S. E.; Asher S. A., *Appl. Spectrosc.* **1984**, *38*, 847.

5. Haacke, G.; Panzer, H. P.; Magliocco, L. G.; Asher, S. A.*U.S. Patent 5,266,238*, **1993.**

6. Asher, S. A.; Weissman, J. M.; Sunkara, H. B.; Pan, G.; Holtz, J.; Liu, L.; Kasavamoorthy, R. *In Polymers for Advances Optical Applications*, Jenekhe, S. A., Wynne, K. J., Eds.; Washington, DC, **1997**.

7. Asher, S. A.; Jagannathan, S. *U.S. Patent 5,281,370*, **1994.**

8. Asher, S. A.; Chang, S. Y.; Jagannathan, S.; Kesavamoorthy, R.; Pan, G. U.*S. Patent 5,452,123*, **1995.**

9. Carlson, R. J.; Asher, S. A. *Appl. Spectrosc.* **1984**, *38*, 297.

10. Brnardic, C., M.S. Thesis, University of Pittsburgh, **1992**.

11. Hiltner, P. A.; Papir, Y. S.; Krieger, I. M. *J. Phys. Chem.,* **1971**, *75*,1881.

12. Clark, N. A.; Hurd, A. J.; Ackerson, B. J. *Nature,* **1979**, *281,* 57.

13. Aastuen, D. J. W.; Clark, N. A.; Cotter, L. K.; Ackerson, B. J. *Phys. Rev. Lett.*, **1986**, 57, 1733.

14. Asher, S. A.; Flaugh, P. L.; Washinger, G. *Spectroscopy*, **1986**, *1*, 26.

15. Rundquist, P. A.; Jagannathan, S.; Kesavamoorthy, R.; Brnardic, C.; Xu, S.; Asher, S. A. *J. Chem. Phys.*, **1990**, *94,* 711.

16. Carlson, R. J.; Asher, S. A. *Appl. Spectrosc.,* **1984**, *38,* 297.

17. Verwey, E. J. W.; Overbeek, J. T. G. *Theory of the Stability of Lyophobic Colloids*, Elsevier, New York, **1948.**

18. Weissman, J. M.; Sunkara, H. B.; Tse, A. S.; Asher, S. A. *Science*, **1996**, *274,* 959.

19. Chang, S-Y.; Liu, L.; Asher, S. A. *J. Am. Chem. Soc.*, **1994**, *116*, 6739.

20. Chang, S-Y.; Liu, L.; Asher, S. A. *J. Am. Chem. Soc.,* **1994**, *116,* 6745.

21. Rundquist, P. A.; Photinos, P.; Jagannathan, S.; Asher, S. A. *J. Chem. Phys.*, **1989**, *91,* 4932.

22. Rundquist, P. A.; Kesavamoorthy, R.; Jagannathan, S.; Asher, S. A. *J. Chem. Phys.*, **1991**, *951,* 249.

23. Tse, A. S.; Wu, Z.; Asher, A. S. *Macromolecules*, **1995**, *28,* 6533.

24. Asher, S. A.; Holtz, J.; Liu, L.; Wu, Z. *J. Am. Chem. Soc.,* **1994**, *116,* 4997.

25. Kamenetzky, E. A.; Magliocco, L. G.; Panzer, H. P. *Science*, **1994**, *263,* 207.

26. Haacke, G.; Panzer, H. P.; Magliocco, L. G.; Asher, S. A. *U.S. Patents 5,266,238 and 5,368,781,* **1993**.

27. Asher, S. A.; Jagannathan, S. *U.S. Patent 5,281,370*, **1994**.

28. Haacke, G.; Panzer, H. P.; Maliocco, L. P.; Asher, S. A. *U.S. Patent 5,366,348,* **1993**.

29. Holtz, J. H.; Holtz, J. S. W.; Munro, C. H.; Asher, S. A. *Anal. Chem.,* **1998**, *70,* 780.

30. Hartley, G. S. *J. Chem. Soc.,* **1938**, 633.

31. a) Robertson, J. M.; *J. Chem. Soc.,* **1939**, 232; b) Hampson, G. C.; Robertson, J. M.; *J. Chem. Soc.*, **1941**, 409.

32. Flory, P. J. *Principles of Polymer Chemistry*, Cornell University Press, Ithaca, NY, **1953.**

33. Hiemenz, P. C.; Rajagppalan, R. *Principles of Colloid and Surface Chemistry*, 3rd edition, Marcel Dekker, Inc., **1997**.

34. Huang, Y.; Szleifer, I.; Peppas, N. A. *Macromolecules* **2002**, *35*, 1373.

35. Lee, K., Asher, S. A., *J. Am Chem. Soc*., **2000**, *122*, 9534.

36. Weissman, J. M.; Sunakara, H. B.; Tse, A. S.; Asher, S. A. *Science* **1996**, *274*, 959.

37. Asher, S. A.; Sharma, A. S.; Goponenko, A. V.; Ward, M. M. *Anal. Chem.* **2003**, 75, 1676.

38. Asher, S. A.; Alexeev, V. L.; Goponenko, A. V.; Sharma, A. S.; Lednev, I. K.; Wilcox, C.; Finegold, D. *J. Am. Chem. Soc.,* **2003**, *125*, 3322.

39. Reese, C. E.; Baltusavich, M. E.; Keim, J. P.; Asher, S. A. *Anal. Chem.,* **2001**, *73*, 5038.

40. Crano, J. C.; Guglielmetti, R. J. *Organic Photochromic and Thermochromic Compounds*, Plenum Press, New York, **1999.**

41. McArdle, C. B. *Applied Photochromic Polymer Systems*, Blackie, New York, **1992**.

42. Durr, H.; Bouas-Laurent, H. *Photochromism: Molecules and Systems*, Elsevier Amsterdam, **1990**.

Chapter 2

Epoxide Functionalized Polymerized

Crystalline Colloidal Arrays

This chapter was submitted to *Sensors and Actuators B, Chemistry*. The co-author is Sanford A. Asher.

2. EPOXIDE FUNCTIONALIZED POLYMERIZED CRYSTALLINE COLLOIDAL ARRAYS

2.1. ABSTRACT

We report the development of a novel method for functionalizing polymerized crystalline colloidal arrays (PCCA). This new method enables us to easily incorporate molecular recognition agents into the PCCA to produce chemical sensing materials that report on analyte concentration via diffraction of visible light. We copolymerize glycidyl methacrylate with acrylamide and N,N'-methylenebisacrylamide around crystalline colloidal arrays. The incorporated epoxide groups are available for further PCCA functionalization through reactions with thiol, amine or hydroxyl groups. We fabricated a Pb^{2+} sensor which utilizes a crown ether recognition agent, as well as a glucose sensor which utilizes glucose oxidase.

2.2. INTRODUCTION

We recently developed a new class of chemical sensing materials known as intelligent polymerized crystalline colloidal arrays (IPCCA).[1-8] These materials are composed of an array of colloidal particles immobilized within a hydrogel (PCCA). The array spacing is ~ 200 nm, such that it diffracts visible light. We fabricate a chemical sensing material by adding molecular recognition agents to the PCCA which actuate hydrogel volume changes upon reaction with analytes.[1-8] The resulting hydrogel volume changes are read out by the consequent changes in the diffraction wavelength. We attached the molecular recognition agents either by introducing them during PCCA polymerization, or by attaching the agents after PCCA polymerization. For example, we previously fabricated a lead-sensing IPCCA by copolymerizing a vinyl crown ether into the PCCA.[1,5-8] In contrast, we fabricated a glucose-sensing IPPCA by attaching glucose oxidase using avidin-biotin coupling subsequent to polymerizing the biotin group into the PCCA.[1-3]

We utilize more complex functionalization in our fabrication of glucose-sensing boronic acid IPCCA, where we hydrolyzed the PCCA to form carboxyl groups which we subsequently used to attach molecular recognition groups.[7,8] Only nonionic molecular recognition groups can be copolymerized into the PCCA; charged groups would disorder the colloidal particle array. Thus, we require post-polymerization molecular functionalization strategies for developing IPCCA sensors.

In this paper we describe a new method for incorporating molecular recognition agents into the PCCA. This method involves copolymerization of glycidyl methacrylate, which has a good balance of hydrolytic stability and reactivity with amine groups, and does not destroy the

order of the CCA. This synthesis provides epoxy groups along the hydrogel surface which readily react with thiol, amine or hydroxyl groups.[9,10]

2.3. EXPERIMENTAL

Highly charged, 120 nm diameter monodisperse polystyrene colloidal particles (10 % wt. suspension) were prepared by emulsion polymerization, as described elsewhere.[11,12] Excess ions and surfactants were removed from the colloidal suspensions by dialysis against deionized water. The dialyzed suspension was further cleaned by shaking with an ion-exchange resin (Bio-Rad). The suspension became iridescent due to Bragg diffraction from the CCA.

In order to fabricate the PCCA, acrylamide (50 mg, Fluka) and glycidyl methacrylate (20 μl, Aldrich) were used as monomers, and N,N'-methylenebisacrylamide (3 mg, Fluka) was used as a crosslinker (Figure 1). 10 μl of a 10% solution of diethoxyacetophenone (Acros Organics, v/v) UV photoinitiator in DMSO was added to the suspension. This mixture was injected into a cell consisting of two quartz plates, separated by a 76 μm spacer (two DuraSeal sheets). The cell was exposed to UV light from a Black Ray model B-100, UVP Inc. mercury lamp (365 nm maximum wavelength) to initiate polymerization. After a 30 minute exposure, the cell was opened and the resulting hydrogel film, which adheres to one of the quartz plates, was washed in deionized water in order to remove all unreacted compounds. This PCCA functionalized with epoxy groups is then immediately reacted with the desired species containing terminal amine groups (Figure 2).

The maximum molar ratio of glycidyl methacrylate to acrylamide that was incorporated in the hydrogel was 15% due to the limited solubility of glycidyl methacrylate in water.[13] We observed phase separation at a 20 mol % of glycidyl methacrylate. The concentration of the reactive epoxide groups was determined from absorption measurements of an amine-containing

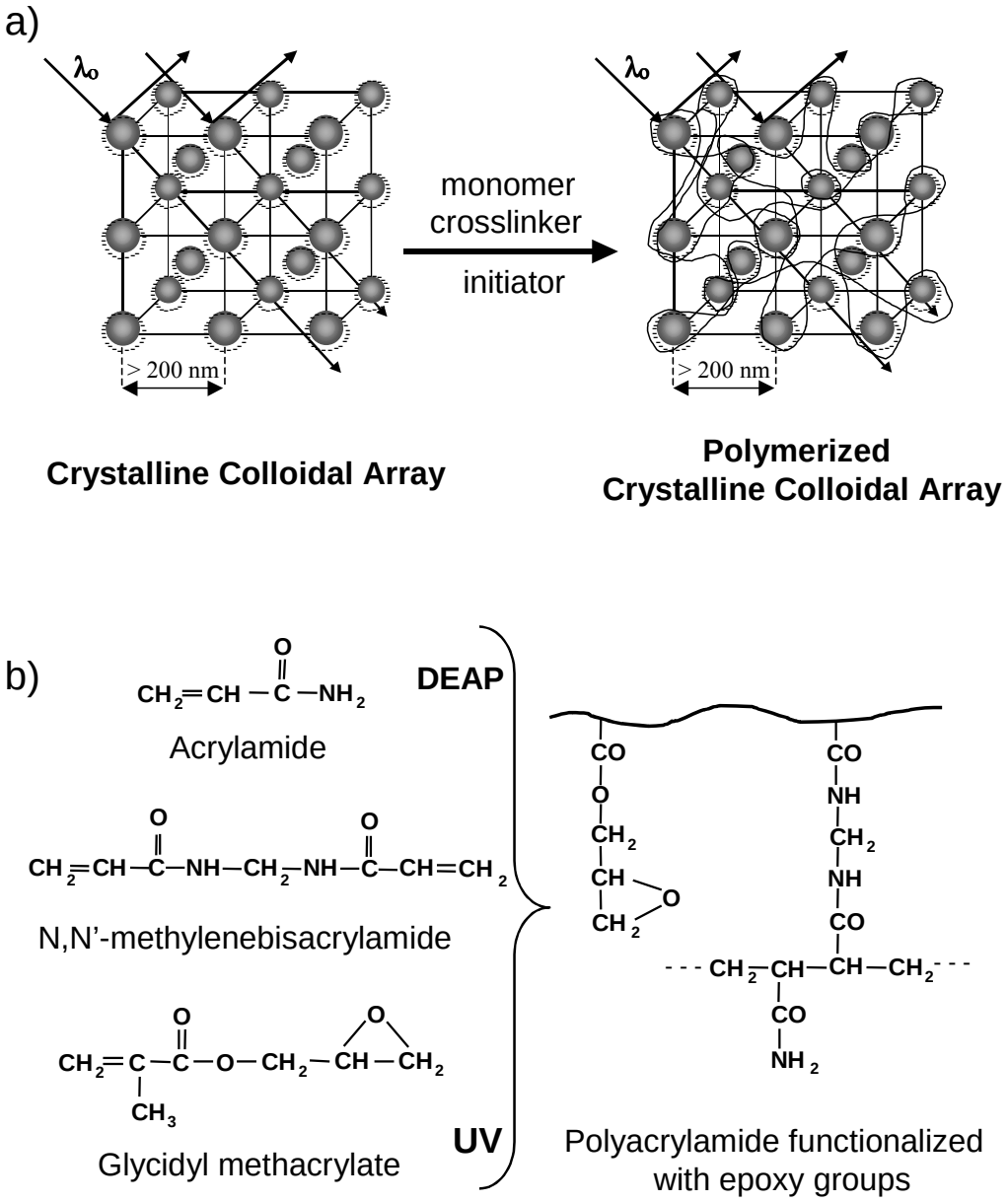

Figure 2.1. a) Polymerized crystalline colloidal array is developed by introducing a monomer (for example, acrylamide) and crosslinker (for example, N,N'-methylenebisacrylamide) inside the CCA liquid solution. CCA is made from 120 nm polystyrene colloidal particles. Schematically shown is the hydrogel polymerized around the CCA. b) Functionalization of PCCA with epoxide groups.

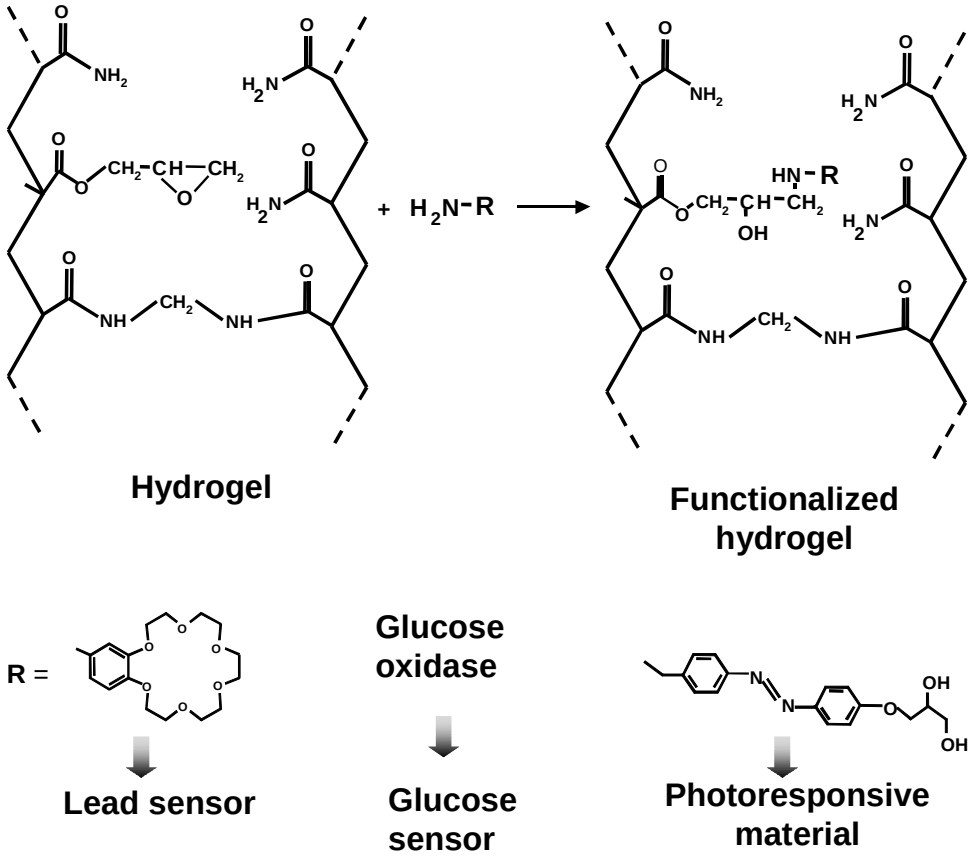

Figure 2.2. PCCA functionalized with epoxy groups is exposed to various compounds with terminal amino groups.

dye, Disperse Orange 3, which shows an absorption maximum around 450 nm in water. This dye was reacted with the glycidyl-PCCA for two hours, and the resulting gel was washed overnight in deionized water. The concentration of dye inside the hydrogel was determined to be ~ 3 mM using a Perkin-Elmer Lambda 9 UV/VIS/NIR spectrophotometer.

We fabricated a lead sensor by exposing the PCCA to an 0.08 M aqueous solution of 4'-aminobenzo-18-crown-6 (Aldrich). The response of this IPCCA was measured by using an Ocean Optics USB2000 Fiber Optic Spectrometer. The wavelength diffracted from the IPCCA sensor monitors the IPCCA's linear dimension. The IPCCA diffraction wavelength shift reached its equilibrium value within 2 minute (for 1 to 10 mM analyte concentrations), or within 10 min (for analyte concentrations < 0.1 mM), since the response is diffusion limited.

We fabricated a glucose-responsive PCCA by covalently attaching glucose oxidase (Sigma, G7016, 50,000 units) to the epoxy-functionalized PCCA. The PCCA was exposed to a 9 X 10^{-5} M aqueous solution of glucose oxidase at room temperature overnight under continuous stirring. The hydrogel was then washed with deionized water.

We also used the glycidyl PCCA to fabricate a photoresponsive PCCA by covalently attaching an amine-containing azobenzene derivative to the epoxy-funtionalized PCCA. The synthesis and properties of this photosensitive PCCA[14] are discussed in Chapter 3.

2.4. RESULTS AND DISCUSSION

2.4.1. Crown Ether Pb^{2+} IPCCA

In previous work, we fabricated a Pb^{2+} IPCCA sensor by copolymerizing acryloyamidobenzo-18-crown-6 with acrylamide and N,N'-methylenebisacrylamide.[1,5-8] In the present study, we copolymerized glycidyl methacrylate to create a PCCA which has the capability of binding any recognition agent containing amine, thiol, or hydroxide functionalities.

We synthesized an analogous Pb^{2+} sensing IPCCA by reacting the glycidyl PCCA with 4'-aminobenzo-18-crown-6. Figure 3 shows the response of this IPCCA sensor to Pb^{2+} in the form of dissolved $Pb(NO_3)_2$. The diffraction red-shifts with increasing Pb^{2+} concentrations in a manner similar to that observed previously.[1,5-8]

Figure 3b shows that the diffraction red-shift increases as the epoxide group concentration increases, presumably due to the attachment of a larger amount of 4'-aminobenzo-18-crown-6. The IPCCA reached a saturated response within 2 minutes of analyte addition.

This IPCCA red-shift results from hydrogel swelling due to a Donnan potential established by the increased concentration of mobile counterions to the Pb^{2+} chelated to the 18-crown-6.[1,3,5,8] The slope of the calibration plot for Pb^{2+} is determined by the association constant of the crown ether, the concentration of crown ethers in the IPCCA and the hydrogel crosslink density, which determines the IPCCA elasticity.[1,3,5,8] We used 2% N,N'-methylene-bisacrylamide crosslinking to give us a robust 76 μm thick gel.

This IPCCA fully responds to Pb^{2+} within a few minutes. For example, Figure 4 shows that the diffraction of the top surface of an IPCCA gives a saturating 30 nm red-shift due to a 1 mM $Pb(NO_3)_2$ solution within ~1 min under constant stirring. In these measurements the diffraction peak was monitored until no further change in diffraction occurred. The IPCCA reaches its equilibrium diffraction more slowly at low analyte concentrations (< 0.1 mM) because the response is diffusion limited.

2.4.2. Glucose Oxidase IPCCA

We previously fabricated a glucose IPCCA sensor based on glucose oxidase by attaching biotin to the PCCA, and using the well-known avidin-biotin interaction to attach avidinated

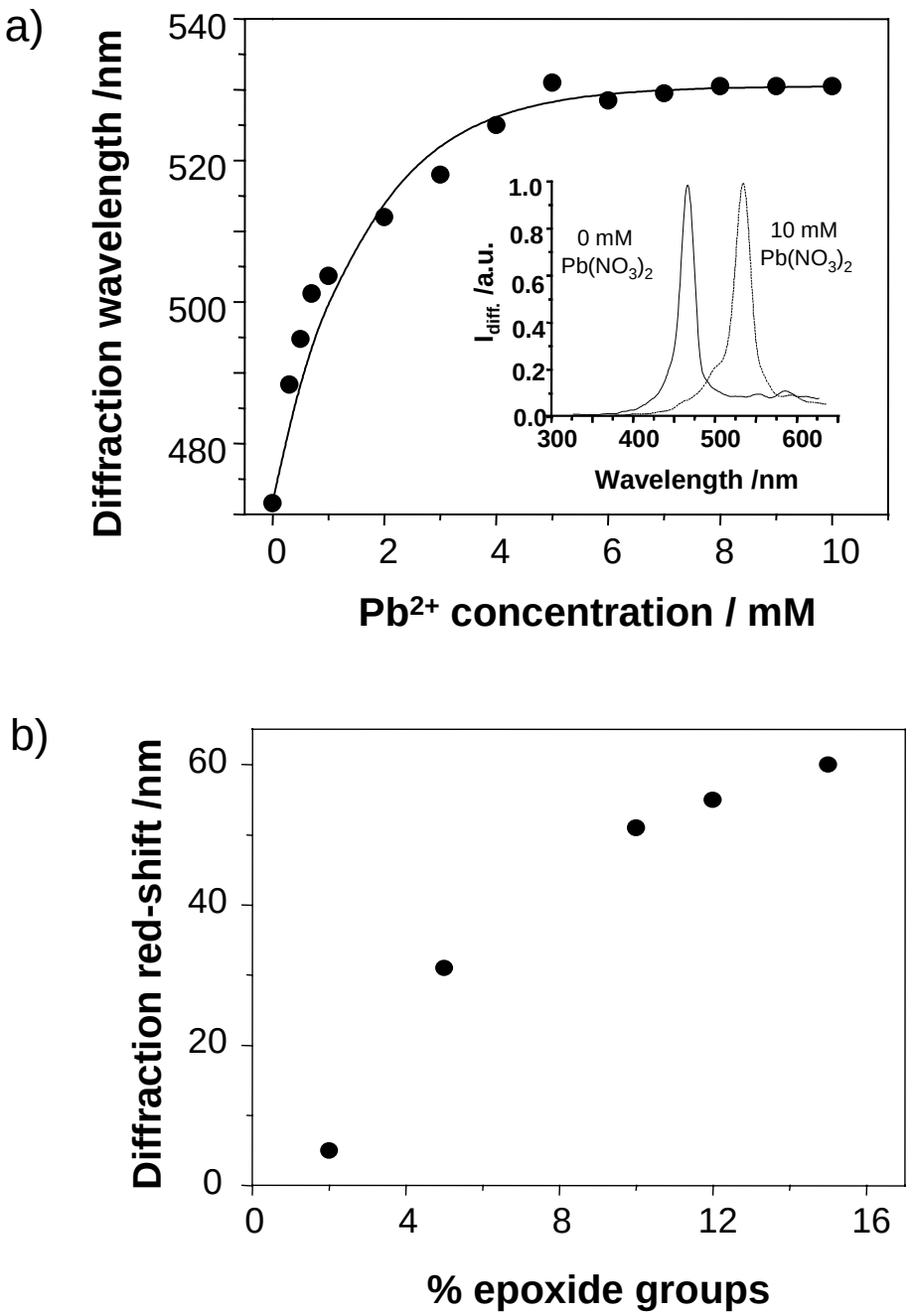

Figure 2.3. a) Diffraction wavelength change as a function of Pb^{2+} concentration (15% epoxide groups). Inset: IPCCA functionalized with 15% glycidyl methacrylate responds to 10 mM $Pb(NO_3)_2$. The 60 nm red-shift of diffraction peak is shown. CCD spectrophotometer was used to measure reflected light from the IPCCA. b) Red-shift of diffraction wavelength dependence on epoxide concentration inside the lead responsive PCCA (gel exposed to 10 mM $Pb(NO_3)_2$).

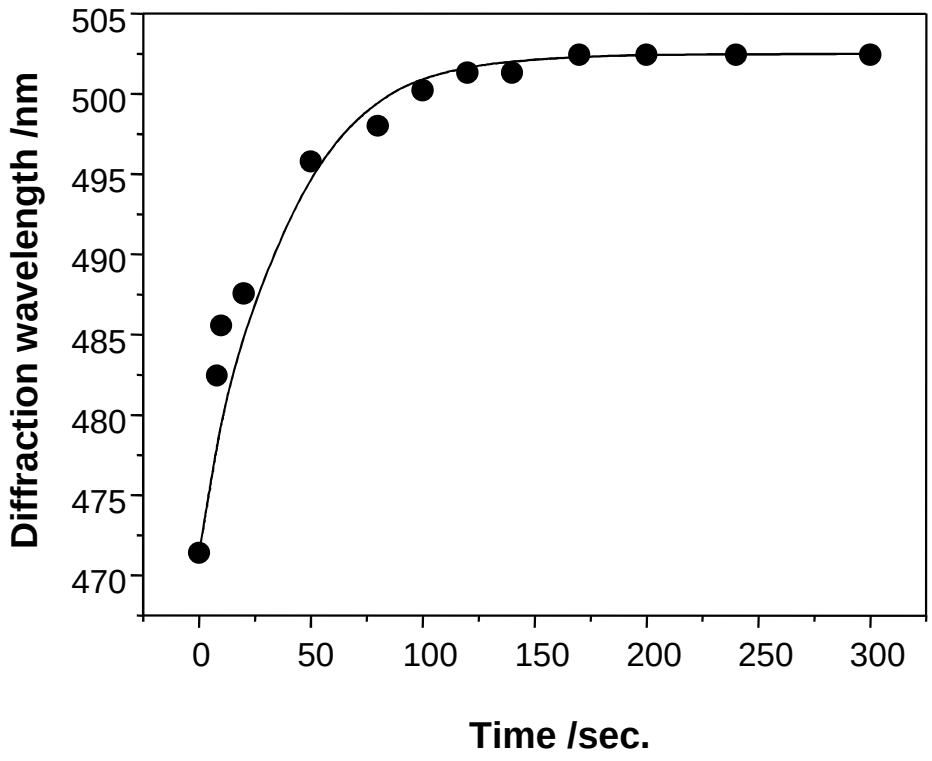

Figure 2.4. Kinetic measurement for the IPCCA exposed to 1 mM Pb^{2+} concentration. The gel tested here has 15% mol of epoxide groups incorporated.

glucose oxidase to the hydrogel.[1,3] In the present work, we describe a method which more simply binds glucose oxidase through its exposed amine groups.

Glucose oxidase is an ellipsoidal flavin-containing glycoprotein with dimensions of 60 Å x 52 Å x 37 Å. The monomer is folded into two structural domains, one which binds flavin and the other which is involved with substrate binding. At neutral pH, the oxidized flavin is uncharged, but the reduced flavin is anionic.[1,3,15,16]

Glucose oxidase converts glucose to gluconic acid in a two-step process.[15,16] In the first step, glucose is converted to gluconic acid, and the enzyme is reduced. In the second step, the enzyme is reconverted to its oxidized form by oxygen present in the solution, producing hydrogen peroxide as a byproduct:

$$\text{EnzymeH(oxidized)} + \text{glucose} \rightarrow \text{enzyme}^- \text{(reduced)} + \text{gluconic acid} + H^+$$

$$2\ \text{Enzyme}^- \text{(reduced)} + 2\ H^+ + O_2 \rightarrow 2\ \text{EnzymeH(oxidized)} + H_2O_2$$

We showed previously[1,3] that the reaction of glucose with the glucose oxidase IPCCA reduced the flavin prosthetic group, which becomes an anion, resulting in a Donnan-potential induced hydrogel expansion in low ionic strength solutions.

Figure 5a shows the UV-visible absorption spectra of a dehydrated glycidyl acrylamide PCCA which eliminates the visible diffraction peak. Figure 5a compares the absorption of the dried glycidyl gel and a similar gel reacted with glucose oxidase. The glucose oxidase Flavin Adenine Dinucleotide (FAD) prosthetic group absorption bands at 380 nm and 450 nm demonstrate the attachment of the glucose oxidase protein.

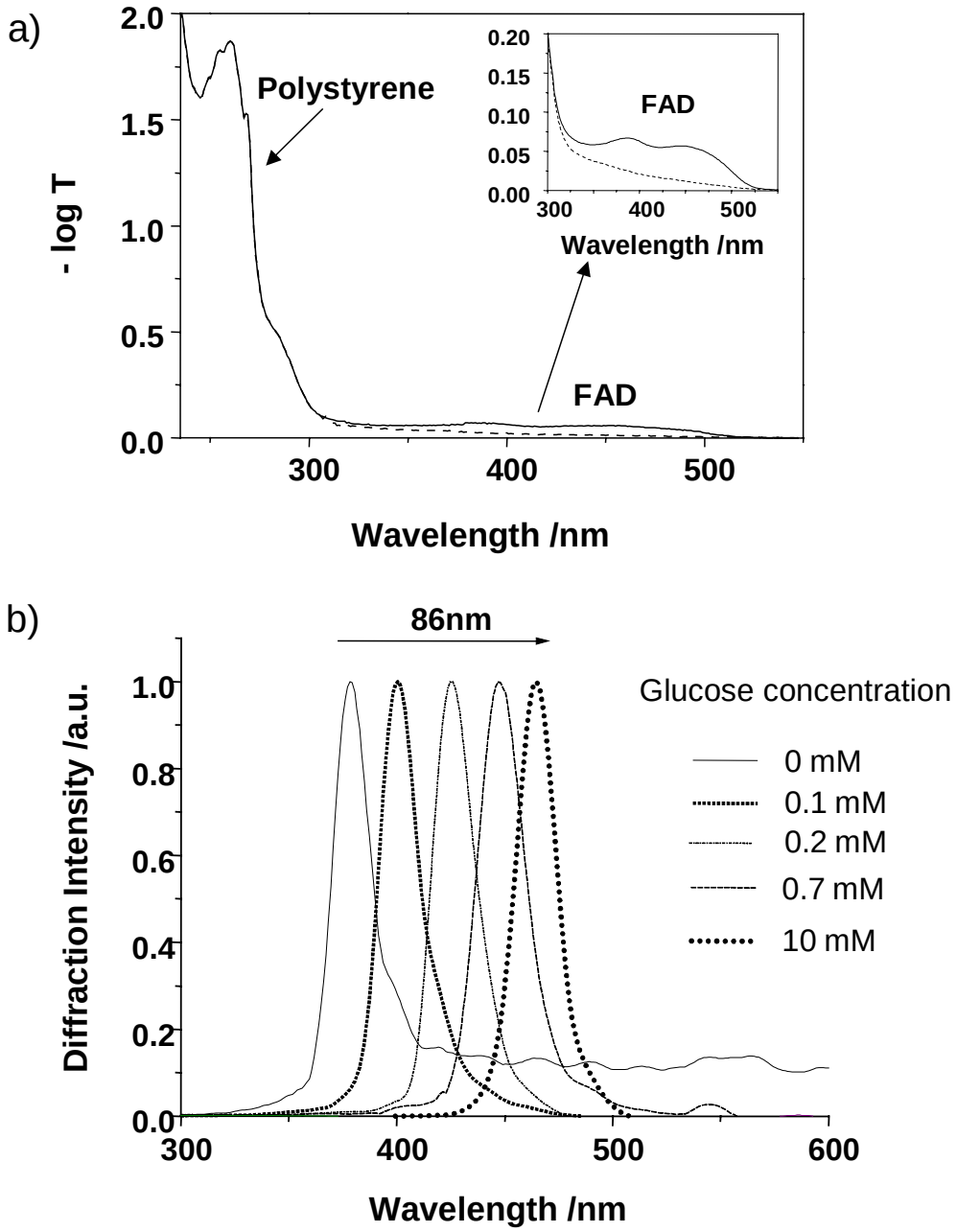

Figure 2.5. a) Absorption spectra of dehydrated glycidyl acrylamide hydrogel (---) before and after (—) reaction with glucose oxidase. The FAD absorption peaks indicate the successful attachment of glucose oxidase. b) β-D(+)Glucose concentration dependence of diffraction for glucose oxidase IPCCA.

Figure 5b shows that the glucose oxidase IPCCA (containing a 15% molar ratio of glycidyl methacrylate) monotonically red-shifts with increasing glucose concentrations. The diffraction red-shifts 86 nm in the presence of 10 mM glucose. This behavior is similar to that of our glucose oxidase sensors attached through avidin biotin coupling. This indicates that the glycidyl attachment has not deactivated the glucose oxidase.

We examined the time dependence of the diffraction red-shift of our glucose oxidase sensor under an N_2 atmosphere. Figure 6 shows the time dependence for a 10 mM glucose solution. The response saturated within 1 min. Measurements for 0.1 mM and 100 mM glucose solutions showed saturation at 3 min and 30 sec, respectively. The response rate is determined by the mass transport of substrate into the gel, the rate of enzyme reaction and the collective diffusion constant of the hydrogel.

2.5. CONCLUSION

Our new method of creating a functionizable PCCA by copolymerizing glycidyl methacrylate into the PCCA makes it convenient to attach molecular recognition groups. The only requirement for attachment is the presence of either thiol, amine or hydroxyl groups on the recognition agent. This advance will help in developing IPCCA sensing materials for additional analytes.

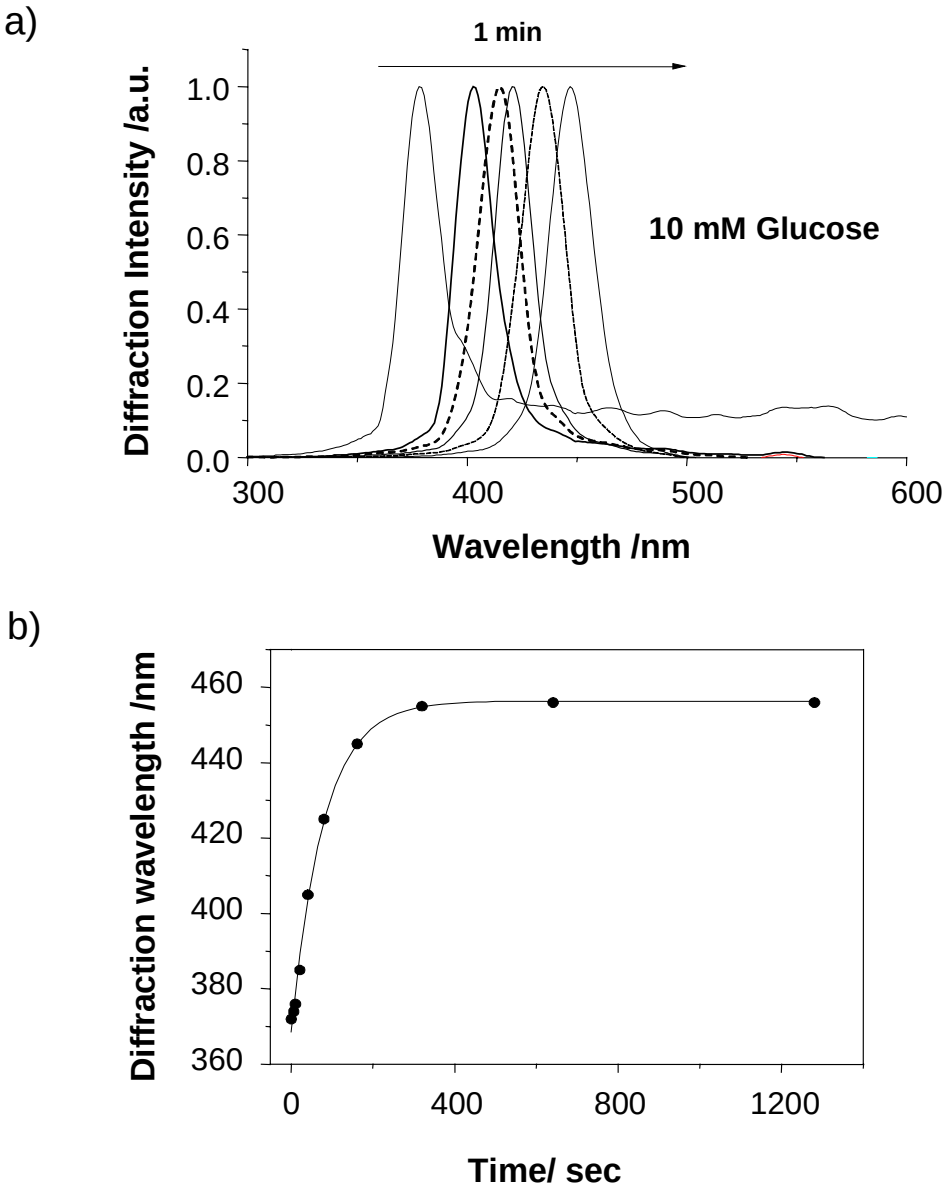

Figure 2.6. a) Time dependence of diffraction of glucose oxidase IPCCA upon exposure to 10 mM glucose solution. b) The response saturates in less than 5 min.

2.6. REFERENCES

1. Holtz, J. H.; Asher, S. A. *Nature*, **1997**, *389*, 829.

2. a) Asher, S.A.; Holtz, J. H. *U.S. Patent 5,854,078*, **1998**. b) Asher, S. A.; Holtz, J. H.; *U.S. Patent 5,898,004*, **1999**.

3. Holtz, J. H.; Holtz, J. S. W.; Munro, C. H.; Asher, S. A. *Anal. Chem.*, **1998**, *70*, 780.

4. Reese, C. E.; Baltusavich, M. E.; Keim, J. P.; Asher, S. A. *Anal. Chem.* **2001**, *73*, 5038.

5. Lee, K.; Asher, S. A. *J. Am. Chem. Soc*., **2000**, *122*, 9534.

6. Asher, S. A.; Alexeev, V. L.; Goponenko, A. V.; Sharma, A. C.; Lednev, I. K.; Wilcox, C. S.; Finegold, D. N. *J. Am. Chem. Soc.,* **2003**, *125*, 3322.

7. Alexeev, V. L.; Sharma, A. C.; Goponenko, A. V.; Das, S.; Lednev, I. K.; Wilcox, C. S.; Finegold, D. N.; Asher, S. A. *Anal. Chem.*, **2003**, *75*, 2316.

8. Asher, S. A.; Peteu, S.; Reese, C.; Lin, M.; Finegold, D. *Analy. and Bioanaly. Chem.,* 2002, *373*, 632.

9. Hermanson, G. T.; Mallia, A. K.; Smith, P. K. *Immobilized Affinity Ligands Techniques*, Academic Press, San Diego, California, **1992**.

10. Aslam, B.; Dent, A. *Bioconjugation*, Macmillan Reference Ltd., **1998**.

11. Reese, C. E.; Guerrero, C. D.; Weissman, J. M.; Lee, K.; Asher, S. A. *J. Colloid Interface Sci.*, **2000**, *232*, 76.

12. Reese, C. E.; Asher, S. A. *J. Colloid Interface Sci.*, **2002**, *248*, 41.

13. Brandrup, J.; Immergut, E. H.; Grulke, E. A. *Polymer Handbook*, John Wiley & Sons, Inc., New York, 4th edn., **1999**.

14. a) Kamenjicki, M.; Lednev, I. K.; Mikhonin, K. A.; Kasavamoorthy, R.; Asher, S. A. *Adv. Funct. Mater*. **2003**, *13*, 774. b) Asher, S. A.; Kamenjicki, M.; Lednev, I. K. *US Patent 6,589,452*, **2003**.

15. Burtis, C. A.; Ashwood, E. R. *Tietz Textbook of Clinical Chemistry*, W.B. Saunders Company, Pennsylvania, 3rd edn., **1999**.

16. Hassan, C. M.; Doyle, F. J.; Peppas, N. A.*Macromolecules,* **1997**, *30,* 6166.

Chapter 3

Photoresponsive Azobenzene Photonic Crystals

This chapter was submitted to *Nano Letters*. The co-authors are Igor Lednev and Sanford Asher.

3. PHOTORESPONSIVE AZOBENZENE PHOTONIC CRYSTALS

3.1. INTRODUCTION

Many groups are developing fabrication methods to produce photonic crystals with bandgaps in the visible, infrared and microwave spectral regions.[1-6] Photonic crystals are materials with a periodic variation in their dielectric constant. The resulting periodic variations in the refractive index lead to diffraction of light and to the occurrence of photonic bandgaps. Light of frequencies within the bandgap cannot propagate. This provides the opportunity to control the flow of light. Photonic crystals may be the key to all-optical integrated circuits.[7]

The earliest chemical approach to fabricating photonic crystals was through the self-assembly of highly charged monodisperse colloidal particles into crystalline colloidal arrays (CCA).[8] These CCA are complex fluids which self-assemble due to long range electrostatic repulsions between particles into plastic face centered cubic (fcc) crystalline arrays. The CCA Bragg diffract ultraviolet, visible or near-infrared light depending on the colloidal particle array spacings.[8,9]

Robust semi-solid polymerized crystalline colloidal array (PCCA) materials were fabricated by embedding the CCA into a hydrogel network.[9] PCCAs can be made from a stimuli–responsive polymer network,[10,11] where appropriate stimuli alter the PCCA volume and the resulting CCA plane spacings and diffraction wavelengths.[12-14] In this regard we describe here a novel photochemically actuated photonic crystal, where photoisomerization of a covalently attached azobenzene derivative changes the hydrogel free energy of mixing. The resulting PCCA volume change alters the lattice constant and shifts the diffracted wavelength. We alter the wavelength of the diffraction with light outside the photon bandgap. The volume

phase transition of the photocontrolled PCCA (PCPCCA) induced by the azobenzene photoisomerization occurs in the 10 sec time domain. Chapter 4 will examine the highly complex short time dynamics of a similar PCCA.[15]

We fabricated this photochemically controlled photonic crystal by attaching an epoxide functionality to the PCCA. This was accomplished by copolymerizing glycidyl methacrylate,[16-20] polyacrylamide and N,N'-methylenebisacrylamide within a CCA of 140 nm fluorinated polymer colloidal particles. We utilized fluorinated colloids to minimize absorption in the UV region in order to monitor the trans-azobenzene ~350 nm absorption band. These highly sulfonated, monodisperse fluorinated colloidal particles were prepared by emulsion polymerization.[21] The PCCA epoxy groups were reacted with the primary amine of the water soluble azobenzene derivative shown in Figure 1. As far as we know, this azobenzene derivative is the first to display photochromism in water.

3.2. RESULTS AND DISCUSSION

As shown in Figure 1, this 76 μm thick PCCA diffracts slightly more than 50 % of the light in a band centered around 670 nm red light. The light is incident normal to the fcc (111) planes and is only partially diffracted due to the small refractive index difference between the particles (n_p~1.38) and the mainly aqueous (n_w~1.33) hydrogel medium.[21] PCCA made from polystyrene colloidal spheres diffract essentially all of the incident light.[12-14]

The photoisomerization of the azobenzene derivative attached to the PCCA is shown in Figure 1. In the dark equilibrium state, the azobenzene molecules are in their trans form and absorb strongly at 350 nm. The 365 nm excitation occurs within this strong 350 nm trans-azobenzene $\pi \rightarrow \pi^*$ transition which photoisomerizes the trans-azobenzene to the cis-form. Thus,

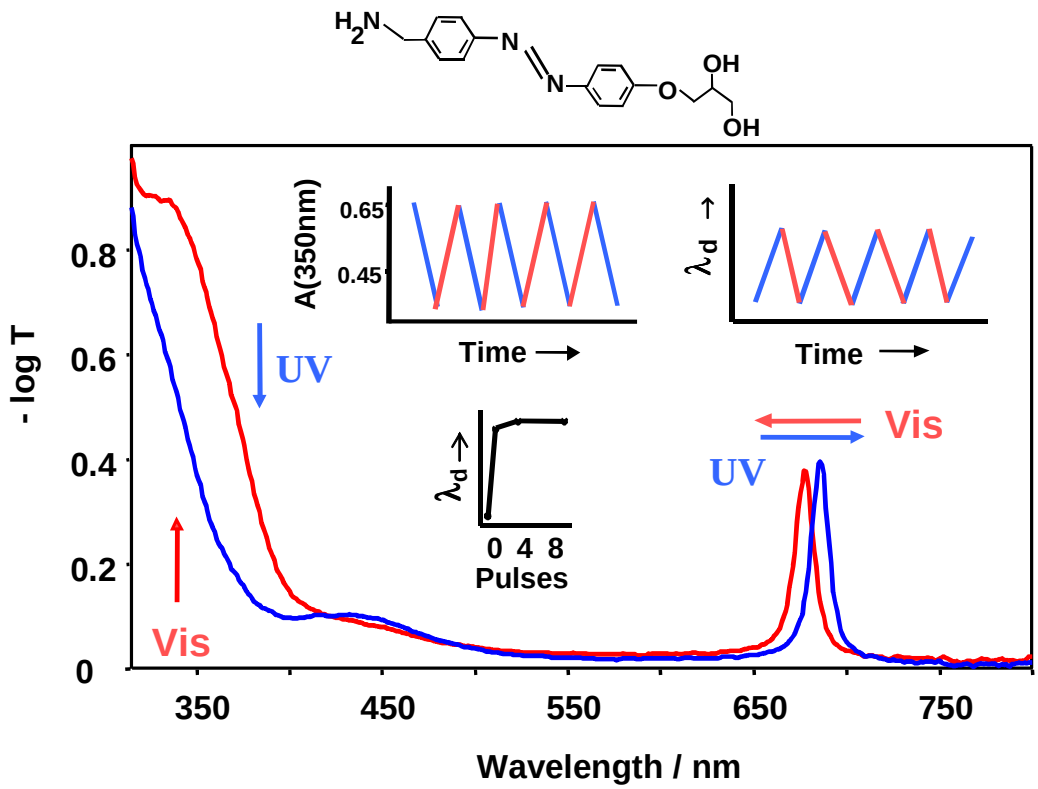

Figure 3.1. Structure of water soluble azobenzene derivative and photoresponse of the azobenzene functionalized PCCA to UV and vis light. PCCA is 76 μm thick and contained 5 % crosslinks. It was fabricated from 140 nm diameter fluorinated colloids. The spectra show fully reversible changes in the azobenzene absorption (300 to 550 nm) and ~670 nm diffraction shifts upon alternating excitation with 365 nm and 488 nm light.

the 350 nm trans-azobenzene $\pi \rightarrow \pi^*$ absorption bleaches, and the 440 nm cis-azobenzene $n \rightarrow \pi^*$ transition appears.[22-26] This process can be reversed either by excitation within this ~440 nm absorption band or by dark cis $\rightarrow$ trans conversion, which restores the 350 nm trans absorption band and the original diffraction in ~ 10 days (Figure 2).

The response time of the PCPCCA diffraction shift is controlled by either the incident light power or by the collective diffusion constant of the hydrogel polymer network and the rate of water flow. Figure 2 shows a situation where the time response of the PCCA is limited by the 350 nm photon flux.

The photochemical conversion from trans to cis is very efficient (ϕ~0.2), and the photoswitching effect can be actuated by a single ns pulse of the laser (1.2 mJ/cm^2, Figure 1-inset). In this case, the diffraction shifts are limited by the polymer and water time response, and occur ~10 sec after the laser pulse (Figure 2). The PCCA absorption and diffraction can be toggled back and forth indefinitely by illumination alternatively with UV light followed by visible light (insets to Figure 1).

The volume of the PCCA hydrogel is controlled by the balance between the free energy of mixing of the polymer hydrogel with water and the elastic restoring force of the hydrogel crosslinks.[12-15] The higher dipole moment of the cis-azobenzene form results in an increased solubility in water, which increases the free energy of mixing of the hydrogel, causing the polymer network to swell and the PCPCCA diffraction to red-shift. As expected, the magnitude of the diffraction peak shift linearly increases with the increase in azobenzene concentration from 2 to 4 mM due to the resulting increased free energy of mixing.

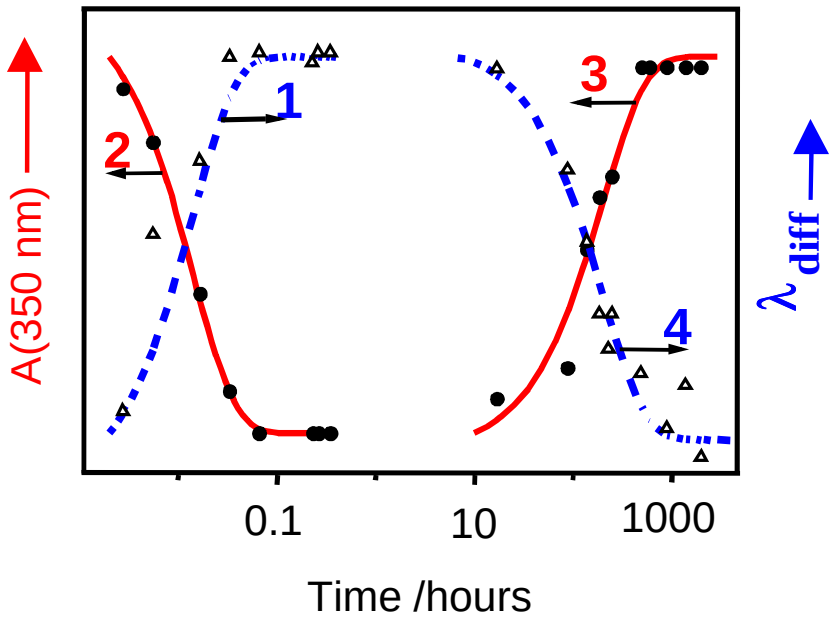

Figure 3.2. Time dependence of 350 nm absorbance and the diffraction wavelength with incident illumination. For lines 1 and 2 the shift is limited by the photon flux. Lines 3 and 4 indicate the time course of changes which occur in the dark.

This PCCA functions as a novel recordable and erasable memory device. Light absorption actuates the diffraction shift, which is read out at wavelengths which are not absorbed. This information is erased by exciting the photonic crystal with 488 nm visible light. The size of a pixel can be as small as ~1 μm, the smallest region which can give rise to a narrow diffraction band. If the diffraction shift is increased, this material could act as a display device. The response of the material is rather slow, and is limited by the collective diffusion time of the hydrogel polymer and the required flow of water into and out of the hydrogel. However, reading this device is limited only by the speed with which the material can be scanned by a laser beam. This is the first example of direct photochemical control of the wavelength of photonic crystal diffraction. However, other approaches have utilized photons to control the diffraction efficiency.[6,27-29]

3.3. REFERENCES

1. Ozin, G. A.; Yang, S. M. *Adv. Func. Mat*. **2001**, *11*, 95.

2. Jiang, P.; Ostojic, G. N.; Narat, R.; Mittleman, D.; Colvin, V. L. *Adv. Mat.* **2001**, *13*, 389.

3. Goldenberg, J. M.; Wagner, J.; Stumpe, J.; Paulke, B.-R.; Gornitz, E. *Physica E*, **2003**, *17*, 433.

4. Rogach, A. L.; Kotov, N. A.; Koktysh, D. S.; Ostrander, J. W.; Ragoisha, G. A. *Chem. Mater.* **2000**, *12*, 2721.

5. Meseguer, F.; Blanco, A.; Migues, H.; Garcia-Santamaria, F.; Ibisate, M.; Lopes, C. *Colloids and Surfaces A*, **2002**, *202*, 281.

6. Kubo, S.; Gu, Z.; Takahashi, K.; Ohko, Y.; Sato, O.; Fujishima, A. *J. Am. Chem. Soc.* **2002**, *124*, 10950.

7. Joannopoulos, J. D.; Meade, R. D.; Winn, J. N. *"Photonic Crystals: Molding the Flow of Light"* (Princeton University Press, New York, **1995**).

8. a) Asher, S.A. *U.S. Patents 4,627,689 and 4,632,517*, **1986**. b) Carlson, R. J.; Asher, S. A. *Applied Spectroscopy*, **1984**, *38*, 3. c) Asher, S. A.; Flaugh, P. L.; Washinger, G. *Spectroscopy*, **1986**, *1*, 12, 26.

9. a) Asher, S. A.; Holtz, J.; Liu, L.; Wu, Z. *J. Am. Chem. Soc.,* **1994**, *116*, 4997. b) Asher, S. A.; Jagannathan, S. *U.S. Patent 5,281,370*, **1994**. c) Haacke, G.; Panzer, H. P.; Magliocco, L. G.; Asher, S. A. *U.S. Patent 5,266,238,* **1993**.

10. a) Li, Y.; Tanaka, T. *Annu. Rev. Mat. Sci.* **1992**, *22*, 243. b) Osada, Y.; Gong, J. *Prog. Polym. Sci.* **1993**, *18*, 187.

11. a) Irie, M. *Adv. Poly. Sci.* **1993**, *110*, 49. b) Harmon, M. E.; Kuckling, D.; Frank, C. W. *Macromolecules.* **2003**, *36*, 162. c) Kang, M.-S.; Gupta, V. K.; *J. Phys. Chem. B,* **2002**, *106*, 4127.

12. Holtz, J. H.; Asher, S. A. *Nature*, **1997**, *389*, 829.

13. Weissman, J. M.; Sunkara, H. B.; Tse, A. S.; Asher, S.A. *Science*, **1996**, *274,* 959.

14. Lee, K.; Asher, S. A. *J. Am. Chem. Soc.*, **2000**, 122, 9534.

15. Kamenjicki, M.; Lednev, I.; Mikhonin, A.; Kasavamoorthy, R.; Asher, S. A. *Adv. Func. Mat.* **2003**, *13*, 774.

16. Paul, S.; Ranby, B. *J. Polym. Sci., Polym. Chem. Ed.*, **1976**, *14,* 2449.

17. Hild, G.; Lamps, J. P.; Rempp, P. *Polymer*, **1993**, *34,* 2875.

18. Iwakura, Y.; Kurosaki, T.; Ariga, N.; Ito, T. *Makromol. Chem.,* **1966**, *97,* 128.

19. Fitch, R. M. *Polymer Colloids: A Comprehensive Introduction*, Academic Press, San Diego, **1997**.

20. Hermanson, G. T. *Bioconjugate Techniques*, Academic Press, **1996**.

21. Pan, G.; Tse, A. S.; Kasavamoorthy, R.; Asher, S. A. *J. Am. Chem. Soc.,* **1998**, *120*, 6518.

22. Lednev, I. K.; Ye, Y.-Q.; Hester, R. E.; Moore, J. N. *J. Phys. Chem.,* **1996**, *100*, 13338.

23. Lednev, I. K.; Ye, Y.-Q.; Matousek, P.; Towrie, M.; Foggi, P.; Neuwahl, F. V. R.; Umapathy, S.; Hester, R. E.; Moore, J. N. *Chem. Phys. Lett,* **1998**, *290*, 68.

24. Rau, H. *Angew. Chem. Internat. Edit.* **1973**, *12*, 224.

25. Griffiths, J. *Colour and Constitution of Organic Molecules*, Academic Press, **1976**.

26. Crano, J. C.; Guglielmetti, R. J. *Organic Photochromic and Thermochromic Compounds*, Plenum Press, **1999**.

27. Weissman, J. M.; Sunkara, H. B.; Tse, A. S.; Asher, S. A. *Science* **1996**, *274*, 959.

28. Reese, C.; Mikhonin, A.; Kamenjicki, M.; Tikhonov, A.; Asher, S. A. *J. Am. Chem. Soc.* **2004**, *126*, 1493.

29. a) Kesavamoorthy, R.; Super, M. S.; Asher, S. A. *J. Appl. Phys.* **1992**, *71*, 1116. b) Asher, S. A.; Kesavamoorthy, R.; Jagannathan, S.; Rundquist, P. *Nonlinear Optics III*, **1992**, *1626*, 238. c) Pan, G.; Kesavamoorthy, R.; Asher, S. A. *Phys. Rev. Lett.* **1997**, *78*, 3860. d) Pan, G.; Tse, A. S.; Kesavamoorthy, R.; Asher, S. A. *J. Am. Chem. Soc*. **1998**, *120*, 6518. e) Pan, G.; Kesavamoorthy, R.; Asher, S. A. *J. Am. Chem. Soc.* **1998**, 120, 6525.

Chapter 4

Photochemically Controlled Photonic Crystals

This chapter was published in *Advanced Functional Materials*, **2003**, 13, No.13, 774. The co-authors are Igor K. Lednev, Alexander Mikhonin, Rasu Kesavamoorthy and Sanford A. Asher;

4. PHOTOCHEMICALLY CONTROLLED PHOTONIC CRYSTALS

4.1. ABSTRACT

We have developed photochemically controlled photonic crystals which may be useful in novel recordable and erasable memory and/or display devices. These materials can operate in the UV, visible or near IR spectral regions. Information is recorded and erased by exciting the photonic crystal with UV light or visible light. The information recorded is read out by measuring the photonic crystal diffraction wavelength. The active element of the device is an azobenzene-functionalized hydrogel, which contains an embedded crystalline colloidal array. UV excitation forms cis-azobenzene while visible excitation forms trans-azobenzene. The more favorable free energy of mixing of cis-azobenzene causes the hydrogel to swell and to red-shift the photonic crystal diffraction. We also observe fast ns, μs and ms transient dynamics associated with fast heating lattice constant changes, refractive index changes and thermal relaxations.

4.2. INTRODUCTION

The recent intense interest in photonic bandgap crystals stems from their potential ability to increase light waveguiding efficiency, to increase the efficiency of stimulated emission processes, and to localize light.[1] Numerous groups around the world are developing fabrication methods to produce photonic crystals with bandgaps in the visible, infrared and microwave spectral regions.[2]

The simplest photonic crystal can be fabricated by the close-packing of spheres, similar to that which in nature forms opals.[3] The earliest chemical approach fabricated large face centered cubic (fcc) photonic bandgap crystals through the self-assembly of highly charged, monodisperse colloidal particles into crystalline colloidal arrays (CCAs). The CCAs self-assemble due to long-range electrostatic repulsions between particles.[4]

These CCAs are complex fluids consisting of colloidal particles which self- assemble into plastic fcc crystalline arrays which Bragg-diffract ultraviolet, visible or near-infrared light, depending on the colloidal particle array spacings. More recently, robust semi-solid photonic crystal (PCCA) materials were fabricated by polymerizing a hydrogel network around the self-assembled CCA array[5] (Figure 1). This new photonic crystal material can utilize environmentally responsive hydrogels[6] to create a PCCA in which thermal or chemical environmental alterations results in PCCA volume change, thereby altering the CCA photonic crystal plane spacings and diffraction wavelengths.[7-11]

We report here the development of a photochemically actuated PCCA (120 nm diameter polystyrene CCA), where photoisomerization of a covalently attached chromophore changes the hydrogel free energy of mixing. The resulting photocontrolled PCCA (PCPCCA) volume change alters the lattice constant and shifts the diffracted wavelength. Thus, we have a material

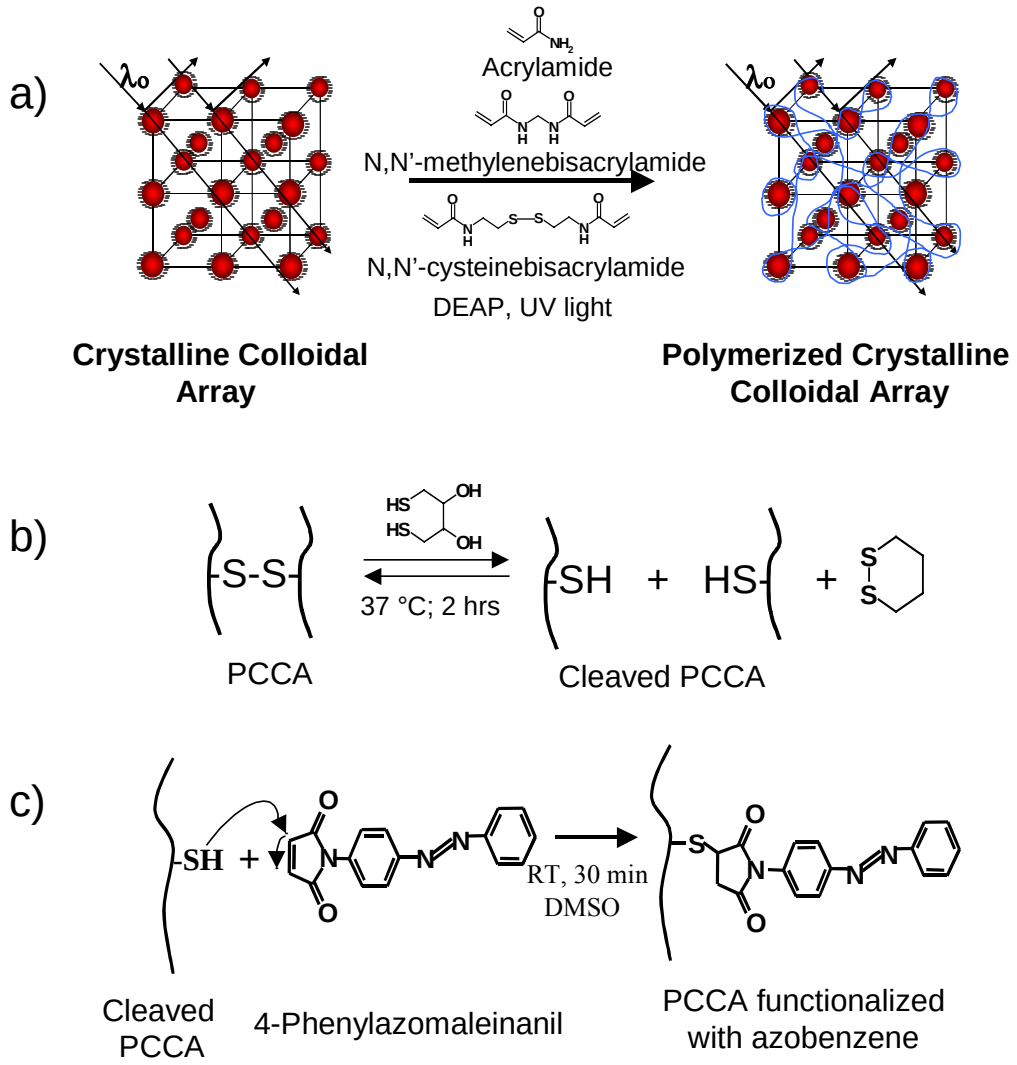

Figure 4.1. a) Synthesis of the PCCA-containing disulfide bonds. b) Cleaving disulfide bonds with dithiolthreitol (DTT). c) Maleimide-thiol attachment of azobenzene to PCCA.

in which we modulate the diffracted light by the independent absorption of light outside the diffraction bandgap.

4.3. EXPERIMENTAL

The highly sulfonated, 120 nm diameter monodisperse colloidal particles were prepared by emulsion polymerization.[12] After dialyzing against water for one week, these particles readily self-assemble into highly ordered CCA. N,N'-cystaminebisacrylamide (5 mg; Aldrich) dissolved in 20 μl dimethylsulfoxide (DMSO) was added to 4 mg of a solution of 10 % diethoxyacetophenone (DEAP, Aldrich, v/v) in DMSO. The PCCA were prepared by adding this solution to a solution containing 50 mg acrylamide (Sigma), 3 mg N,N'-methylenebisacrylamide (Sigma), and 1 g of a 10 wt% dispersion of diffracting polystyrene CCA (Figure 1a). This solution was injected into a cell made of two quartz plates separated by a 76 μm thick spacer and exposed to UV light (Black-Ray model B-100A, UVP Inc.). After 30 min illumination, the cell was opened and the gel was washed with water. The PCCA remained attached to one of the quartz plates.

Dithiolthreitol (DTT, ACROS Organics) was used to cleave the PCCA disulfide bonds (Figure 1b), which leaves reactive thiol groups attached to the PCCA.[13,14] The PCCA diffraction red-shifts upon cleavage of these disulfide bond crosslinks due to the resulting decrease in the PCCA elastic constant.

The medium within the cleaved PCCA was slowly exchanged with pure DMSO; the PCCA diffraction efficiency decreased due to the smaller refractive index difference between the polystyrene colloids (n = 1.60) and the DMSO (n = 1.47) containing medium, compared to that of water (n = 1.33). The PCCA volume decreased somewhat, due to the decrease in the free energy of mixing between the PCCA and DMSO, compared to water.

The PCCA was incubated under stirring for ~2 hours with a solution of 4-phenylazomaleinanil (Polysciences, Inc) (Fig. 1c) in DMSO (7 mM). Figure 2 compares the absorption spectrum of the PCCA before and after attachment of the azobenzene derivative. In the absence of azobenzene the PCCA shows diffraction from the fcc (111) planes at ~540 nm. Below 300 nm, the spectrum also shows contributions from higher order diffraction, as well as from the polystyrene colloid particle absorption.

In contrast, the PCCA containing covalently attached azobenzene additionally shows the trans azobenzene 322 nm absorption band. We can vary the amount of attached azobenzene by controlling the sulfhydryl group concentration within the PCCA.

4.4. RESULTS AND DISCUSSION

4.4.1. Photochemistry of 4-phenylazomaleinanil solution

Azobenzene derivatives, normally in their ground state trans forms at room temperature in the dark,[15-20] show strong $\pi \rightarrow \pi^*$ absorption bands at ~340 nm (Figure 3). 4-phenylazomaleinanil shows the typical azobenzene photochemistry, where irradiation with 365 nm UV light bleaches the strong ~340 nm trans $\pi \rightarrow \pi^*$ UV absorption band as it converts trans- azobenzene to the cis form. A weaker cis $n \rightarrow \pi^*$ absorption band at ~435 nm (Figure 3a) appears. Figure 3a shows that irradiation of a DMSO solution of 4-phenylazomaleinanil by ~13 mW/cm^2 of 365 nm UV light from a mercury lamp gives rise to a photostationary state within 2 min. This is expected from the ~20 s observed bleaching time of the ~ 340 nm trans band of the 4-phenylazomaleinanil DMSO solution (Figure 3a inset). Subsequent irradiation with white light (~3 mW/cm^2, 488 nm from an Ar^+ laser) photoconverts the cis form back to the trans form, as evident by the restored ~340 nm trans

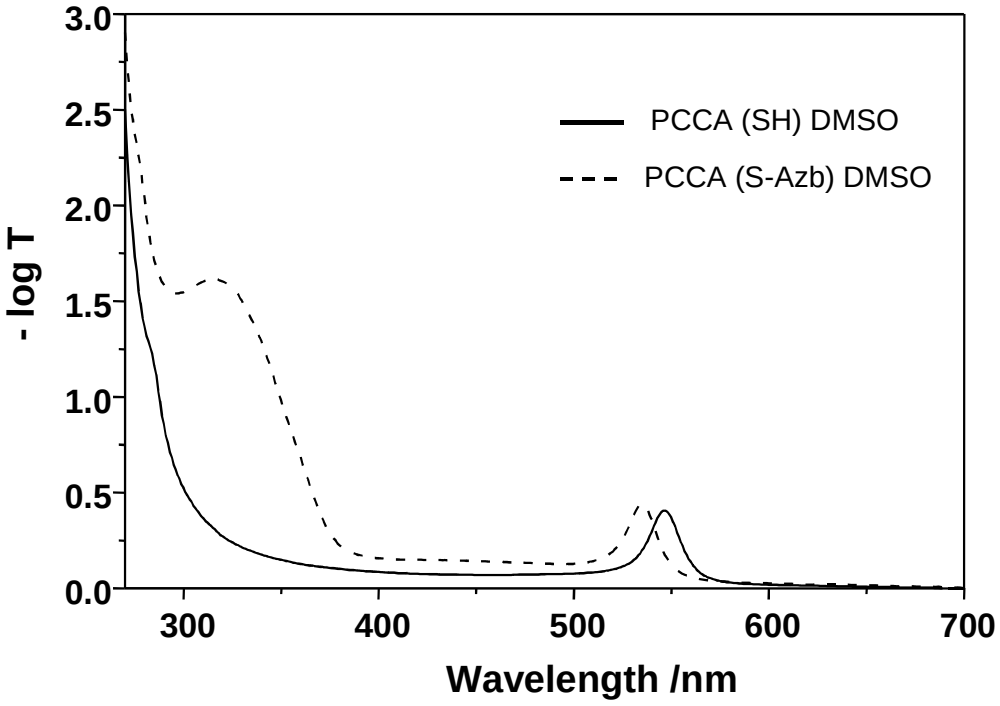

Figure 4.2. Absorption spectra of 76 μm thick PCCA before and after attachment of a 4-phenylazomaleinanil.

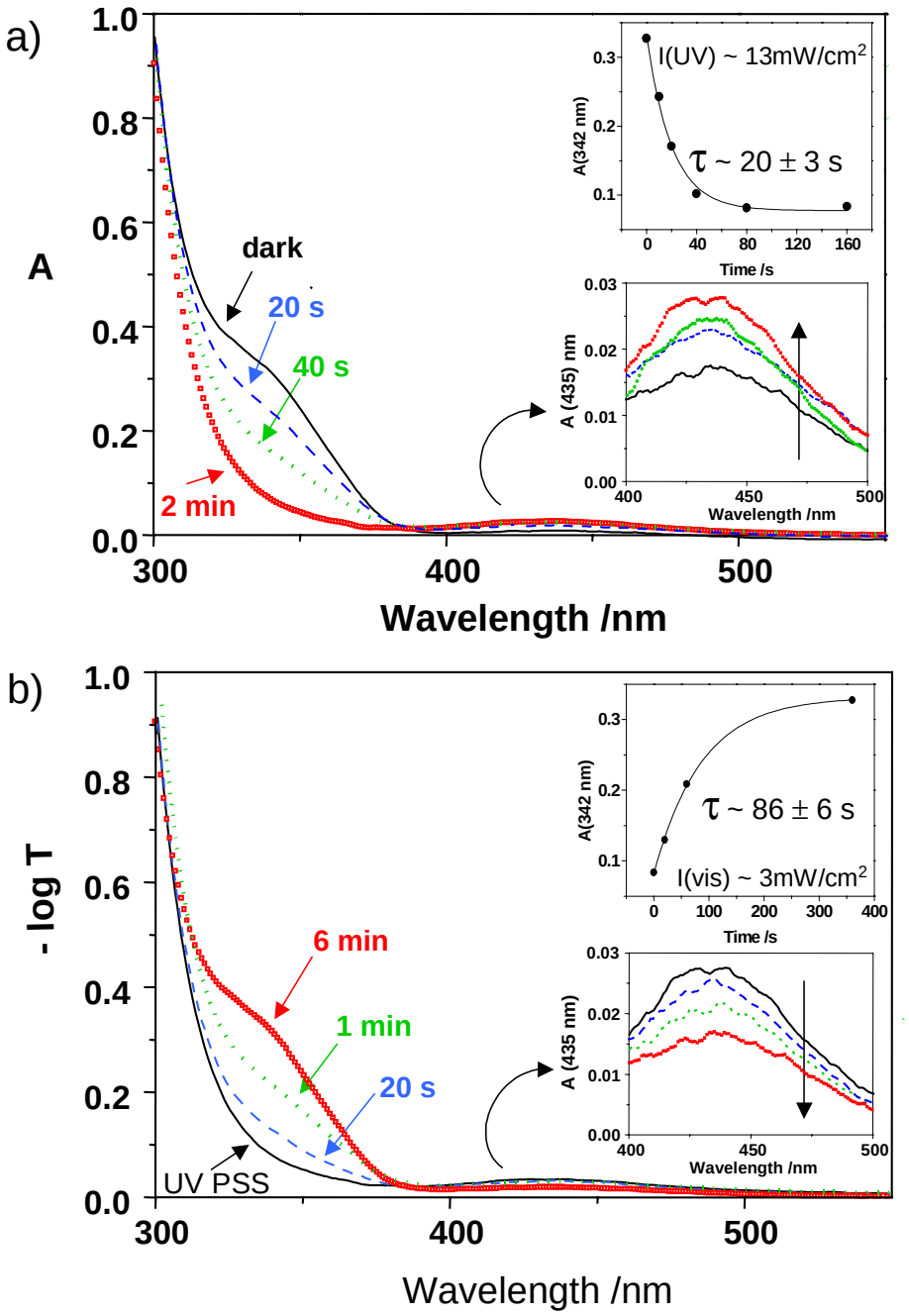

Figure 4.3. Photochemistry of 60 μM 4-phenylazomaleinanil in DMSO in a 1 mm quartz cuvette. a) Absorption changes upon irradiation with 13 mW/cm^2 of 365 nm light. b) Absorption changes upon irradiation with 3 mW/cm^2 of white light. The UV PSS curve shows the photostationary state absorption reached with UV light excitation.

$\pi \rightarrow \pi^*$ absorption (Figure 3b). The Figure 3b inset indicates a ~86 s characteristic time for photoisomerization back to the trans form.

We have estimated that the trans to cis quantum yield, Φ, is ~ 0.07 for our 4-phenylazomaleinanil in isooctane for 355 nm excitation. This quantum yield is comparable to that of azobenzene in isooctane (Φ ~ 0.12).[21-25] In addition, we observe that 4-phenylazomaleinanil dissolved in DMSO (4.5 mM) shows very similar kinetics to 4.5 mM 4-phenylazomaleinanil attached to a PCCA, which also indicates similar quantum yields.

4.4.2. Photophysics of PCCA functionalized with azobenzene

Figure 4 shows the absorption spectrum of a PCCA containing covalently attached azobenzene (PCPCCA). The PCPCCA photochemistry observed is essentially identical to that of 4-phenylazomaleinanil in DMSO. Excitation with 365 nm UV light (~13 mW/cm^2) results in a decrease in the 322 nm ($\pi \rightarrow \pi^*$) trans absorption and an increase in the 430 nm ($n \rightarrow \pi^*$) cis absorption, due to the photoconversion of the trans to cis form (the absorption shifts to 322 nm upon attachment to the PCCA).

The PCCA was oriented such that the beam was incident normal to the fcc (111) planes, which at this normal incidence diffracts ~530 nm light. The conversion of trans-azobenzene to the cis form causes the (111) plane diffraction to shift from ~530 nm to ~580 nm. Excitation with visible light (~3 mW/cm^2) shifts the diffraction back to ~530 nm.

The diffraction red-shift is due to an increase in the free energy of mixing of the hydrogel polymer network with the medium upon UV light illumination, while the blue-shift results from a decrease in the free energy of mixing upon return of the azobenzene to its trans form.

This photochemically driven diffraction change is reversible as shown in Figure 5, which shows a sample cycled numerous times by UV and visible excitation. Irradiation of a cycled

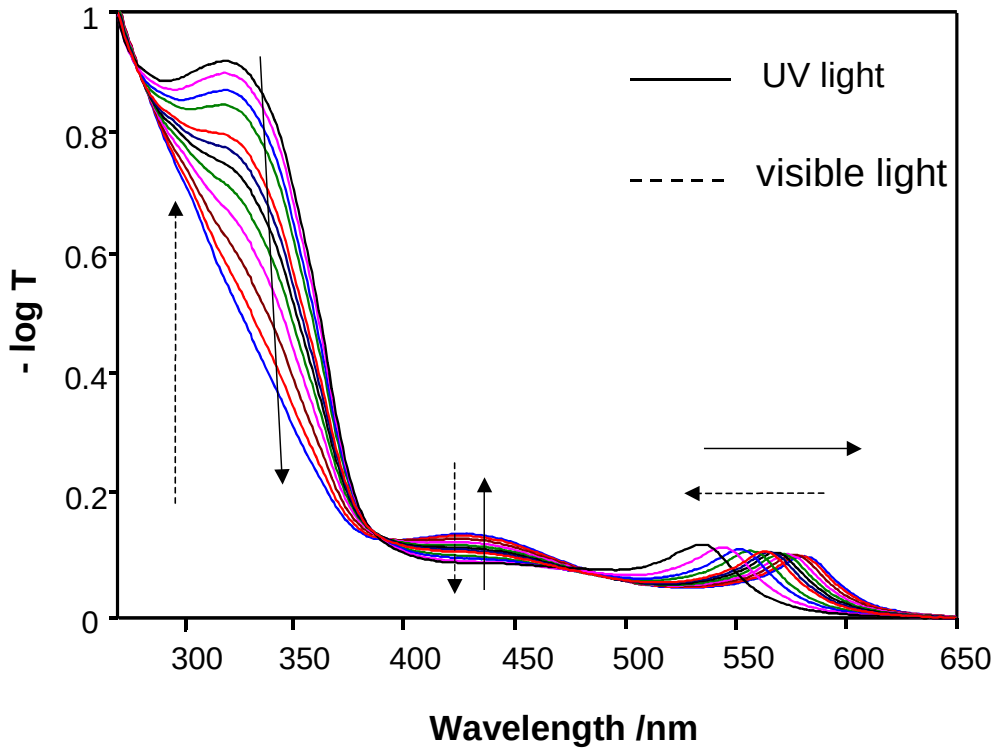

Figure 4.4. 38 μm thick PCCA functionalized with 4-phenylazomaleinanil (3 mM) shows a 50 nm diffraction red-shift upon UV excitation. Solid arrows show spectral changes due to the UV irradiation, while the dashed arrows show changes due to visible light illumination. The 530 to 580 nm peak derives from diffraction by the PCCA fcc (111) planes. The (111) plane spacing, $d_{111} = \lambda_0/2n$ for light at normal incidence.

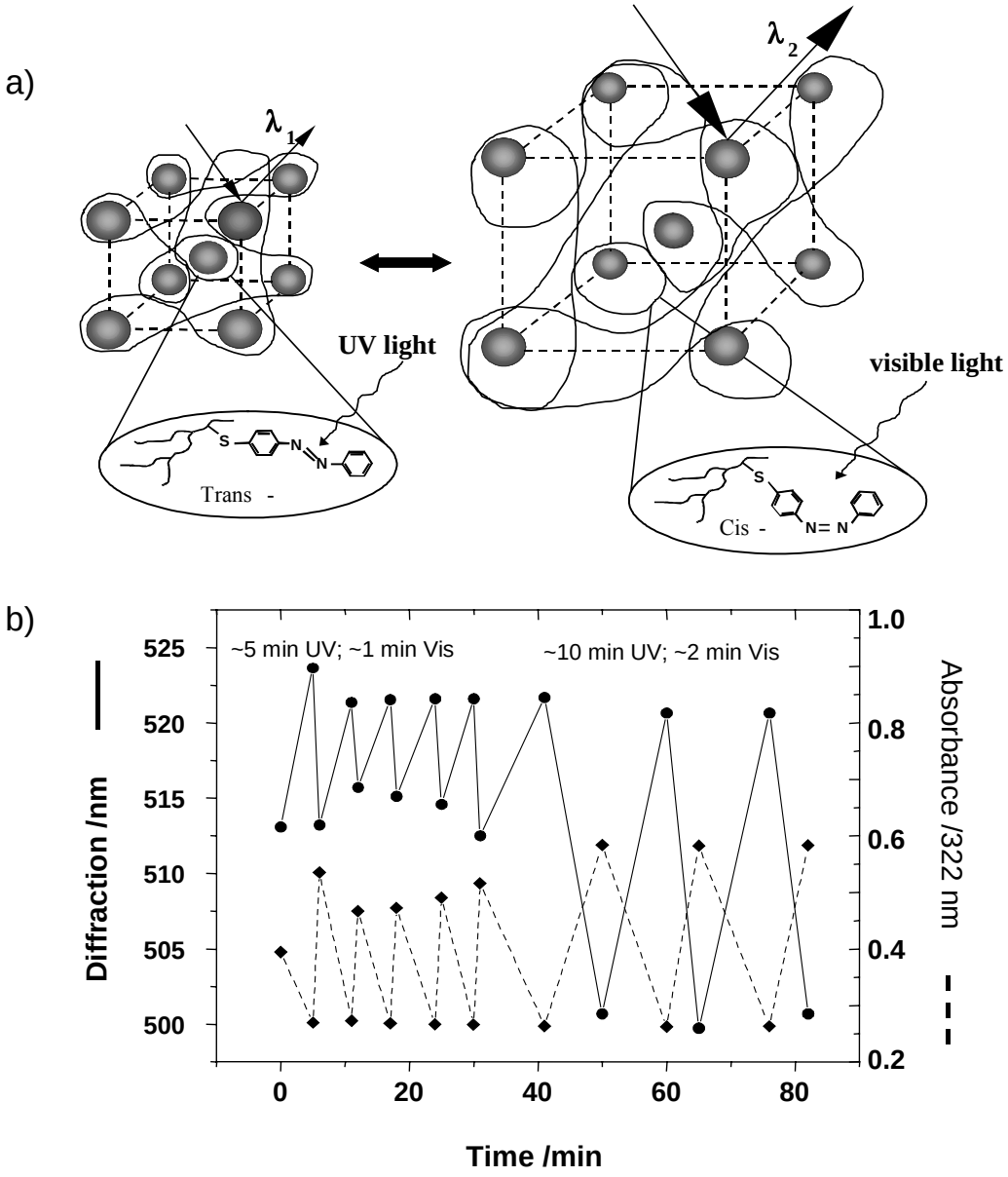

Figure 4.5. a) UV light photoisomerizes the trans to the cis derivative, while visible light photoisomerizes the cis to the trans form. b) Reversible photochemistry: UV light red-shifts the diffraction and bleaches the trans 322 nm absorption, while subsequent excitation with visible light blue-shifts the diffraction and increases the 322 nm absorption.

PCPCCA (where the fcc (111) plane diffracts at ~513 nm) for 5 min with ~10 mW/cm^2 UV light causes a ~0.2 absorbance decrease at ~322 nm and a ~8 nm diffraction red-shift, which is completely reversed by a 1 min illumination with ~50 mW/cm^2 visible light. Doubling the UV illumination time decreases the 322 nm trans absorption by ~0.4 and causes the diffraction shift to double. The ~520 nm maximum diffraction value occurs in a sample which was converted to the trans form and which shows a maximum trans photobleach. The PCPCCA absorption and diffraction can be cycled back and forth indefinitely.

Thermal cis → trans relaxation in the dark gradually blue-shifts the diffraction (Figure 6a) as the azobenzene relaxes to its thermodynamically more stable trans state, restoring the 322 nm trans absorption (Figure 6b). This dark relaxation is very slow (~83 hours at 27 °C) compared to the observed photoisomerization rates.

In our study we determined the activation energy for the ground state cis-trans isomerization by measuring the thermal relaxation for the cis-trans process in dark at different temperatures. Characteristic times were determined for seven different temperatures, from which we calculated an activation energy of ~28 KCal/mol for the ground state cis-trans isomerization of the 4-phenylazomaleinanil functionalized PCCA (Table 1).

The magnitude of the diffraction shift photoresponse increases monotonically with increasing azobenzene concentration (Figure 7) due to the resulting increased free energy of mixing. As expected, the photoresponse decreases as the hydrogel crosslinking density increases, due to the resulting increased elastic constants of the PCCA. No photoresponse occurs for >10 % concentrations of N,N'-methylenebisacrylamide relative to acrylamide (Figure 8). The crosslink concentrations displayed are those expected for the stoichiometric incorporation of

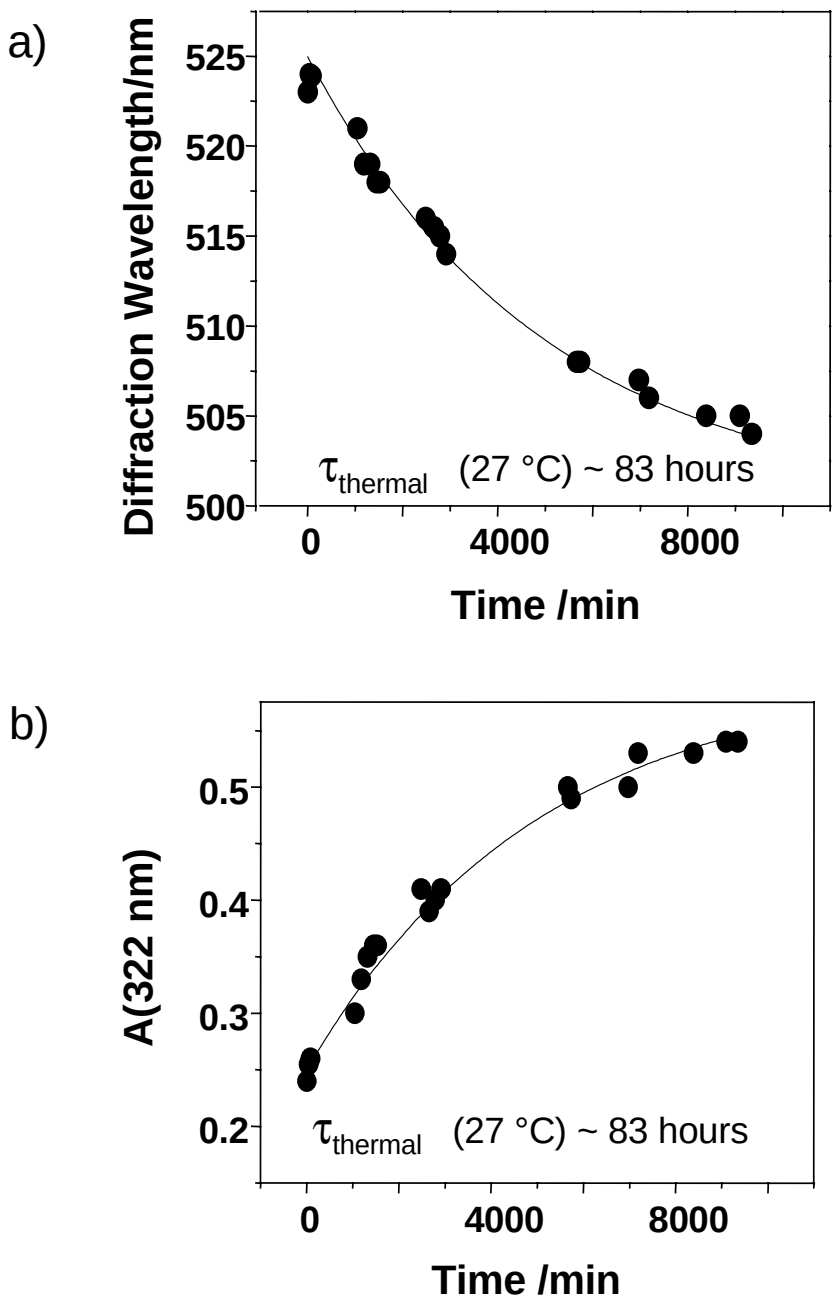

Figure 4.6. Thermal isomerization of azobenzene attached to a PCCA at 27 °C in the dark. a) Diffraction wavelength and b) 322 nm absorption changes.

Table 4.1. Temperature dependence of the PCPCCA - dark thermal relaxation.

Temp (°C)	τ (hrs)
27	83
28	64
35	28
36	23
42	13
49	3
56	1.4

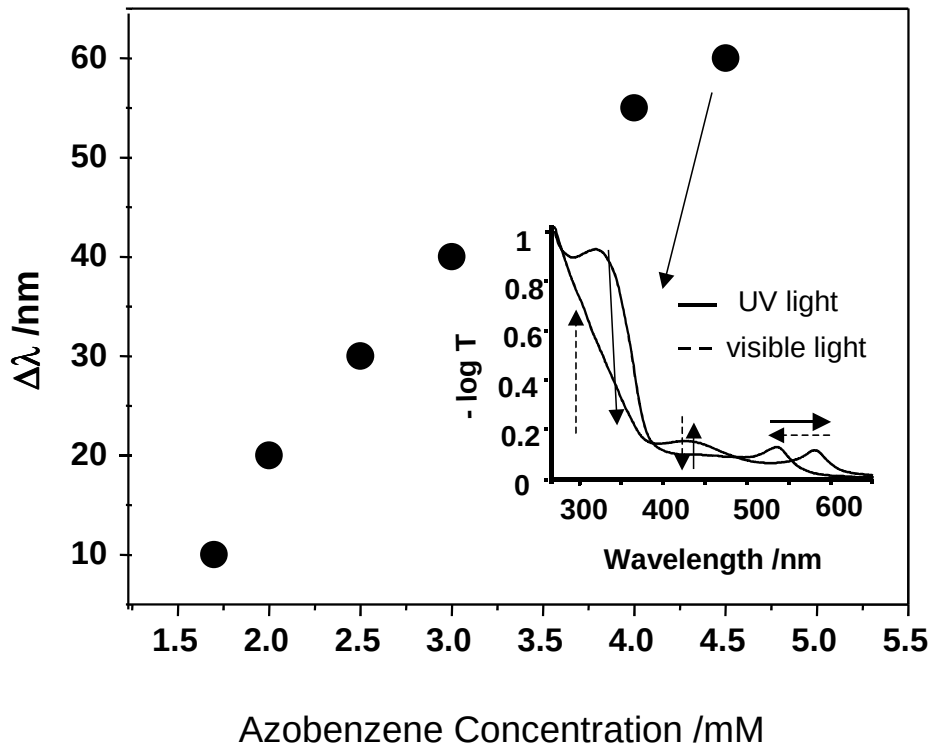

Figure 4.7. Dependence of photoresponse on 4-phenylazomaleinanil concentration (in DMSO medium). Inset shows the absorption spectrum of a PCPCCA containing 4.5 mM of 4-phenylazomaleinanil.

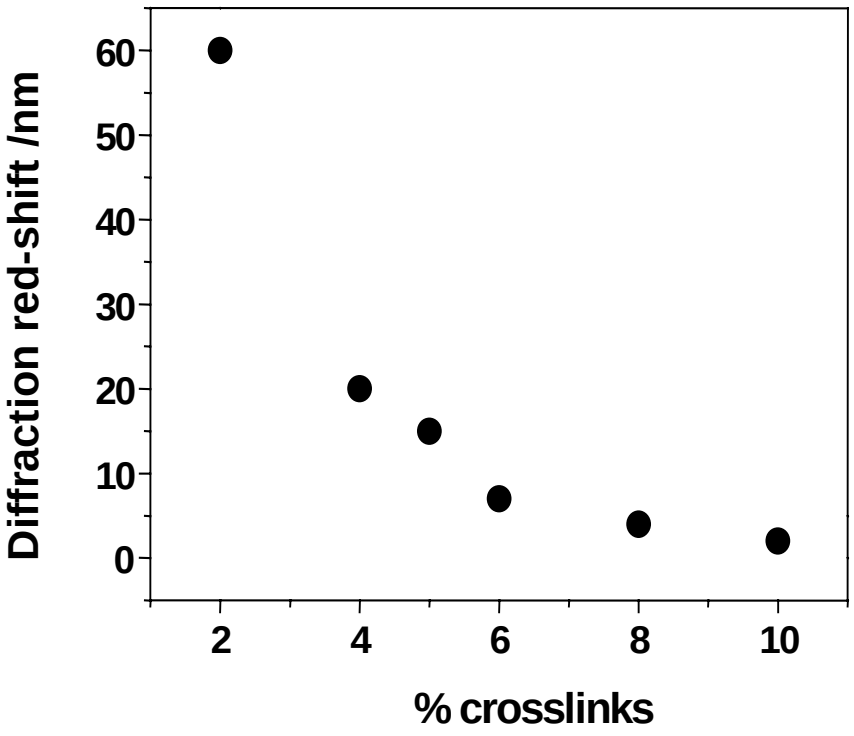

Figure 4.8. Dependence of diffraction shift on the crosslink concentration (N,N'-methylenebisacrylamide relative to acrylamide). We expect a much smaller actual crosslink density.[8] The gel thickness is 76 μm and contains 4.5 mM azobenzene.

N,N'-methylenebisacrylamide as PCCA crosslinks, assuming that all of the N,N'-cystaminebisacrylamide disulfide bonds are broken. However, it should be noted that the effective crosslink concentration is usually found to be significantly below this stoichiometric concentration; Lee and Asher[8] demonstrated that only a small fraction of the N,N'-methylenebiscrylamide crosslinker forms effective hydrogel crosslinks.

4.4.3. Diffraction Kinetics

The response time of the PCPCCA diffraction shift can be limited by the incident power, the photolysis rates and the collective diffusion constant of the hydrogel polymer network. Our diffraction shifts can be actuated by a single ns laser pulse. Figure 9a shows that a single 0.4 mJ/cm^2, 3 ns, 355 nm pulse from a YAG laser actuates a trans bleach and causes a ~7 nm diffraction red-shift for a PCPCCA which normally diffracts at ~440 nm.

The response of the sample is additive; three 355 nm pulses cause ~3 times the red-shift (Figure 9a). As shown in Figure 9b, we can achieve the same red-shift with one 1.2 mJ/cm^2 pulse. The response can be erased with visible light, and it is completely reversible over an indefinite number of cycles.

We examined the kinetics of the diffraction changes by monitoring changes in the transmission spectrum of the sample after applying one 355 nm YAG pulse (1.2 mJ/cm^2, 3 ns duration). We used a 120 ns pulsed Xe flashlamp (IBH Model 5000XeF) and an Ocean Optics USB2000 Miniature Fiber Optic Spectrometer (Figure 10) to record spectra after time delays of 0.3 μs to 6 ms, and 3 s to 2 min subsequent to UV pulses. As an example, Figure 11a shows spectra recorded before (black) and at various times (0.3 μs – 6000 μs) after excitation (red) by a 3 ns 355 nm pulse. The final state of the sample was recorded 1 min after this UV pulse (blue).

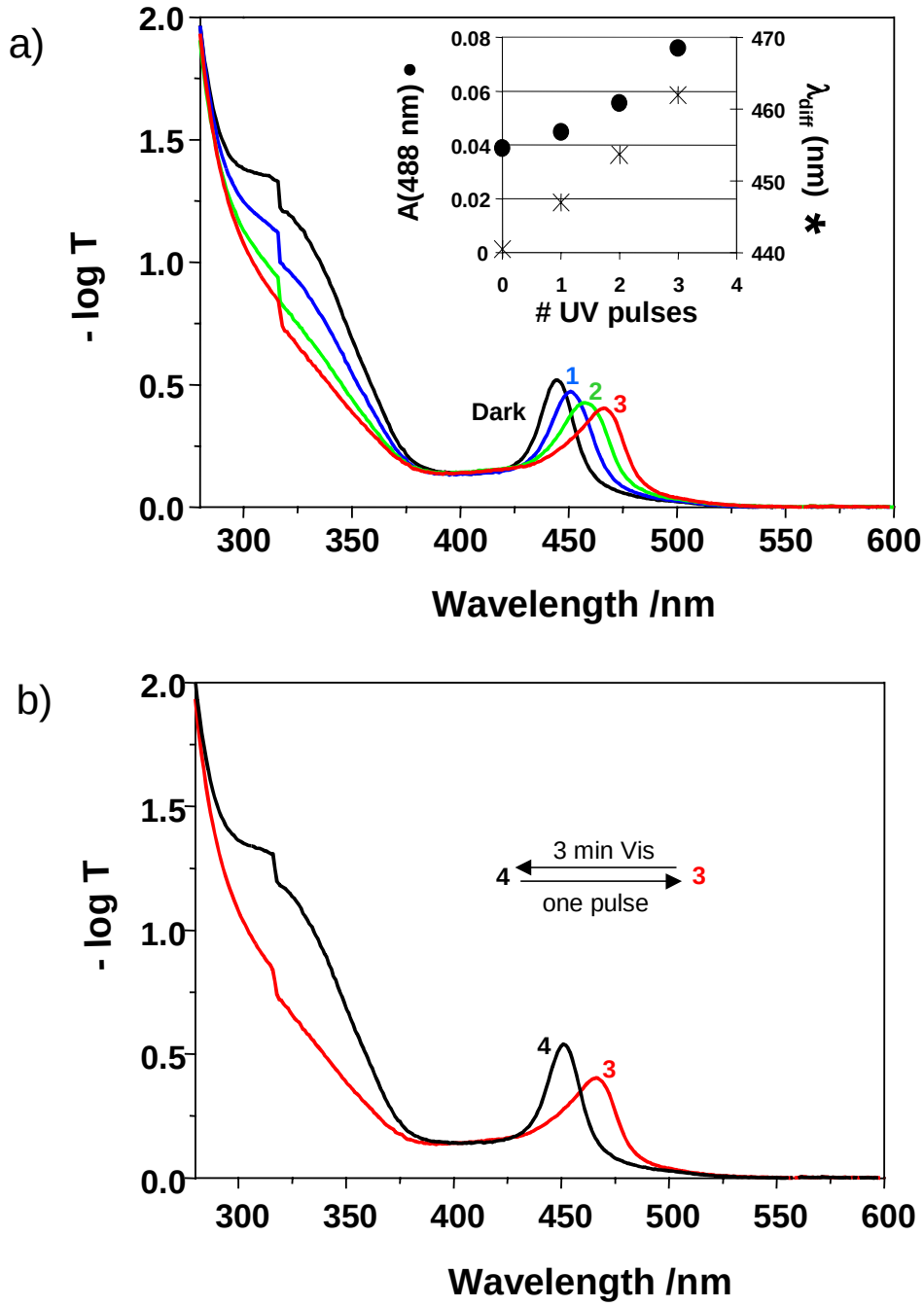

Figure 4.9. a) Extinction changes induced in PCPCCA by three laser pulses (355 nm, 0.4 J/cm^2). b) System returns back to the original state after 3 min of ~50 mJ/cm^2 visible irradiation (3 to 4). One 1.2 J/cm^2 355 nm laser pulse induces a 14 nm diffraction red-shift (4 to 3).

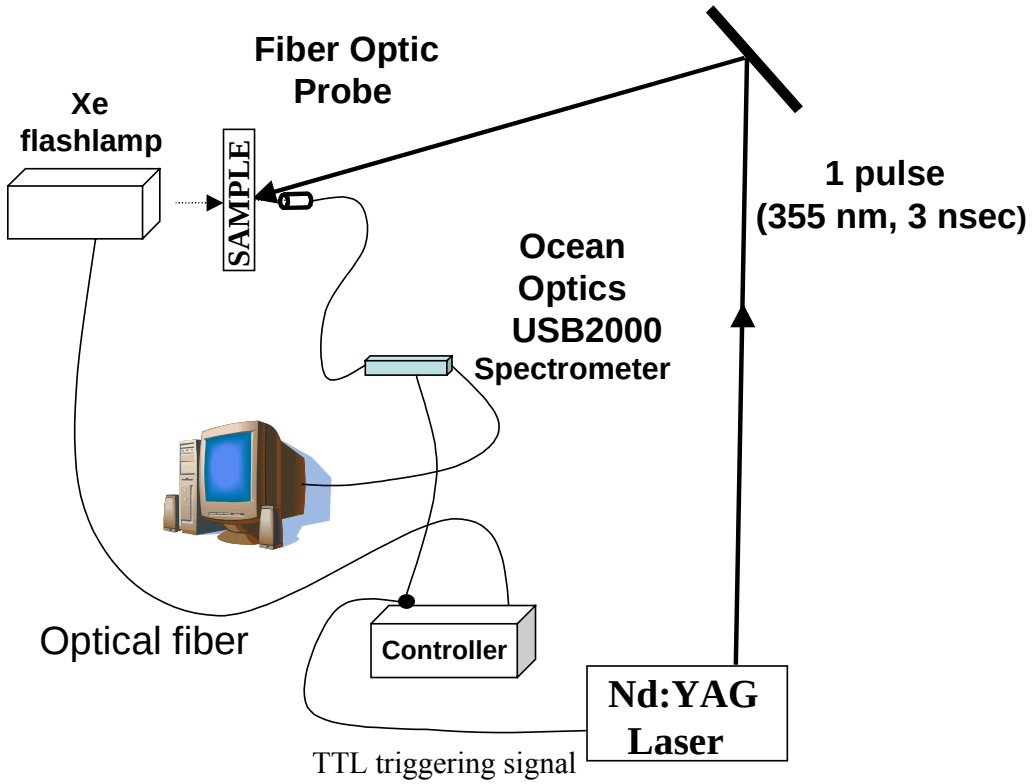

Figure 4.10. Transient absorption spectrophotometer used to measure PCPCCA spectral kinetic responses to 355 nm light.

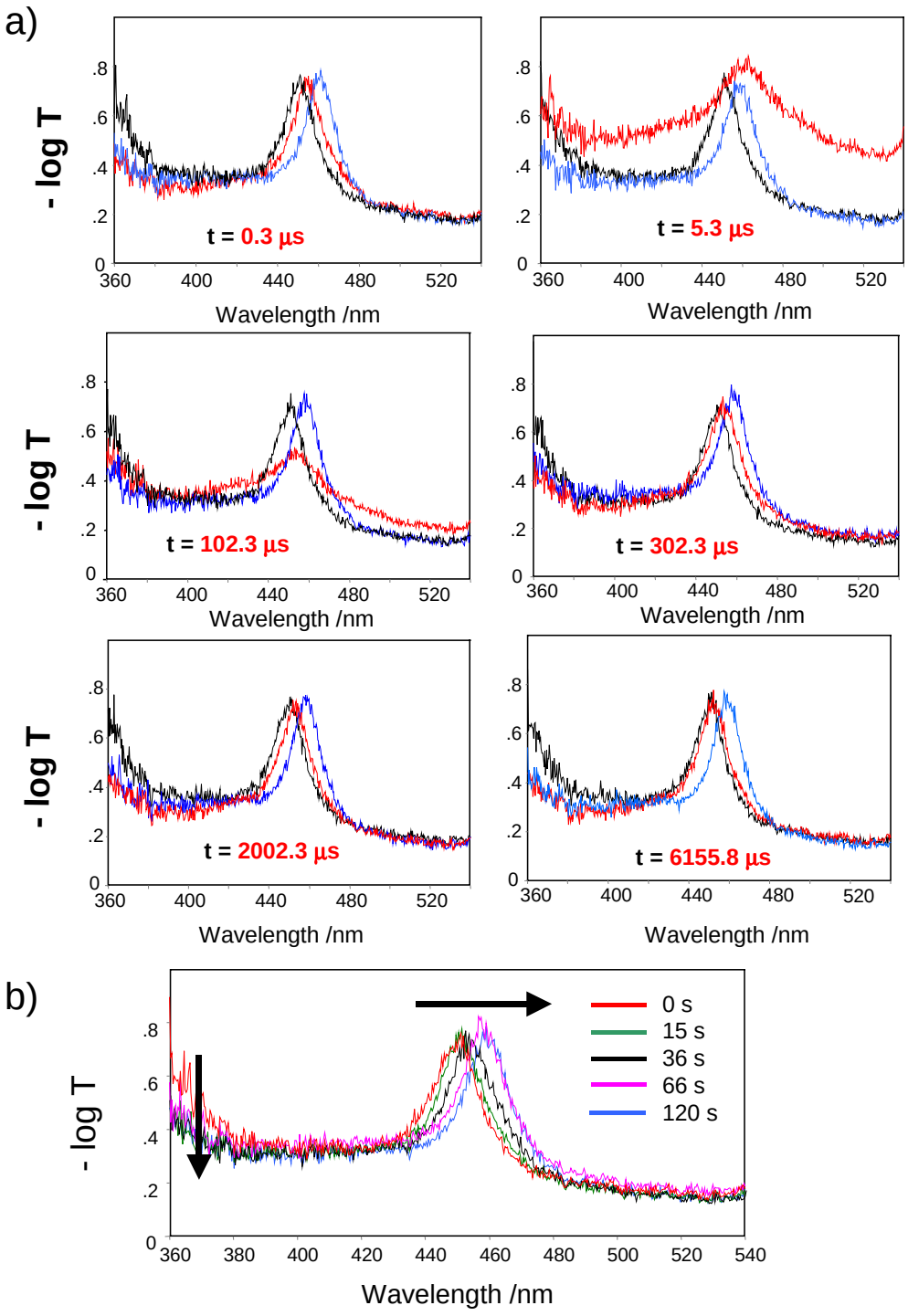

Figure 4.11. a) PCPCCA in dark (black), at the indicated time subsequent to excitation by one 3 ns 355 nm pulse (red), and after 1 min (blue). b) Absorption spectral changes in second time regime.

In addition, Figure 12 graphically shows the time dependence of the diffraction maximum wavelength in the slow sec timescale.

A diffraction red-shift of ~5 nm occurs within 300 ns, and the diffraction peak remains sharp and symmetric. At 1.3 μs we see more complex dynamics where the background increases and the diffraction broadens. The diffraction continues to red-shift until ~12 μs. By 100 μs the diffraction begins to narrow and the diffraction band blue-shifts. At 302 μs only a small diffraction red-shift remains; the diffraction spectrum is close to that prior to the UV pulse.

Much larger diffraction changes (~10 nm) occur at much longer times (~30 s, Figures 11b, 12). The fact that the 365 nm absorption remains bleached demonstrates that this slow process does not involve azobenzene trans to cis ground-state photochemistry. This slow time scale is typically observed[9] for macroscopic volume phase transitions of 3 cm X 3 cm X 76 μm photonic crystals in response to changes in the free energy of mixing or changes in the Donnan potential. This process is delayed by the polymer collective diffusion constant and by the necessity of mass flow in order for the DMSO solvent outside the hydrogel to flow into the swelling polymer.[26] Thus, this slow diffraction shift results from a hydrogel volume phase transition driven by the change in the free energy of mixing of cis-azobenzene compared to trans-azobenzene.

Clearly, other dynamical phenomena come into play in the shorter time regimes. The prompt (0.3 μs) ~5 nm rigid diffraction band red-shift, which preserves the diffraction peak shape, appears to directly result from heating of the PCCA by the incident UV beam. The PCCA, which is rigidly attached to a quartz surface, is composed mainly of DMSO, which shows a temperature-dependent density change around room temperature of $d\rho/dT = -0.0012$.[27] We calculated that our UV pulse beam essentially instantly induced a 20 °C temperature jump in the

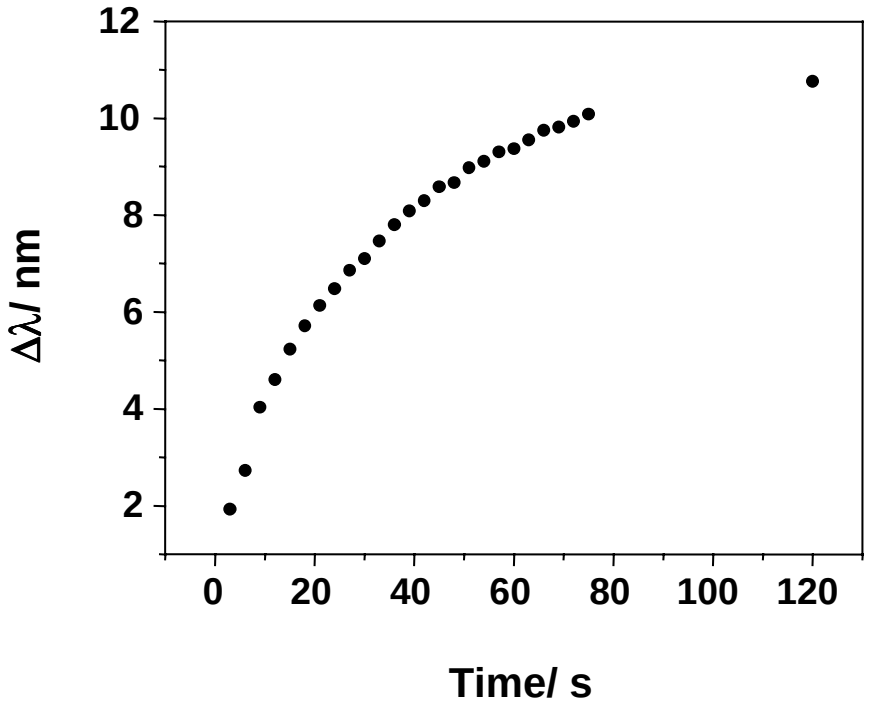

Figure 4.12. Temporal dependence of diffraction peak wavelength after excitation by a 3 ns 355 nm laser pulse.

sample which expands the PCCA volume, increasing d_{111} to red-shift the diffraction. A counteracting diffracted wavelength blue-shift must also accompany the resulting temperature induced refractive index decrease (dn/dT = -0.00035 for DMSO).[27]

In general, we find that the total volume change of a hydrogel is determined by its thermodynamics. The exact diffraction change depends upon whether the hydrogel expansion is constrained. If the hydrogel is unconstrained, the linear dimensional change in any direction d'_{111} / d_{111} is given by $(V'/ V)^{1/3}$. In contrast, for hydrogels attached to a quartz surface, the entire volume change can only occur along the normal to the surface and thus, $d'_{111} / d_{111} = V' / V$. In this case, the 20 °C temperature rise would increase the volume by ~2 %, which would increase d_{111} and the wavelength diffracted by a maximum of 9 nm. In contrast, the 0.007 decrease in n would decrease the diffracted wavelength by 3 nm. The resultant 6 nm estimated shift is very close to the 5 nm shift observed.

This hypothesis of heating as being responsible for this prompt diffraction shift is supported by observations of rapid temperature jump diffraction red-shifts for samples where azobenzene is dissolved in the hydrogel at identical concentrations rather than being attached, and by our observations that the magnitude of the red-shift scales with pulse energy.

The scattering baseline increases and the diffraction band broadens during the 5 to 100 μs time scale after the UV pulse. These phenomena must result from transient disordering within the PCCA. Although our mesoscopically inhomogenous material unevenly absorbs the UV light to give rise to an instantaneous mesoscopic inhomogenous temperature redistribution, the temperature should become uniformly distributed well within 50 ns.[28]

The ~50 μs disorder dynamics must originate from longer scale phenomena in the sample. The PCCA can be thought of as 120 nm slabs containing colloidal particles arrayed

within a hydrogel containing DMSO, separated by ~30 nm slabs of a hydrogel containing DMSO. We excite an internal 2 mm X 2 mm X 76 μm volume element of the PCCA by a UV pulse. This heated volume element must then expand against the adjacent cooler hydrogel, resulting in lateral constraining forces. These compressive restoring forces create an instability in the heated hydrogel.

It is well known that smectic liquid crystals (which have analogous structures) respond to such constraints by having their layers buckle at high strains forming parabolic focal conics.[29,30] Analogous forces in our case will cause the (111) layers to buckle, causing the (111) planes to show a distribution of shallow tilt angles relative to the excitation beam. This causes the diffraction band to broaden. Other defect structures that form will cause additional light scattering.

This constraint decreases as the probed volume thermally reequilibrates on the ~200 μs timescale, restoring the original diffraction peak after 6 ms. In the multisecond time domain, the system undergoes a free energy of mixing change volume phase transition driven by the trans-cis photoisomerization of azobenzene.

This PCPCCA functions as a slow display device, and may be used as a novel recordable and erasable memory material. Light absorption actuates the diffraction shift, which is read out at a wavelength where no absorption occurs. Our photonic crystal material can be addressed and read out in small areas. For example, we should be able to utilize pixels as small as ~1 μm, the smallest region which can give rise to a narrow diffraction band. Reading this device is limited only by the speed with which the material can be scanned or imaged by a laser beam.

4.5. CONCLUSIONS

Diffraction switching in our PCPCCA results from both azobenzene photoisomerization and laser heating. In the fast ns time regime, heating increases the material volume and red-shifts the diffraction. This volume change relaxes in the μs time domain. At longer times the volume of the PCPCCA hydrogel is controlled by the balance between the free energy of mixing of the polymer hydrogel with DMSO and the elastic restoring force of the hydrogel crosslinks. The higher cis-isomer dipole moment results in an increased solubility in DMSO, causing an increase in the free energy of mixing. Thus, the PCPCCA swells and a diffraction red-shift is observed. To our knowledge, this is the first example of the photochemical control of a photonic crystal.

4.6. REFERENCES

1. Joannopoulos, J. D.; Meade, R. D.; Winn, J. N. *Photonic Crystals: Molding the Flow of Light* (Princeton University Press, New York) **1995**.

2. a) Krauss, T. F.; De La Rue, R. M., *Prog. Quant. Elect.* **1999**, *23*, 51. b) Ozin, G. A.; Yang, S. M. *Adv. Func. Mat.* **2001**, *11*, 95. c) Jiang, P.; Ostojic, G. N.; Narat, R.; Mittleman, D.; Colvin, V. L. *Adv. Mat.* **2001**, *13*, 389. d) Norris, D. J.; Vlasov, Y. A. *Adv. Mat.* **2001**, *13*, 371.

3. a) Pieranski, P. *Contemp. Phys.*, **1983**, *24*, 25. b) Striemer, C. C.; Krishnan, R.; Fauchet, P. M.; Tsybeskov, L.; Xie, Q. *Nano Letters*, **2001**, *1,* 643.

4. a) Asher, S. A.; Flaugh, P. L.; Washinger, G. *Spectroscopy* **1986**, *1*, 26. b) Clark, N. A.; Hurd, A. J.; Ackerson, B. J. *Nature* **1979**, *281*, 57. c) Carlson, R. J.; Asher, S. A.; *Appl. Spectrosc.* **1984**, *38*, 297. d) Reese, C.; Asher, S. A. *J. Colloid and Interface Science* **2002**, *248*, 41. e) Asher, S. A. *US Patents 4,627,689* and *4,632,517*, **1986**.

5. a) Haacke, G.; Panzer, H. P.; Magliocco, L. G.; Asher, S. A. *US Patent 5,266,238*, **1993**. b) Asher, S. A.; Jagannathan, S. *US Patent 5,281,370*, **1994**. c) Asher, S. A.; Holtz, J. H.; Liu, L.; Wu, Z. *J. Am. Chem. Soc.* **1994**, *116*, 4997.

6. a) Irie, M. *Advances in Polymer Science*, **1993**, 110, 49. b) Osada, Y.; Gong, J. *Prog. Polym. Sci.* **1993**, *18*, 187.

7. Weissman, J. M.; Sunkara, H. B.; Tse, A. S.; Asher, S. A. *Science* **1996**, *274*, 959.

8. Lee, K.; Asher, S. A. *J. Am. Chem. Soc.* **2000**, *122*, 9534.

9. Holtz, J. H.; Asher, S. A. *Nature*, **1997**, *389*, 829.

10. Asher, S. A.; Alexeev, V. L.; Goponenko, A. V.; Sharma, A. C.; Lednev, I. K.; Wilcox, C. S.; Finegold, D. N. *J. Am. Chem. Soc*. **2003**, *125,* 3322.

11. Holtz, J. H.; Holtz, J. S. W.; Munro, C. H.; Asher, S. A. *Anal. Chem*. **1998**, *70*, 780.

12. Reese, C. E.; Guerrero, C. D.; Weissman, J. M.; Lee, K.; Asher, S. A. *J. Colloid and Interface Science* **2000**, *232*, 76.

13. Aslam, M.; Dent, A. *Bioconjugation*, Grove's Dictionaries Inc., **1998**.

14. Hermanson, G. T. *Bioconjugate Techniques,* Academic Press, **1996**.

15. Rabek, J. F. *Photochemistry and Photophysics*, Vol.2, CRC Press, **1990**, 119.

16. Lednev, K. I.; Ye, Y. -Q.; Hester, R. E.; Moore, J. N. *J. Phys. Chem.* **1996**, *100*, 13338.

17. Lednev, K. I.; Ye, Y. -Q.; Matousek, P.; Towrie, M.; Foggi, P.; Neuwahl, F. V. R.; Umapathy, S.; Hester, R. E.; Moore, J. N. *Chem. Phys. Lett.* **1998**, *290,* 68.

18. Rau, H. *Angew. Chem. Internat. Edit.* **1973**, *12*, 224.

19. Yamashita, S.; Ono, H.; Toyama, O. *Bull. Chem. Soc. Jpn.* **1962**, *35*, 1849.

20. Hartley, G. S. *Nature*, **1937**, *140*, 281.

21. Zimmerman, G. M.; Chow L. Y.; Paik, U. J. *J. Am. Chem. Soc*. **1958**, *80,* 3528.

22. Zimmerman, G.; Chow, L.; Paik, U. *J. Chem. Phys.* **1955**, *23*, 825.

23. Griffiths, J. *Colour and Constitution of Organic Molecules*, Academic Press, **1976**.

24. Bortous, P.; Monti S. *J. Phys. Chem.*, **1979**, *83*, 648.

25. Malkin, S.; Fisher, E. *J. Phys. Chem.*, **1962**, *66*, 2482.

26. a) Tanaka, T.; Hocker, L. O.; Benedek, G. B. *J. Chem. Phys.* **1973**, *69*, 5151. b) Tanaka, T.; Filmore, D. J. *J. Chem. Phys.* **1979**, *70*, 1214. c) Peters A.; Candau, S. J. *Macromolecules* **1986**, *19*, 1952. d) Peters, A.; Candau, S. J. *Macromolecules* **1988**, *21*, 2278. e) Li, Y.; Tanaka, T. *J. Chem. Phys.* **1990**, *92*, 1365. f) Annaka, M.; Tanaka, T. *Nature*, **1992**, *355*, 430. g) Durning, C. J.; Mormon, K. N. Jr., *J. Chem. Phys.* **1993**, *98*, 4275. h) Tokita, M.; Miyamoto, K.; Komai, T. *J. Chem. Phys.* **2000**, *113*,1647. i) Kang, M-S.; Gupta, V. K. *J. Phys. Chem. B,* **2002**, *106*, 4127.

27. Lide, D. R. *Handbook of Chemistry and Physics*, CRC Press, 73rd edition, **1992**.

28. Kesavamoorthy, R.; Super, M. S.; Asher, S. A. *J. Appl. Phys.* **1992**, *71*, 1116.

29. Asher, S. A.; Pershan, P. S. *J. de Physique* **1979**, *40*, 161.

30. Asher, S. A.; Pershan, P. S. *Biophys. J.* **1979,** *27*, 393.

Chapter 5

Photochemically Controlled Crosslinking in Polymerized Crystalline Colloidal Array Photonic Crystals

This chapter was submitted to *Macromolecules*. The co-author is Sanford A. Asher.

5. PHOTOCHEMICALLY CONTROLLED CROSSLINKING IN POLYMERIZED CRYSTALLINE COLLOIDAL ARRAY PHOTONIC CRYSTALS

5.1. ABSTRACT

We developed photochemically controlled photonic crystals which may be useful in novel recordable and erasable memories and/or display devices. These materials can operate in the UV, visible or near IR spectral regions. Information is recorded and erased by exciting the photonic crystal with 355 nm UV light or 488 nm visible light. The recorded information is read out by measuring the photonic crystal diffraction wavelength. The active element of the device is an azobenzene crosslinked hydrogel which contains an embedded crystalline colloidal array. This material is similar to our previously developed photonic crystals, which contained azobenzene functional groups. However, in contrast to the previous photonic crystals where the azobenzene was attached as a pendant group, the azobenzene here is attached at both ends and crosslinks the photonic crystal material. UV excitation forms cis-azobenzene crosslinks while visible excitation forms trans-azobenzene crosslinks. The less favorable free energy of mixing of the cis-azobenzene crosslinked species causes the hydrogel to shrink and blue-shift the photonic crystal diffraction. This is completely the opposite behavior as observed from the pendant azobenzene groups we reported previously. We also observe fast ns, μs and msec transient dynamics associated with fast heating lattice constant changes, refractive index changes and thermal relaxations.

5.2. INTRODUCTION

The recent intense interest in photonic bandgap crystals stems from their potential ability to increase light waveguiding efficiency, to increase the efficiency of stimulated emission processes, and to localize light.[1] Numerous groups around the world are developing fabrication methods to produce photonic crystals with bandgaps in the visible, infrared and microwave spectral regions.[2]

The simplest photonic crystal can be fabricated by the close-packing of spheres similar to that which in nature forms opals. The earliest chemical approach fabricated large face centered cubic (fcc) photonic bandgap crystals through the self-assembly of highly charged, monodisperse colloidal particles into crystalline colloidal arrays (CCAs). The CCAs self-assemble due to long range electrostatic repulsions between particles.[3,4]

These CCAs are complex fluids which consist of colloidal particles which self-assemble into plastic fcc crystalline arrays which Bragg diffract ultraviolet, visible or near-infrared light, depending on the colloidal particle array spacings. More recently, robust semi-solid photonic crystal (PCCA) materials were fabricated by polymerizing a hydrogel network around the self-assembled CCA array[5] (Figure 1). This new photonic crystal material can be made environmentally responsive such that thermal or chemical environmental alterations result in PCCA volume changes, thereby altering the CCA photonic crystal plane spacings and diffraction wavelengths.[6-10]

We report here the development of a second[11] example of a photochemically actuated PCCA, where photoisomerization of a covalently attached crosslinking chromophore changes the hydrogel free energy of mixing. The resulting photocontrolled PCCA volume change alters the

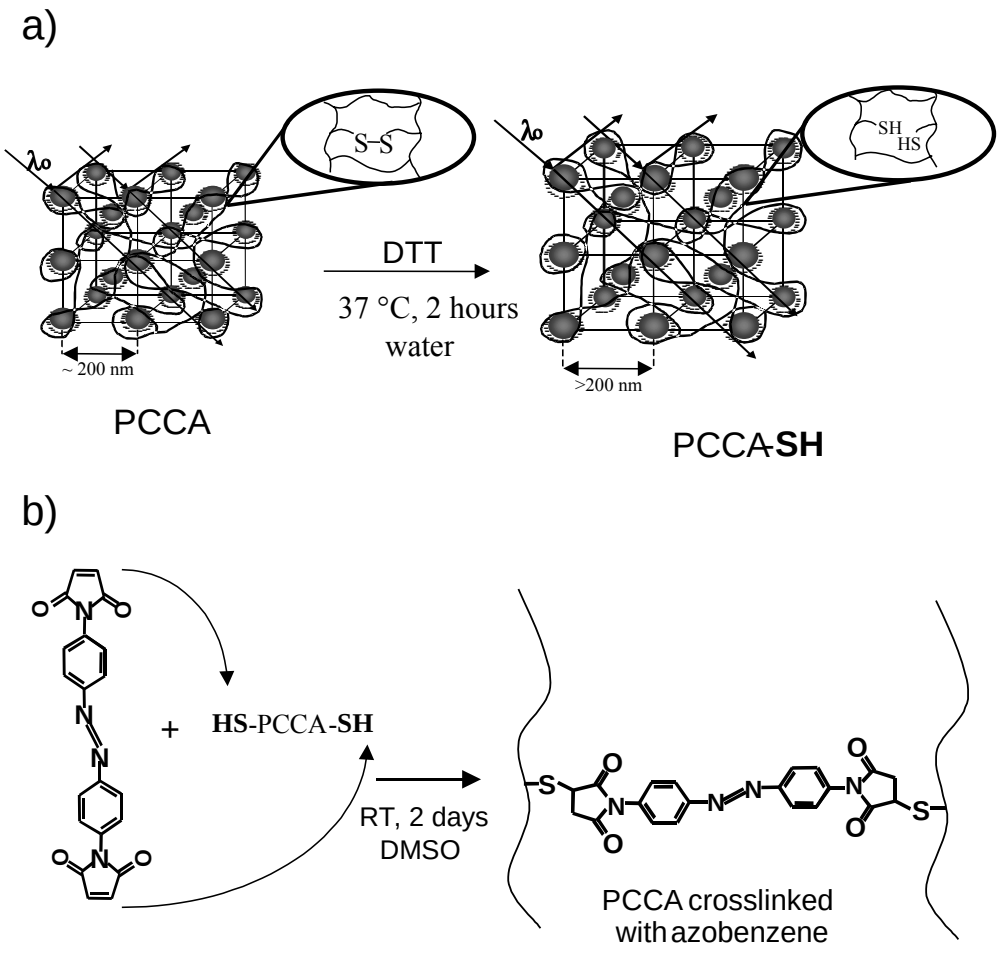

Figure 5.1. a) Synthesis of thiol functionalized PCCA. b) Synthesizing a photoresponsive PCCA by crosslinking the thiol functionalized PCCA with azophenyl-p-N,N'-dimaleimide.

lattice constant and shifts the diffracted wavelength. Thus, we have a material in which we can modulate the diffracted light by exciting the material either with 355 nm or 488 nm light, far from the diffraction bandgap.

The photonic crystal PCCA described here utilizes photoisomerization of azobenzene crosslinks to alter the PCCA diffraction. Photoisomerization of the azobenzene crosslink from its normally trans to its cis form blue-shifts the diffraction. In contrast, our previously demonstrated pendent azobenzene PCCA, showed a diffraction red-shift upon azobenzene isomerization to the cis form.[11] Although the photochemistries are identical, as are the mechanisms of diffraction shifting, the detailed thermodynamics differ.

5.3. EXPERIMENTAL

5.3.1. Synthesis of the azobenzene cross-linker

We synthesized azophenyl-p-N,N'-dimaleimide by dissolving 2 g of 4,4'-diaminoazobenzene (Lancaster) in 20 ml of dimethylformamide (DMF, Aldrich) and mixing it into a solution of 5 g of maleic anhydride (Fisher) in 5 ml DMF.[12] After 2 hrs, yellow crystals of azophenyl-p-N,N'-dimaleimide were filtered out, dried and dissolved in 250 ml of acetic anhydride (Fisher) and 12 g sodium acetate (Aldrich). The liquid was decanted, and its volume reduced under vacuum to 50 ml. 300 g ice was added to the solution, and after 2 hours the crystals were collected and washed with water. Re-crystallization of the sample was done twice in (1:1) dioxane-ethanol mixtures. The sample was dissolved in chloroform and its structure confirmed by NMR.

5.3.2. Synthesis of the photoresponsive PCCA with photochromic crosslinks

Monodisperse polystyrene colloidal particles (120 nm diameter) with thousands of sulfonate groups on their surface were synthesized by emulsion polymerization.[13] We dialyzed

the colloidal suspension against water for one week, after which these particles self-assembled into highly ordered crystalline colloidal arrays (CCA).

Polymerized crystalline colloidal array (PCCA) were prepared by dissolving 50 mg acrylamide (Sigma) and 3 mg N,N'-methylenebisacrylamide (Sigma) in 1 g of a 12 % by weight colloidal suspension of the polystyrene colloids prepared above. N,N'-cystaminebisacrylamide (5 mg; Aldrich) and a 10 μl solution of 10 % diethoxyacetophenone (DEAP, Aldrich, v/v) in DMSO were then added to the above mixture.

This solution was injected into a cell made of two quartz plates separated by a 76 μm thick spacer and exposed to UV light (Black-Ray model B-100A, UVP Inc.). After 30 min illumination, the cell was opened, the gel was washed with water in order to remove unreacted monomer. The PCCA swells slightly (2 nm diffraction red-shift, diffraction peak at ~455 nm) as it assumes its equilibrium volume in water.

Dithiolthreitol (DTT, 0.3 mM aqueous solution, ACROS Organics) was used to cleave the PCCA disulfide bonds leaving reactive thiol groups on the PCCA (Figure 1a).[14,15] This disulfide crosslink cleavage red-shifts the PCCA diffraction 41 nm (from 455 nm to 496 nm) due to the resulting decrease in the PCCA elastic constant.[10,16]

The PCCA cleavage medium was slowly exchanged stepwise with pure DMSO after which the PCCA showed a diffraction peak maximum at 487 nm (Figure 2). The 9 nm diffraction peak blue-shift resulted from the decrease in the free energy of mixing between the PCCA and DMSO, compared to water. The PCCA diffraction efficiency decreased due to the smaller refractive index difference between the polystyrene colloids (n=1.60) and the DMSO medium (n=1.47), compared to that of water (n=1.33). Below 300 nm, the absorption spectrum shows contributions from diffraction, as well as from the polystyrene absorption (Figure 2).

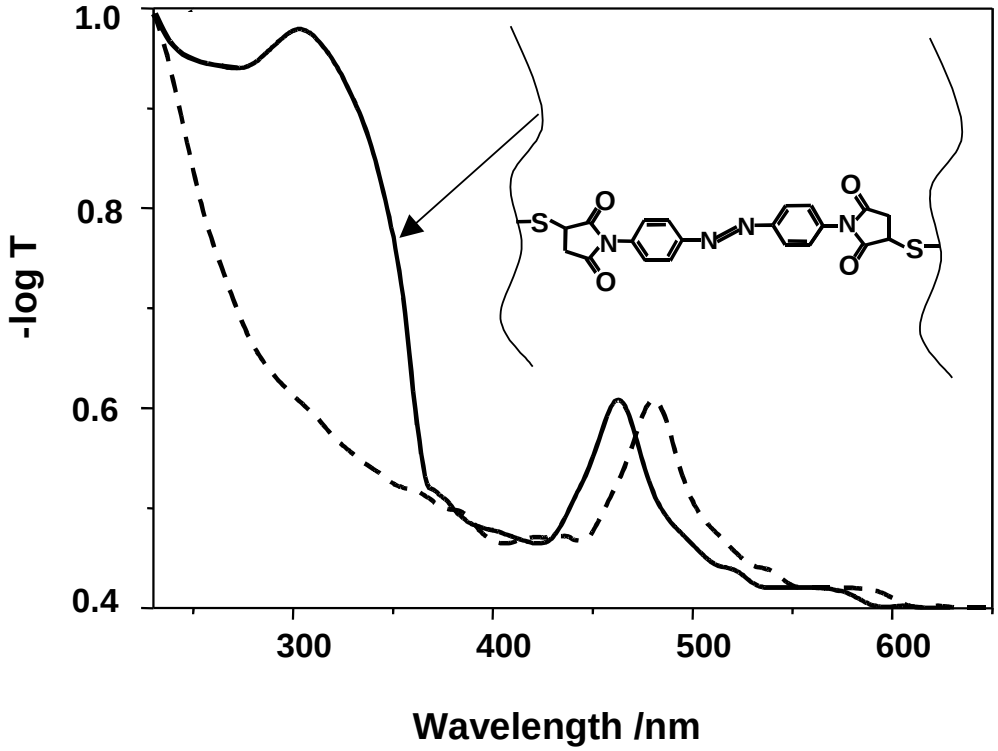

Figure 5.2. PCCA before (dashed) and after (solid) crosslinking with azophenyl-p-N,N'-dimaleimide.

The cleaved PCCA, which diffracted at 487 nm, was incubated for 2 days at room temperature with a DMSO solution of azophenyl-p-N,N'-dimaleimide (10 mM). Both maleimide groups of azophenyl-p-N,N'-dimaleimide quickly and quantitatively react with the PCCA sulfhydryl groups to form PCCA crosslinks.[14,15] The azobenzene PCCA shows a strong trans azobenzene $\pi \rightarrow \pi^*$ absorption band at 334 nm and diffracts at 464 nm (Figure 2).

5.4. RESULTS AND DISCUSSION

Figure 3 shows an azobenzene crosslinked PCCA, which has a 475 nm diffraction peak, as well as a strong trans-azobenzene $\pi \rightarrow \pi^*$ absorption band at 334 nm. A single 1.2 mJ/cm^2, 3 ns, 355 nm UV laser pulse converts the trans-azobenzene to the cis form, as evident from the decreased absorbance of the 334 nm absorption band. In response, at long times (sec to min) the diffraction peak blue-shifts 11 nm.

This blue-shift is exactly opposite to the red-shift we previously demonstrated[11] in azobenzene PCCA where the azobenzenes were attached as pendant groups; in that case the formation of cis-azobenzene caused swelling of the hydrogel, and red-shifted the PCCA diffraction. This observed blue-shift is completely reversible; visible excitation converts the azobenzene back to the trans form and the diffraction red-shifts back to the original diffraction wavelength.

Figure 4 shows the kinetics of the diffraction changes induced by UV excitation in the ns and μs time regimes. The response time of the PCCA depends on the incident power, the photophysics rate and the collective diffusion constant of the hydrogel. We examined the kinetics of the diffraction changes by monitoring changes in the transmission spectrum of the sample after applying a single 3 ns 355 nm YAG pulse (1.2 mJ/cm^2). A 120 ns pulsed Xe

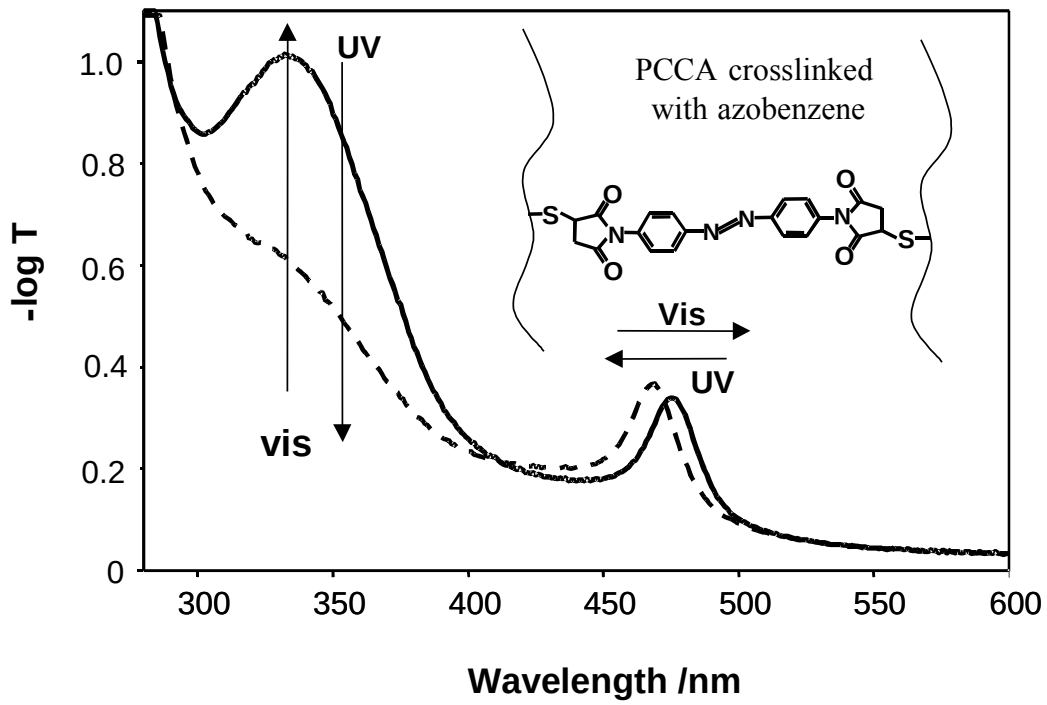

Figure 5.3. Response of azobenzene crosslinked PCCA to UV and visible light irradiation. UV irradiation by a 3 ns pulse of 355 nm light (1.2 mJ/cm2) converts most of the trans azobenzene to the cis form. This results in a ~10 nm blue-shift of the ~ 475 nm diffraction peak. Excitation in the visible converts the cis-azobenzene back to the trans form and red-shifts the diffraction peak.

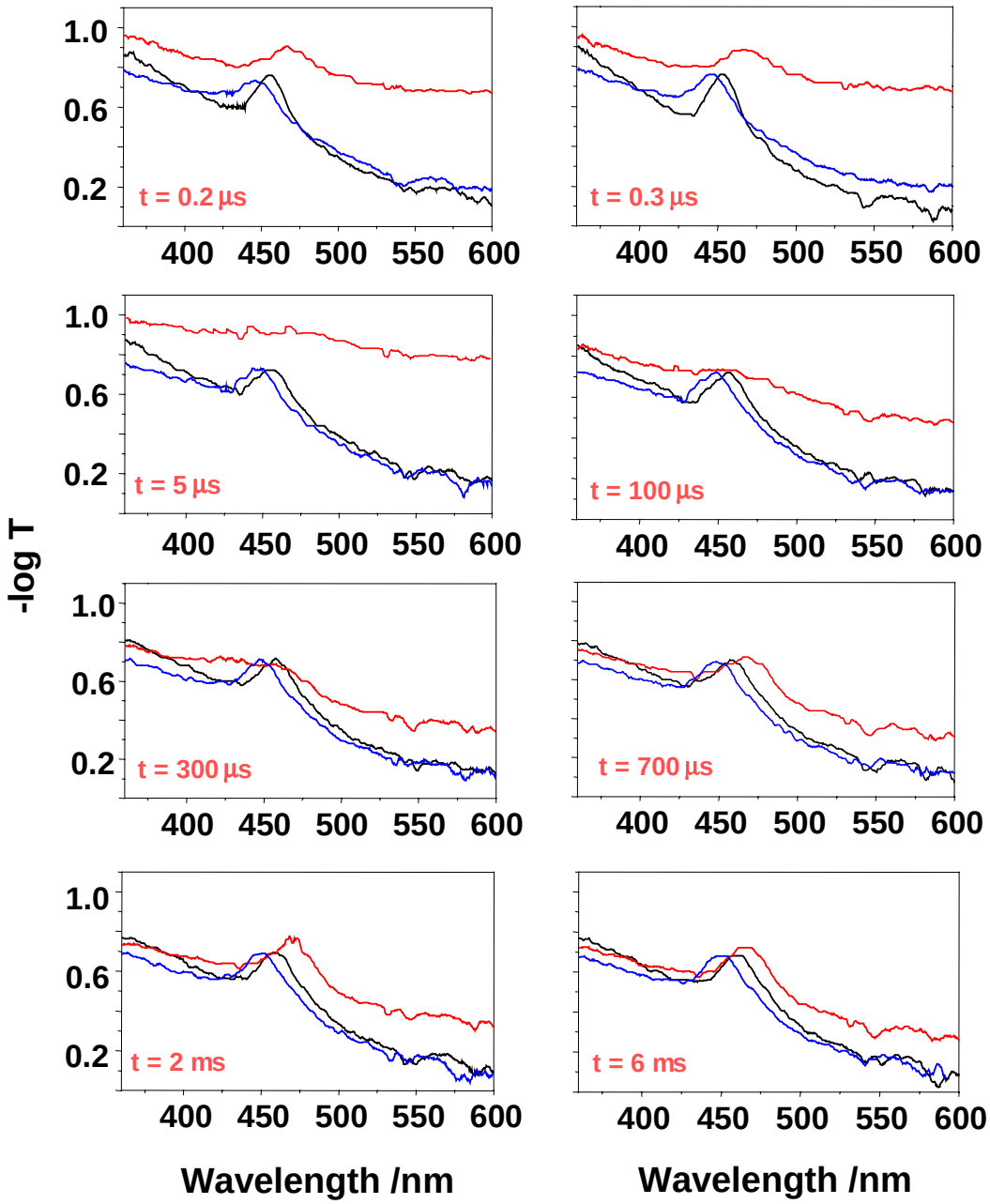

Figure 5.4. Azobenzene crosslinked PCCA prior to UV excitation (black), at the indicated time subsequent to UV excitation by a single 3 ns 355 nm pulse (red), and 1 min (blue) after UV excitation.

flashlamp (IBH Model 5000XeF) and Ocean Optics USB2000 Miniature Fiber Optic Spectrometer recorded the transmission spectra at variable time delays between 200 ns to 6 ms subsequent to the UV pulse. Figure 4 also shows spectra recorded before (black) and 1 min after the UV pulse (blue). Figure 5 graphically shows the time dependence of the diffraction maximum wavelength in the μs and sec timescales.

We observe a ~17 nm initial red-shift at 300 ns due to heating of the sample by the UV laser pulse.[11] This shift is ~three-fold greater than that observed for our previous pendant[11] azobenzene PCCA. Presumably, this larger red-shift results from the larger temperature jump induced by the ~two-fold increased azobenzene concentration present in the azobenzene crosslinked PCCA. We calculate that our UV pulse beam induces a ~20 °C temperature jump in the sample which expands the PCCA volume, which increases the d_{111} spacing to red-shift the diffraction.

The PCCA transiently disorders in the 100 μs time scale, which causes the diffraction band to broaden and disappear. The system then thermally re-equilibrates in the ~ 700 μs to 6 ms time scale (Figure 5).

At longer times the pendent azobenzene PCCA hydrogel (Chapter 4) response to the more favorable free energy of mixing of the larger dipole moment cis-azobenzene with the DMSO. This red-shifted the diffraction. In contrast, the azobenzene crosslinked PCCA diffraction blue-shifts by ~10 nm with a characteristic time of ~12 s, showing just the opposite behavior to the pendant azobenzene PCCA derivatives. The origin of the blue-shift is most likely the formation of less soluble hydrogel aggregates by the cis-azobenzene crosslinked

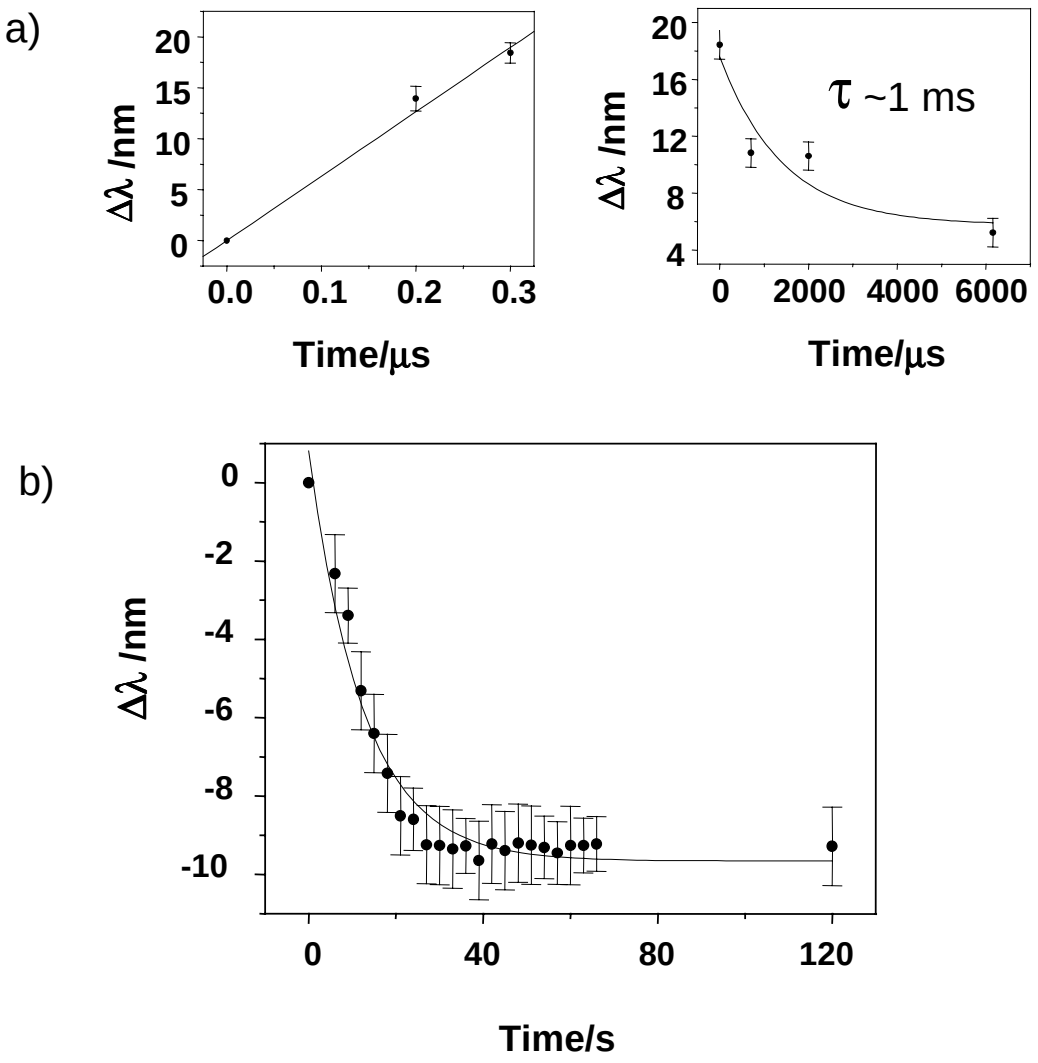

Figure 5.5. Time dependence of diffraction maximum wavelength in the microsecond (a) and second timescales (b).

species. Evidence for this phenomenon comes from the study of Kang et al.,[19] who examined the temperature dependence of the volume phase transition of poly-(N-isopropyl acrylamide) hydrogels with azobenzene crosslinks. They found a lower transition temperature for the cis compared to the trans-azobenzene derivative, and gave an entropic argument to explain the phenomena. Similar photochemistry was used by Wilcox et al.[17,18] in their development of a "precipiton" solubility switch activated by isomerization.

We choose to utilize a more molecular explanation which notes that the decreased transition temperature requires a more hydrophobic and less soluble hydrogel in the presence of the cis-azobenzene crosslink. This suggests that the blue-shift results from a less favorable free energy of mixing of the cis-derivative with the medium. This is occurring in spite of an increased dipole moment, which in the pendant PCCA results in a red-shift. It appears that the change in structure of the cis crosslinked hydrogel species causes a more than compensating solubility decrease.

The azobenzene crosslink tethers two segments of hydrogel chains at the crosslink sites, which at the length of the trans derivative possess separate sheaths of solvent. In contrast, in the cis derivative, the distance between hydrogel chains is too small for separate sheaths of solvent. As a result, the hydrogel locally collapses and the volume on average contracts. The resulting crosslinked segment appears less soluble, which causes the hydrogel to shrink and blue-shift. The smaller cis-azobenzene crosslink creates an excluded volume for solvent molecules in which the hydrogel chains form less soluble segments.

5.5. CONCLUSION

We have developed a new optical memory material which utilizes a PCCA containing azobenzene crosslinks. The trans crosslinks are indefinitely stable in the dark. UV excitation

converts the ground state trans-azobenzene crosslinks to cis-azobenzene crosslinks. Blue light converts the cis crosslinks back to trans. UV excitation results in short and long time diffraction changes. In the fast ns time regime, heating increases the PCCA volume and red-shifts the diffraction. This volume change relaxes in the ms time domain. At longer times the volume of this PCCA hydrogel is controlled by the balance between the free energy of mixing of the polymer hydrogel with DMSO and the elastic restoring force of the hydrogel crosslinks. We observe a decreased free energy of mixing of the PCCA with the DMSO solvent for the cis-azobenzene derivative.

We can photochemically control the diffraction of this photonic crystal; a UV light pulse can write information and a visible blue pulse can erase it. The information is read out from the diffraction, which can occur at any desired wavelength. To our knowledge, this is only the second[12] example of the photochemical control of a photonic crystal.

5.6. REFERENCES

1. Joannopoulos, J. D.; Meade, R. D.; Winn, J. N. *Photonic Crystals: Molding the Flow of Light* (Princeton University Press, New York), **1995**.

2. a) Krauss, T. F.; De La Rue, R. M. *Prog. Quant. Elect.* **1999**, *23*, 51. b) Ozin, G. A.; Yang, S. M. *Adv. Func. Mat.* **2001**, *11*, 95. c) Jiang, P.; Ostojic, G. N.; Narat, R.; Mittleman, D.; Colvin, V. L. *Adv. Mat.* **2001**, *13*, 389. d) Norris, D. J.; Vlasov, Y. A.; *Adv. Mat.* **2001**, *13*, 371.

3. a) Hiltner, P. A.; Krieger, I. M. *J. Phys. Chem.* **1969**, *73*, 2386. b) Goodwin, J. W.; Ottewill, R. H.; Parentich, A. *J. Phys. Chem.* **1980**, *84*, 1580.

4. a) Asher, S. A.; Flaugh, P. L.; Washinger, G. *Spectroscopy* **1986**, *1*, 26. b) Clark, N. A.; Hurd, A. J.; Ackerson, B. J. *Nature* **1979**, *281*, 57. c) Carlson, R. J.; Asher, S. A.; *Appl. Spectrosc.* **1984**, *38*, 297. d) Reese, C.; Asher, S. A. *J. Colloid and Interface Science* **2002**, *248*, 41.

5. a) Asher, S. A.; Holtz, J.; Liu, L.; Wu, Z. *J. Am. Chem. Soc.* **1994**, *116*, 4997. b) Asher, S. A. *US Patents 4,627,689* and *4,632,517*, **1986**.

6. Holtz, J. H.; Asher, S. A. *Nature*, **1997**, *389*, 829.

7. Asher, S. A.; Peteu, S.; Reese, C.; Lin, M.; Finegold, D. *Analy. and Bioanaly. Chem.*, **2002**, *373*, 632.

8. a) Haacke, G.; Panzer, H. P.; Magliocco, L. G.; Asher, S. A. *US Patent 5,266,238*, **1993**. b) Asher, S. A.; Jagannathan, S. *US Patent 5,281,370*, **1994**.

9. Weissman, J. M.; Sunkara, H. B.; Tse, A. S.; Asher, S. A. *Science* **1996**, *274*, 959.

10. Lee, K.; Asher, S. A. *J. Am. Chem. Soc.* **2000**, *122*, 9534.

11. Kamenjicki, M.; Lednev, I.; Mikhonin, A.; Kasavamoorthy, R.; Asher, S. A. *Adv. Func. Mat.* **2003,** *13*, 774.

12. Fasold, H.; Groschel-Stewart, U.; Turba, F. *Biochemische Zeitschrift*, **1963**, *337*, 425.

13. Reese, C. E.; Guerrero, C. D.; Weissman, J. M.; Lee, K.; Asher, S. A. *J. Colloid and Interface Science* **2000**, *232*, 76.

14. Aslam, M.; Dent, A. *Bioconjugation*, Grove's Dictionaries Inc., **1998**.

15. Hermanson, G. T. *Bioconjugate Techniques,* Academic Press, **1996**.

16. Holtz, H.; Holtz, J. S. W.; Munro, C. H.; Asher, S. A. *Anal. Chem*. **1998**, *70*, 780.

17. Bosanac, T.; Yang, J.; Wilcox, C. S. *Angew. Chem. Int. Ed*., **2001**, *40*, 1875.

18. Bosanac, T.; Wilcox, C. S. *Tetrahedron Lett*., **2001**, *42*, 4309.

19. Kang, M-S.; Gupta, V. K. *J. Phys. Chem. B,* **2002**, 106.

Chapter 6

Photoswitchable Spirobenzopyran-based Photochemically Controlled Photonic Crystals

This chapter was submitted to *Advanced Functional Materials*. The co-authors are Igor K. Lednev and Sanford A. Asher.

6. PHOTOSWITCHABLE SPIROBENZOPYRAN-BASED PHOTOCHEMICALLY CONTROLLED PHOTONIC CRYSTALS

6.1. ABSTRACT

We have developed a photochemically controlled photonic crystal material by covalently attaching spiropyran derivatives to polymerized crystalline colloidal arrays (PCCA). These PCCAs consist of colloidal particles that self-assemble into crystalline colloidal arrays (CCA), which are embedded in crosslinked hydrogels. Photoresponsive PCCA were made two ways: 1) by functionalizing the hydrogel network with spiropyran derivatives, and 2) by functionalizing the colloidal particles with spiropyran derivatives. These materials can diffract light in the UV, visible, or near-IR spectral regions. The diffraction of the PCCA is modulated exciting the spiropyran with UV light, thereby red-shifting the diffraction. Alternatively, the diffraction is blue-shifted by exciting the spiropyran with visible irradiation. Thus, this material acts as a memory storage material where information is recorded by illumination of the PCCA, and information is read out by measuring the photonic crystal diffraction wavelength. UV excitation forms the open spiropyran form while visible excitation forms the closed spiropyran form. The diffraction shifts result from changes in the free energy of mixing of the PCCA system as the spiropyran is photoexcited to its different stable forms.

6.2. INTRODUCTION

There is intense interest in fabricating materials with bandgaps in the visible, infrared and microwave spectral regions.[1,2] The idea is to develop materials which can be used for light waveguiding where light is used for processing information. The simplest method for producing materials with photonic bandgaps involves the use of crystalline colloidal array (CCA) self-assembly where monodisperse, highly charged nano and mesoscale colloidal particles form cubic arrays (Figure 1).[3] These particles are generally negatively charged due to the ionization of surface strong acid groups. The electrostatic repulsive interactions result in the formation of fcc or bcc arrays where the particles are spaced by distances significantly larger than their diameters. The periodic spacings diffract the light and form bandgaps at angles that fulfill the Bragg condition.[3-5]

Our group developed methods to polymerize hydrogels around the highly plastic CCA to form more robust solid materials called polymerized crystalline colloidal arrays (PCCAs, Figure 1).[6,7] These PCCAs contain the periodic array that gives rise to the photonic bandgap. A major advantage of the PCCA is that it can be further chemically modified to make it responsive to its chemical, thermal and photonic environments.[8-12] For example, we made chemical sensors where the photon bandgap shifts in frequency in response to changing analyte concentrations.[8,9] We also made thermally responsive PCCA where poly-N-isopropylacrylamide (NIPAM) was used for the hydrogel. This NIPAM shows a temperature driven volume phase transition such that the photonic bandgap wavelength can be tuned throughout the visible spectral region by varying the temperature between 10 and 40 °C.[11] In addition, we recently demonstrated a photoresponsive azobenzene-based PCCA,[12] where the photochemistry of the azobenzene

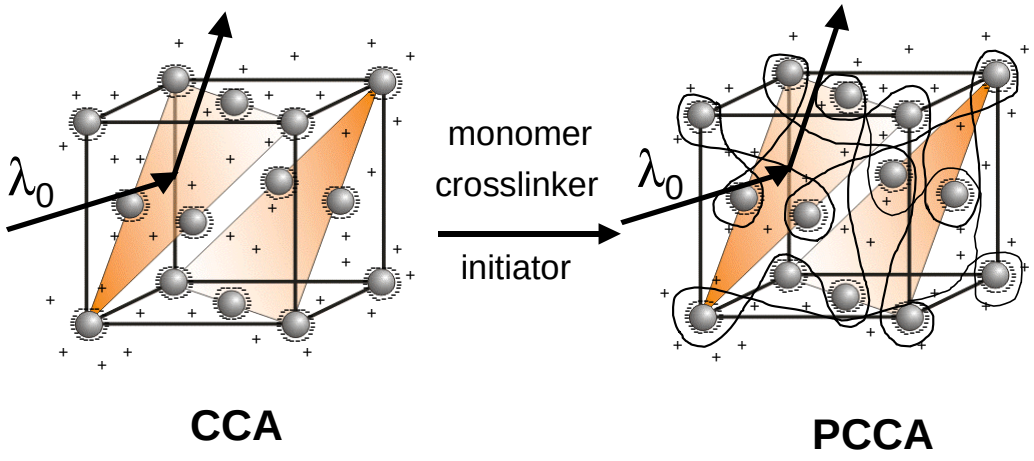

Figure 6.1. Synthesis of polymerized crystalline colloidal array (PCCA).

derivative was used to drive shifts in the bandgap diffraction wavelength upon excitation with UV and visible light.

In this work, we demonstrate another example of a photochemically-actuated PCCA in which photoisomerization of a covalently attached spirobenzopyran modulates the PCCA's bandgap. Photoisomerization of a PCCA with a covalently attached spirobenzopyran chromophore changes the hydrogel's free energy of mixing due to the large change in charge distribution within the spirobenzopyran molecule.[13] The resulting PCCA volume change alters the CCA lattice constant and shifts the bandgap and the diffracted wavelength.

6.3. EXPERIMENTAL

6.3.1. Synthesis of photoresponsive hydrogel-linked spirobenzopyran PCCA

Spirobenzopyran-containing PCCAs were fabricated by covalently attaching a spirobenzopyran derivative to the hydrogel network. We accomplished this by reacting N-[p-maleimidophenyl]isocyanate (PMPI; Pierce), a sulfohydryl-reactive and hydroxyl-reactive heterobifunctional crosslinker,[14] with a spirobenzopyran derivative containing a hydroxyl group (Figure 2). The isocyanate end of PMPI reacts with the hydroxyl groups on the spirobenzopyran, forming urethane linkages. This product contains maleimide ends, which, when coupled to a thiol-containing PCCA, forms stable thioether linkages (Figure 2).[14,15]

The HS-PCCA was made by dissolving 5 mg of N,N'-cystaminebisacrylamide (Aldrich), 50 mg acrylamide, 3 mg N,N'-methylenebisacrylamide and 10 μl DEAP in 1 g of a 10 wt % polystyrene CCA dispersion. This dispersion was injected into a cell made of two quartz plates separated by a 76 μm thick spacer (DuraSeal) and exposed to UV light (Black Ray model B-100, UVP Inc. mercury lamp). After 30 min irradiation, the cell was opened and the gel was

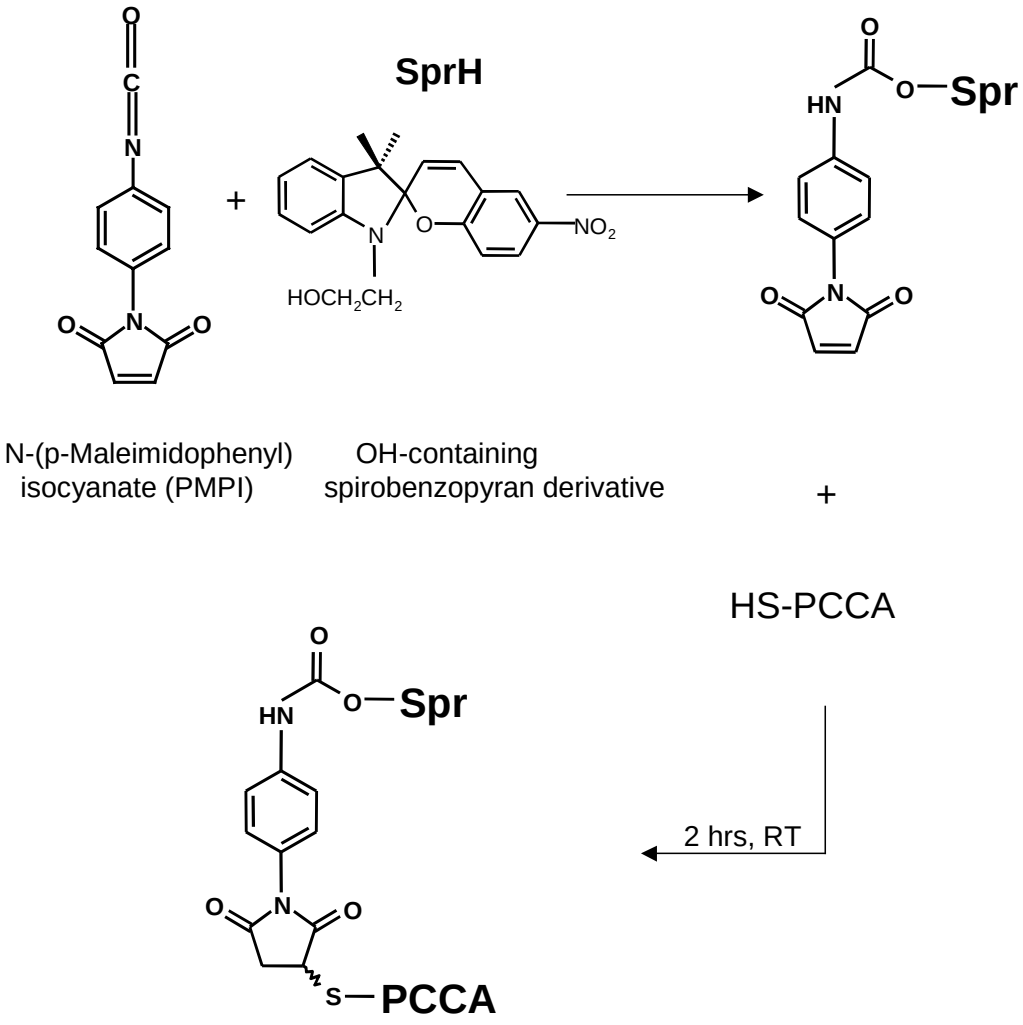

Figure 6.2. Reaction between hydroxylated spirobenzopyran (SprH) and PMPI, and subsequent functionalization of the sulfhydryl-containing PCCA with maleimide-containing spirobenzopyran.

washed with nanopure water. Exposing this PCCA (3 cm X 3 cm X 76 μm) to an aqueous solution of dithiolthreitol (DTT, ACROS Organics) cleaved the disulfide bonds to leave reactive thiol groups within the PCCA.[15] During this process, the hydrogel swelled due to the breaking of crosslinks, and the diffraction wavelength red-shifted 40 nm, to 590 nm. This 76 μm thick PCCA was then incubated with a 6 mM solution of maleimide-functionalized spirobenzopyran in DMSO for two hours at room temperature. From absorption measurements we calculate that we have a 5 mM concentration of spirobenzopyran within the PCCA.

6.3.2. Synthesis of photoresponsive spirobenzopyran-linked colloidal particle PCCA

6.3.2.1. Synthesis of chloromethyl-functionalized polystyrene particles

Chloromethyl-functionalized polystyrene particles were synthesized by emulsion polymerization by using a 10% weight suspension of previously synthesized 120 nm polystyrene colloidal particles as seed particles.[16] These highly charged, monodisperse polystyrene colloidal particles were prepared via emulsion polymerization, as described elsewhere.[17]

In a 500 mL jacketed reaction flask, 76 g of the 10 wt % seed polystyrene colloid dispersion and 15 mL of nanopure water were purged with nitrogen for 20 minutes. 0.04 mol of styrene (Aldrich) and 0.03 mol of chloromethylstyrene (ACROS Organics) were added to the reaction flask, and the mixture was stirred at 200 rpm at 30°C under nitrogen. The seed particles were allowed to swell for one hour. The reaction temperature was raised to 60°C, and the initiator, consisting of 0.17 g potassium persulfate (Aldrich) and 0.12 g sodium bisulfite (JT Baker) in 5 mL nanopure water, was added. After 4 hours, the resulting crude poly-(styrene-chloromethylstyrene) core-shell colloidal particle dispersion was removed from the reaction vessel and dialyzed against nanopure water for one week (until the conductivity of the dialysate was 1.0 $\mu\Omega^{-1}$/cm). The colloidal suspension was further cleaned by shaking the suspension with

a mixed bed ion-exchange resin (Bio-Rad AG 501-X8), after which it became iridescent due to Bragg diffraction (460 nm at normal incidence) from the 135 nm diameter poly-(styrene-chloromethylstyrene) CCA. Elemental microanalysis of these particles showed 3 % chlorine by weight.

6.3.2.2. Synthesis of spiropyran-linked colloidal particle PCCA

A mixture of 50 mg acrylamide (Sigma), 3 mg N,N'methylenebisacrylamide (Sigma), 10 μl diethoxyacetophenone (Aldrich), and 1 g of a 10 wt % dispersion of 135 nm poly-(styrene-chloromethylstyrene) CCA was injected into a cell made of two quartz plates separated by a 38 μm spacer, and exposed to UV light (Black-Ray model B-100A, UVP Inc.) for 1 hour. The 3 cm X 3 cm X 38 μm gel was then removed from the cell, washed with nanopure water, and gradually transferred to a pure DMSO medium. The PCCA was then exposed to 15 ml of a 6 mM DMSO solution of 1-(2-hydroxyethyl)-3,3-dimethyl-6'-nitrospiro (indoline-2,2'-[2H-1] benzopyran) (Chroma Chemicals, Figure 3a) for 2 days at room temperature, in the dark. This spirobenzopyran derivative contains a hydroxyl group, which can undergo a nucleophilic substitution reaction by the chlorines on the polystyrene colloidal particle surfaces. After 2 days of incubation, we utilized absorption spectroscopy to determine that the spirobenzopyran concentration in the PCCA was 2.5 mM. During this procedure the hydrogel swelled and the diffraction wavelength red-shifted to 650 nm. No attachment of spirobenzopyran occurred in a control experiment where the PCCA was prepared only with pure polystyrene colloidal particles.

In order to measure the photochemical response, we irradiated the PCCA in DMSO with UV light (Black Ray model B-100, UVP Inc. mercury lamp, 365 nm maximum wavelength) and visible light (CUDA Products Corp., Model 1-150 tungsten lamp with a UV rejection filter;

wavelength range between 500-750 nm). In addition, we measured the kinetics of the diffraction change in the sec time range using a YAG (355 nm) and an Ar^+ laser (514.5 nm).

6.4. RESULTS AND DISCUSSION

6.4.1. PCCA with spirobenzopyran linked to hydrogel

Figure 3a shows the molecular structural changes that occur for spirobenzopyran as it photochemically cycles from its spiropyran closed form to its merocyanine open form. Figure 3b shows that for spirobenzopyran in DMSO, the merocyanine form has a visible absorption band at ~ 560 nm, whereas the spiropyran form mainly absorbs light in the ultraviolet region (Figure 3b). Intense UV illumination converts the majority of the spyropyran closed form to the merocyanine open form, resulting in a photostationary state (PSS-UV, Figure 3b-blue line). In contrast, intense visible illumination converts a majority of the spiropyran molecules to their closed form; the ~ 560 nm absorption band decreases, and the system stabilizes in a photostationary state (PSS-Vis, Figure 3b-red line).

The Figure 4a blue line shows the extinction spectrum of the photoresponsive PCCA containing spirobenzopyran linked to the hydrogel network, just after saturating excitation by UV light (mercury lamp, 365 nm, 40 mW/cm^2). In contrast, the Figure 4a red line shows the extinction spectrum after saturating excitation with visible light (tungsten lamp, 500-750 nm, 40 mW/cm^2). UV excitation converts spirobenzopyran from its closed to open form, which increases the ~350 and ~560 nm absorption in a manner similar to that for spirobenzopyran monomer in solution (Figure 3). However, the absorption increase at 350 nm is much greater for the PCCA-spirobenzopyran sample than for the spirobenzopyran monomer in solution (compare Figure 4 to Figure 3).

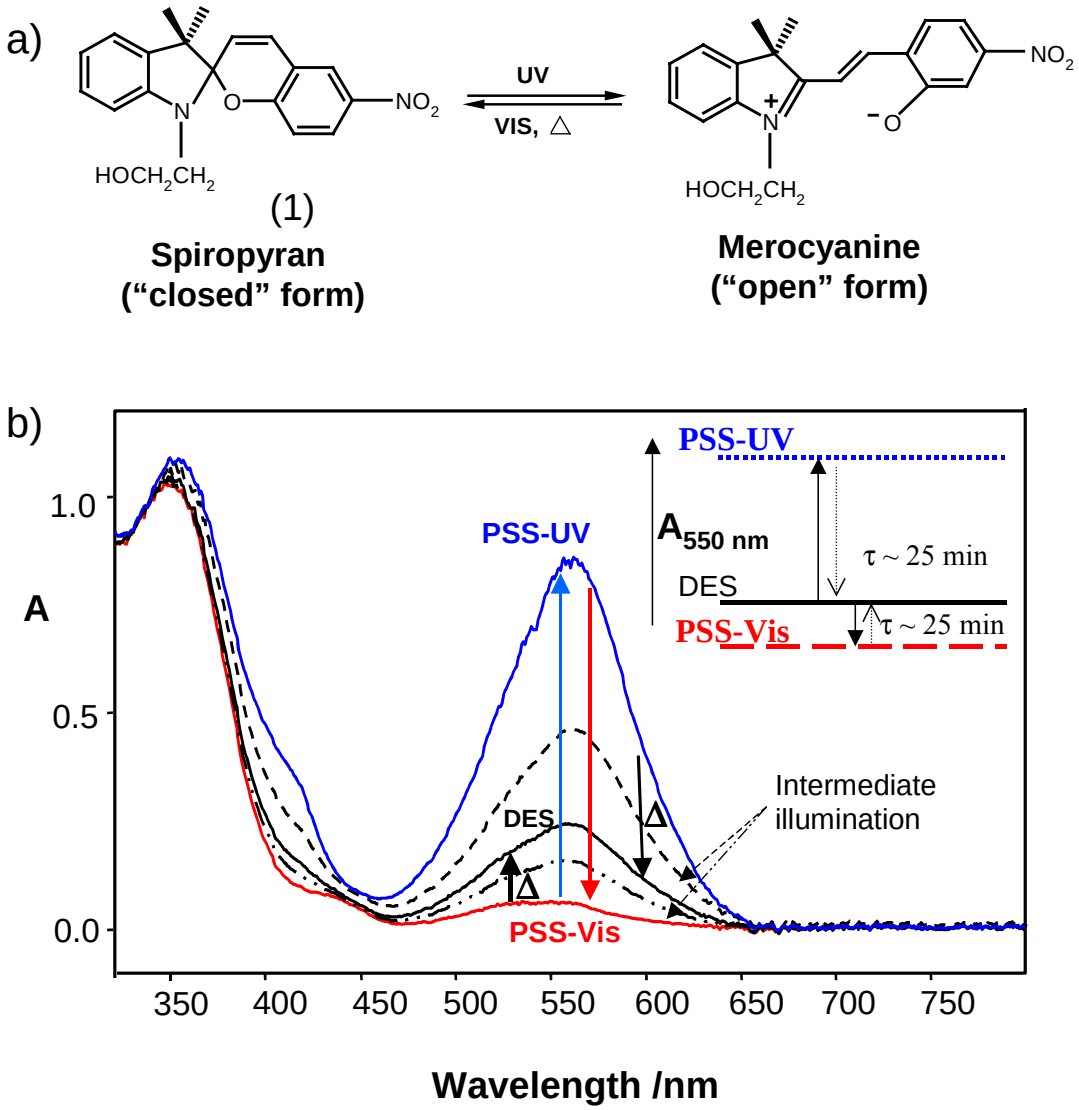

Figure 6.3. a) Molecular structural changes for the spirobenzopyran photochemical interconversion from its closed to open form. b) Photochemistry of spirobenzopyran (1) in DMSO. PSS-UV and PSS-Vis are the photostationary states under UV and visible light irradiation, respectively; Inset: shows 550 nm absorption of photostationary and dark equilibrium states (DES) under UV and visible irradiation (40 mW/cm^2). 1 mm quartz cell, Concentration = 4 x 10^{-4} M.

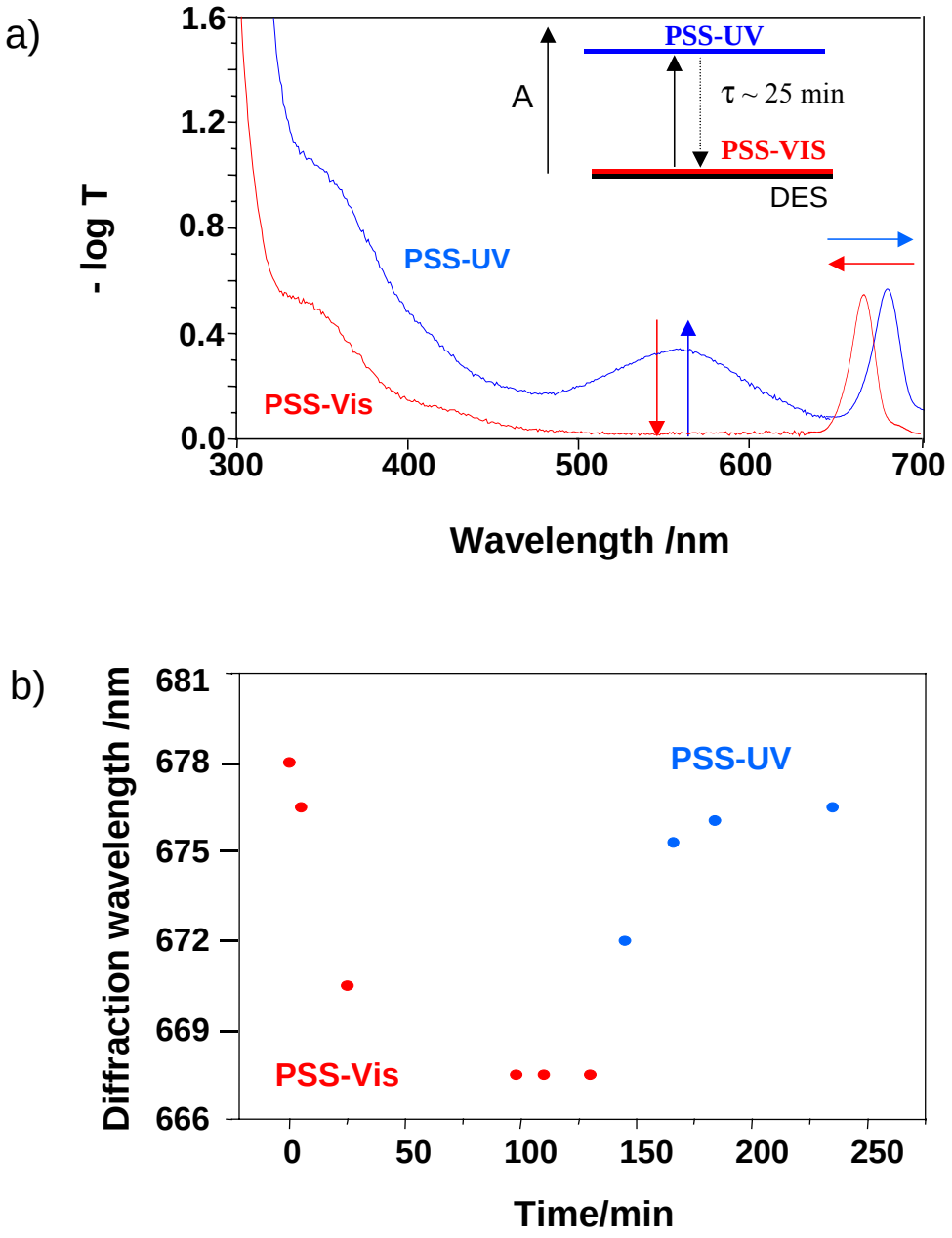

Figure 6.4. a) Extinction spectra of 76 μm PCCA with spirobenzopyran (~5 mM) linked to hydrogel under UV (mercury lamp, ~25 min, 40 mW/cm^2) and visible irradiation (tungsten lamp, ~25 min, 40 mW/cm^2). b) Photoswitching behavior of the PCCA of Figure 4a. The system was exposed to 514.5 nm light (Ar^+ laser, 20 mW/cm^2) and 355 nm (YAG, 20 mW/cm^2).

The PCCA in the DMSO medium was oriented such that the light was incident normal to the fcc (111) planes (glancing angle, $\theta = 90°$), resulting in diffraction of ~680 nm light (λ_{diff}) after saturating UV excitation (Figure 4a). Under these conditions, and with a PCCA refractive index $n \sim 1.48$, the spacing between the (111) planes, d_{111}, is calculated to be 220 nm from Bragg's law ($\lambda_{diff} = 2nd_{111} \sin \theta$). Figure 4 also shows that the UV photostationary state (PSS-UV) 680 nm diffraction peak blue-shifts by 13 nm upon saturation with visible excitation (PSS-Vis). Since little change can occur in the refractive index at these low spirobenzopyran concentrations, the diffraction shifts must arise from volume changes in the PCCA. The 13 nm change represents a 2.5 % shrinkage in the linear dimension, which if isotropic, would arise from a >7% volume shrinkage of the PCCA upon illumination with visible light.

As discussed below, the hydrogel linked spirobenzopyran samples relax in the dark over periods of days to a dark equilibrium state (DES), which has an absorption spectrum essentially identical to that of the PSS-Vis. The inset of Figure 4a shows the magnitude of the absorption at 550 nm for the DES, PSS-Vis and PSS-UV. The DES of spirobenzopyran monomers (Figure 3) has a significantly larger 550 nm absorption than occurs for the hydrogel-linked PCCA (Figure 4). Part of the absorption differences in the 280-330 nm region between Figure 3 and Figure 4 results from the overlapping absorption of the polystyrene particles. It should be noticed that previous studies demonstrated that changes in solvent, pH, and metal binding can greatly influence the spirobenzopyran absorption spectra.[18-23]

Figure 4b shows the results of an experiment in which we excited our sample with 355 nm UV excitation (YAG laser, 20 mW/cm^2) and 514.5 nm visible excitation (Ar^+ laser, 20 mW/cm^2) and monitored the changes in the diffraction wavelength. 514.5 nm excitation of the PSS-UV results in a ~11 nm diffraction blue-shift and formation of the PSS-Vis over a

characteristic time of ~25 min at these intensities. Subsequent UV excitation red-shifts the diffraction ~ 10 nm over a similar time-scale, and forms the PSS-UV.

These diffraction shifts probably derive from difference in the charge distribution and resulting dipole moments between the open and closed forms of spirobenzopyran. UV photoisomerization to the open, merocyanine form results in formation of a zwitterions, which results in a more favorable free energy of mixing of the hydrogel with the DMSO medium. This causes swelling of the hydrogel, resulting in the diffraction red-shift. We previously[12] demonstrated a somewhat similar phenomenon for an azobenzene-derivatized PCCA. In contrast, visible irradiation blue-shifts the diffraction due to formation of the spirobenzopyran closed form, which reduces the dipole moment and shrinks the PCCA (Figure 4b).

Figure 5a shows that the diffraction of our system can be toggled indefinitely by alternating irradiation with UV and visible light. The system shows ~ 10 nm diffraction peak red-shifts and blue-shifts upon alternative irradiation with UV light (20 mW/cm^2) and visible light (20 mW/cm^2). We left the PCCA stabilized in PSS-UV in the dark and monitored the time dependence of diffraction. We found that the characteristic dark thermal recovery time of the PCCA to the DES at 25 °C is ~ 35 hours (Figure 5b). We observe photochemical degradation for these samples at temperatures significantly greater than 25 °C.

6.4.2. PCCA with spiropyran linked to colloidal particles

The photochemistry of spirobenzopyran derivatives depends strongly on their detailed chemical structure and their environment.[24] Spiropyran derivatives can display either “positive” photochromic behavior, where the DES only weakly absorbs visible light, or “negative” photochromic behavior, where the DES shows strong visible absorption.[24] UV wavelength

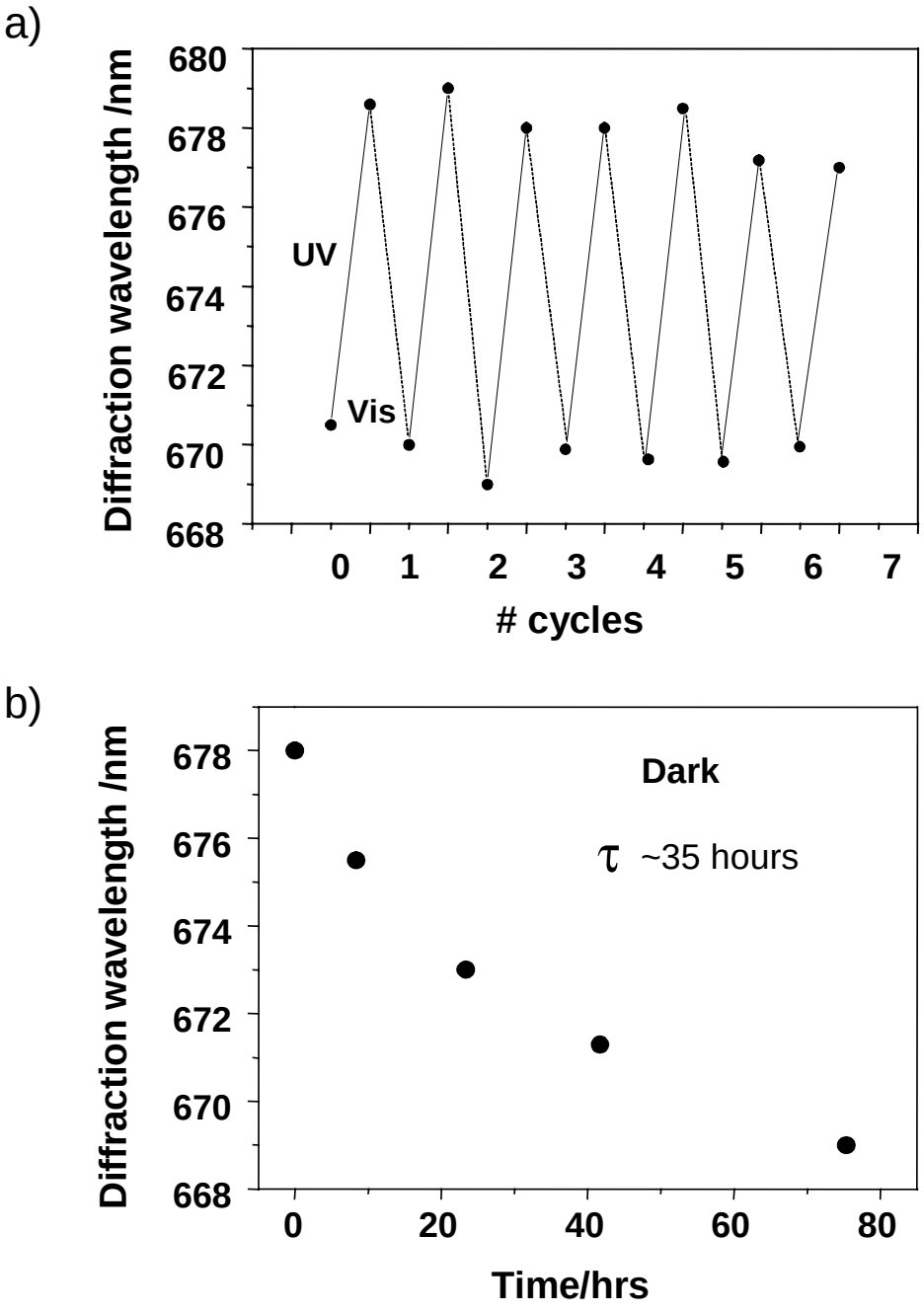

Figure 6.5. a) Photoswitching behavior of the PCCA at 25 °C with spirobenzopyran linked to hydrogel. The system was exposed to alternating irradiation with a YAG laser (355 nm, 20 mW/cm^2) and an Ar^+ laser (514.5 nm, 20 mW/cm^2). b) Thermal relaxation at 25 °C (starting from PSS-UV).

excitation increases the absorption of positive photochromics, but decreases it for the negative photochromics.

Since spirobenzopyrans with low visible absorptions are generally in their closed forms, we expect that positive photochromic behavior involves a transition from the closed to open forms of spiropyran. In contrast, negative photochromics should involve transitions from an open form to a closed form.[25]

Figure 6a (black line) shows the DES extinction spectrum of a 38 μm thick PCCA made from spirobenzopyran-linked poly-(styrene-chloromethylstyrene) colloidal particles. In addition to poly-(styrene-chloromethylstyrene) particle absorption (~280-330 nm), we observe very broad spirobenzopyran UV (~330- 450 nm) and visible absorption (~500-600 nm) bands. Upon UV irradiation (mercury lamp, 365 nm, ~10 min exposure, 40 mW/cm^2), the DES ~650 nm diffraction peak blue-shifts 5 nm, stabilizing in the PSS-UV (Figure 6, blue line). Additional irradiation of this PSS-UV with visible light causes an additional 9 nm diffraction blue-shift (PSS-Vis, Figure 6, red line). Starting from the DES and applying visible (rather than UV) light results in the same PSS-Vis, with a 14 nm diffraction blue-shift. Exciting the PSS-Vis with UV light red-shifts the diffraction 9 nm (Figure 6b).

While we observe changes in the diffraction wavelength upon excitation with visible and UV light, we see little change in the extremely broad visible absorbance. In addition, the visible absorption of the DES is essentially identical to the PSS-UV and PSS-Vis. This behavior dramatically differs from that of the PCCA discussed earlier with the spirobenzopyran linked to the hydrogel, in which a red-shift in the diffraction always occurs with UV irradiation, a blue-shift occurs with visible irradiation (Figure 5a), and significant absorption spectral changes occur at ~560 and ~350 nm (Figure 4a).

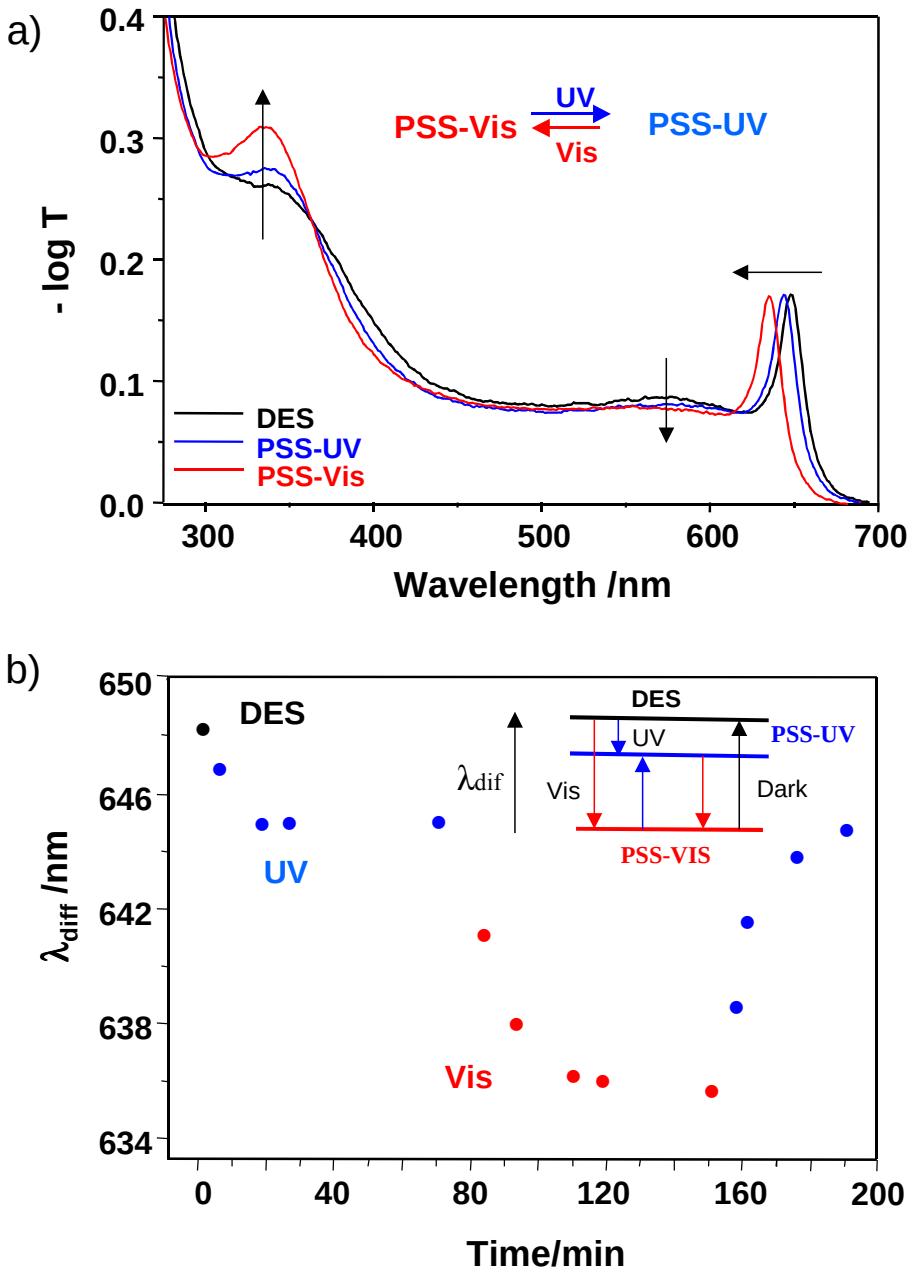

Figure 6.6. 38 µm thick PCCA functionalized with spirobenzopyran derivative linked to colloidal particles in DMSO. PSS-UV and PSS-Vis are the photostationary states under UV, and visible light.

We do not understand the photochemical behavior of the spirobenzopyran-linked particles in detail. The DES shows the most red-shifted diffraction, suggesting dominating presence of the open merocyanine form, which has a more favorable free energy of mixing due to its higher dipole moment. This system can be excited by UV light to a state which is blue-shifted from the DES by 5 nm, with a further 9 nm blue-shift caused by excitation with visible light (Figure 6b). Subsequently, the diffraction can be toggled back and forth 9 nm with alternating UV and visible excitation (Figure 7a). This suggests that the closed form concentration in the PSS-UV is between the closed spiropyran dominated PSS-Vis and the open merocyanine dominated DES.

The different forms of spiropyran in this sample appear to have similar absorbances in the visible region. This may result from additional chemistry that occurs for the spiropyran derivatives bound to the particles, compared to those bound to the PCCA hydrogel. For example, Salhin et al. reported that metal ion interactions with the phenolate anion on the merocyanine form of spirobenzopyran can induce "negative" photochromism.[22,26,27] In addition, Shimizu et al.[28] and Zhou et al.[29] showed that in the presence of acid, the open form may steadily transform into the protonated form (pKa = 3.93), which is also negatively photochromic. Since the pH around the sulfonated colloidal particles is ~3, it is possible that the merocyanine form in the PCCA with spirobenzopyran linked to colloidal particles is completely converted to (or coexists with) the protonated form. Irradiation with visible or UV light causes formation of the closed form, and dark relaxation results in the opposite process. Despite the different photochemistry in this system, the thermal dark relaxation time (30-35 hours, Figures 5b and 7b) and the characteristic photoswitching time between the PSS-Vis and PSS-UV (~ 20 min, Figures

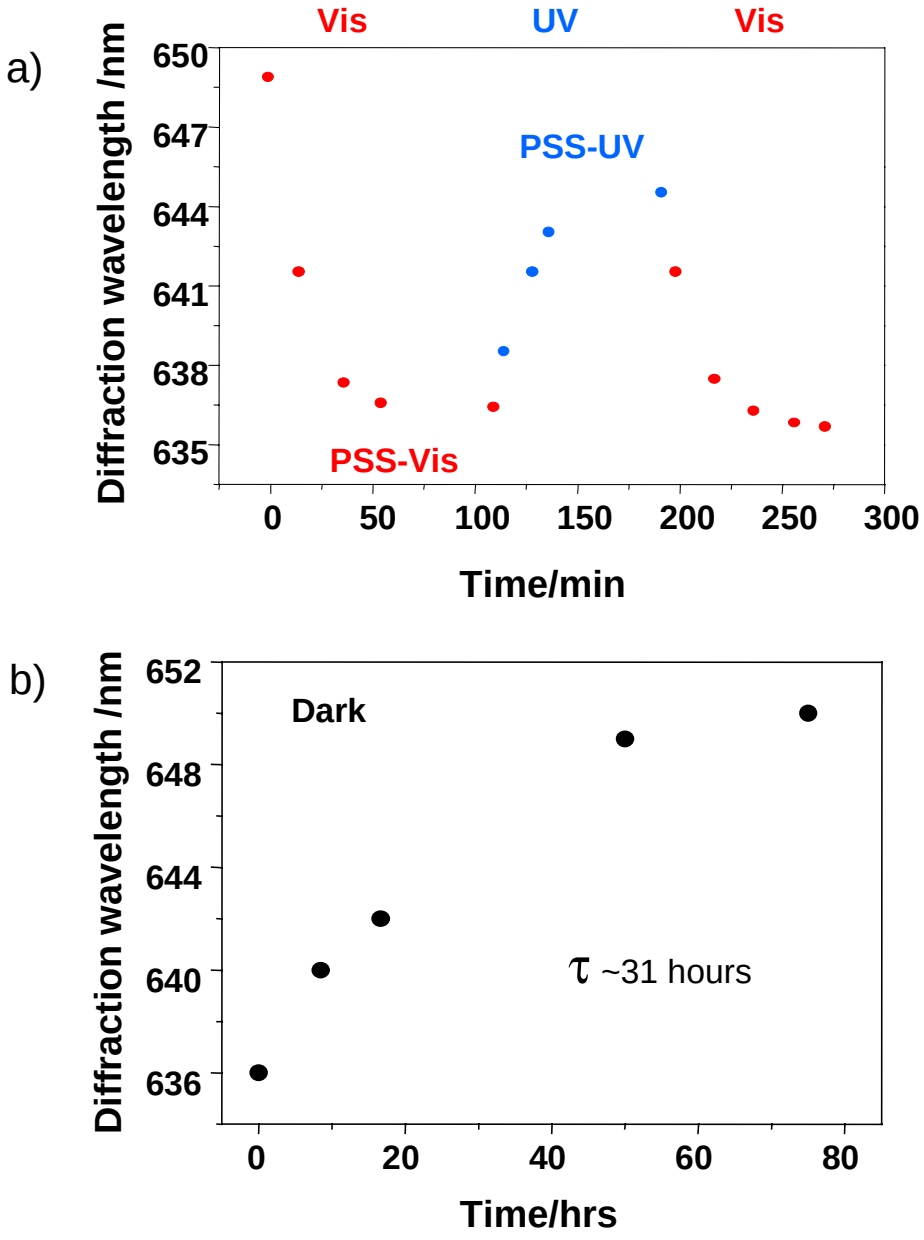

Figure 6.7. a) Irradiation of PCCA with spirobenzopyran linked to colloidal particleswith visible (Ar^+ laser, 514.5 nm, 20 mW/cm2), and UV (YAG laser, 355 nm, 20 mW/cm2) light. b) Dark relaxation at 25 °C (starting from PSS-Vis).

4 and 6) are essentially identical to those of the PCCA with spirobenzopyran linked to the hydrogel.

The change of spirobenzopyran molecules from the closed to open form causes a PCCA diffraction wavelength red-shift due to the change in charge localization of the attached spirobenzopyran. The higher charge localization makes the hydrogel network (in the first system) and colloidal particles (in the second system) more soluble in DMSO, causing an increase in the free energy of mixing of the PCCA. This causes swelling of the hydrogel, red-shifting the PCCA diffraction wavelength.

The system described here could be utilized for slow switching applications (sec to min) such as optical memory devices. The kinetics of gel swelling and shrinking depends on the driving osmotic pressure associated with changes in the free energy of mixing balanced by the collective diffusion constant of the polymer network relative to the solvent.[30-32] The swelling and shrinkage times should scale approximately with the hydrogel length.[33,34] For macroscopic gels the times are secs to mins. However, we recently demonstrated that much smaller, ~200 nm hydrogels can undergo swelling in a few μs.[35]

6.5. REFERENCES

1. Joannopoulos, J. D.; Meade, R. D.; Winn, J. N. *Photonic Crystals: Molding the Flow of Light*, Princeton University Press, Princeton, **1995**.

2. a) Krauss, T. F.; De La Rue, R. M. *Prog. Quantum Electron.* **1999**, *23*, 51. b) Ozin, G. A.; Yang, S. M. *Adv. Funct. Mater.* **2001**, *11*, 95. c) Jiang, P.; Ostojic, G. N.; Narat, R.; Mittleman, D. M.; Colvin, V. L. *Adv. Mater.* **2001**, *13*, 389. d) Norris, D. J.; Vlasov, Y. A. *Adv. Mater.* **2001**, *13*, 371.

3. a) Krieger, I. M.; O'Neil, F. M. *J. Am. Chem. Soc.* **1968**, *90*, 3114. b) Hiltner, P. A.; Papir, H. S.; Krieger, I. M. *J. Phys. Chem.* **1971**, *75*, 1881. c) Clark, N. A.; Hurd, A. J.; Ackerson, B. J. *Nature* **1979**, *281*, 57. d) Pieranski, P. *Contemp. Phys.* **1983**, *24*, 25.

4. a) Asher, S. A. *US Patents 4,627,689* and *4,632,517*, **1986**. b) Asher, S. A.; Flaugh, P. L.; Washinger, G. *Spectroscopy* **1986**, *1*, 26. c) Carlson, R. J.; Asher, S. A. *Appl. Spectrosc.* **1984**, *38*, 297. d) Flaugh, P. L.; O'Donnell, S. E.; Asher, S. A. *Appl. Spectrosc.* **1984**, 847.

5. a) Kesavamorthy, R.; Jagannathan, S.; Rundquist P. A.; Asher, S. A. *J. Chem. Phys.* **1991**, *94*, 5172. b) Rundquist, P. A.; Kasavamoorthy, R.; Jagannathan, S.; Asher, S. A. *J. Chem. Phys.* **1991**, *95*, 1249.

6. a) Haacke, G.; Panzer, H. P.; Magliocco, L. G.; Asher, S. A. *US Patent 5,266,238*, **1993**. b) Asher, S. A.; Jagannathan, S. *US Patent 5,281,370*, **1994**. c) Asher, S. A.; Weissman, J. M.; Sunkara, H. B.; Pan, G.; Holtz, J.; Liu, L.; Kasavamoorthy, R. In *Polymers for Advanced Optical Applications*, Jenekhe, S. A.; Wynne, K. J. Eds., Washington, DC, **1997**.

7. Asher, S. A.; Holtz, J.; Liu, L.; Wu, Z. *J. Am. Chem. Soc.* **1994**, *116*, 4997.

8. a) Holtz, J. H.; Asher, S. A. *Nature*, **1997**, *389*, 829. b) Holtz, J. H.; Holtz, J. S. W.; Munro, C. H.; Asher, S. A. *Anal. Chem.* **1998**, *70*, 780. c) Asher, S. A.; Peteu, S.; Reese, C.; Lin, M.; Finegold, D. *Analy. and Bioanaly. Chem.*, **2002**, *373*, 632.

9. Asher, S. A.; Alexeev, V. L.; Goponenko, A. V.; Sharma, A. C.; Lednev, I. K.; Wilcox, C. S.; Finegold, D. N. *J. Am. Chem. Soc.* **2003**, *125*, 3322.

10. Lee, K.; Asher, S. A. *J. Am. Chem. Soc.* **2000**, *122*, 9534.

11. Weissman, J. M.; Sunkara, H. B.; Tse, A. S.; Asher, S. A. *Science* **1996**, *274*, 959.

12. a) Asher, S. A.; Kamenjicki, M.; Lednev, I. *US Patent* 6,589,452, **2003.** b) Kamenjicki, M.; Lednev, I.; Mikhonin, A.; Kasavamoorthy, R.; Asher, S. A. *Adv. Func. Mat.* **2003,** *13*, 774.

13. Blets, M.; Pfeifer-Fukumura, U.; Kolb, U.; Baumann, W. *J. Phys. Chem. A.* **2002**, *106*, 2232.

14. Annunziato, M. E.; Patel, U. S.; Ranade, M.; Palumbo, P. S. *Bioconjugate Chem.* **1993**, *4*, 212.

15. Hermanson, G. T. *Bioconjugate Techniques,* Academic Press, **1996**.

16. a) Sarobe, J.; Forcada, J. *Colloid Polym. Sci.,* **1996**, *274*, 8. b) Park, J.; Kim, J.; Suh, K. *Colloids and Surfaces A*, **2002**, 191. c) Tsoukatos, T.; Pispas, S.; Hadjichristicks, N. *Macromolecules*, **2000**, *33*, 9504. d) Meyer, U.; Svec, F.; Frechet, J. H. *Macromolecules*, **2000**, *33*, 7769. e) Suh, J.; Oh, S. *J. Org. Chem*. **2000**, *65*, 7534.

17. Reese, C. E.; Guerrero, C. D.; Weissman, J. M.; Lee, K.; Asher, S. A. *J. Colloid Interface Sci.*, **2000**, *232*, 76.

18. Uznanski, P. *Langmuir*, **2003**, *19*, 1919.

19. a) Bertelson, R. C. *Photochromism*; G. H. Brown, Ed.; Techniques of Chemistry. Volume III; Wiley-Interscience: New York. **1971**, 45. b) Zhou, J.; Li, Y.; Tang, Y.; Zhao, F.; Song, X.; Li, E. *J. of Photochemistry and Photobiology,* **1995**, *90*, 117.

20. Tachibana, H.; Yamanaka, Y.; Matsumoto, M. *J. Phys. Chem. B*, **2001**, *105*, 10282.

21. McArdle, C. B.; Blair, H.; Barraud, A. Ruaudel-Teixier, A. *Thin Solid Films*, **1983**, *99*, 181.

22. Tanaka, M.; Nakamura, M.; Salhin, M. A. A.; Ikeda, T.; Kamada, K.; Ando, H.; Shibutani, Y.; Kimura, K. *J. Org. Chem.* **2001**, *66*, 1533.

23. Tanaka, M.; Ikeda, T.; Xu, Q.; Ando, H.; Shibutani, Y.; Nakamura, M.; Sakamoto, H.; Yajima, S.; Kimura, K. *J. Org. Chem.* **2002**, *67*, 2223.

24. a) Kamlet, M. J.; Abboud, J. L.; Taft, R. W. *J. Am, Chem. Soc*. **1977**, *99*, 6027. b) Bohne, C.; Fan, M. C.; Li, Z. J.; Liang, Y. C.; Lusztyk, J.; Scaiano, J. C. *J. Photochem. Photobiol. A: Chem.* **1992**, *66*, 79. c) Kimura, K.; Yamashita, T.; Yokoyama, M. *J. Chem. Soc. Chem. Commun.* **1991**, 147.

25. Garcia, A. A.; Cherian, S.; Park, J.; Gust, D.; Jahnke, F.; Rosario, R. *J. Phys. Chem. A,* **2000**, *104*, 6103.

26. Salhin, A. M. A.; Tanaka, M.; Kamada, K.; Ando, H.; Ikeda, T.; Shibutani, Y.; Yajima, S.; Nakamura, M.; Kimura, K. *Eur. J. Org. Chem.* **2002**, 655.

27. Reichardt, C. *Chem. Rev.* **1994**, *94*, 2319.

28. Shimizu, I.; Nakayama, T.; Kokado, H.; Inoue, E. *Bull. Chem. Soc. Jpn.,* **1970**, *13*, 2244.

29. Li, Y.; Tang, Y.; Zhou, J.; Song, X.; Li, E. *J. Photochem. Photobiol. A: Chem.* **1995**, *90*, 117.

30. Tanaka, T.; Fillmore, D. *J. Chem. Phys.* **1979**, *70*, 121.

31. Peters, A.; Candau, S. J. *Macromolecules* **1986**, *19*, 1952.

32. Matsuo, E. S.; Tanaka, T. *J. Chem. Phys.* **1988**, *89*, 1695.

33. Tokita, M.; Miyamoto, K.; Komai, T. *J. Chem. Phys*. **2000**, *113*, 1647.

34. Tanaka, T.; Hocker, L.; Benedek, G. B. *J. Chem. Phys*. **1973**, *59*, 5151.

35. Reese, C.; Mikhonin, A.; Kamenjicki, M.; Tikhonov, A.; Asher, S. A. *J. Am. Chem. Soc.* **2004**, *126*, 1493.

Chapter 7

Summary

7. SUMMARY

In this dissertation, we investigated topics important to understanding polymerized crystalline colloidal arrays (PCCAs) and development of novel photoresponsive materials and chemical sensors. Our results contribute to the body of information that will be used to understand the phase transition of PCCAs and develop new optical memory, switching, and display devices.

In Chapter 2 of this thesis, we investigated a new method for synthesizing intelligent PCCAs as a class of materials that can be used for chemical sensing. This new procedure enables incorporation of molecular recognition agents into the PCCA to produce an intelligent PCCA without hydrolyzing the hydrogel network. This method includes copolymerization of glycidyl methacrylate in order to incorporate the epoxide groups inside the hydrogel matrix. These epoxide groups are available for further reaction with thiols, amines or hydroxyls immediately after the PCCA is formed. Using this procedure, a lead sensor was created by exposing the epoxide-functionalized PCCA to 4-aminobenzo-18-crown-6. In addition, a glucose sensor was developed by covalently attaching glucose oxidase to the functionalized PCCA. In the future, this procedure will enable us to covalently bind to the PCCA any recognition element containing thiol, amine or hydroxyl groups.

The work described in Chapters 3-6 focuses on the development of a photoresponsive diffracting film which could be used in memory storage, optical displays, and optical switching**.** Photocontrolled diffraction switching behavior was studied in the PCCA functionalized with pendant azobenzene derivatives (Chapters 3 and 4), as well as azobenzene crosslinks (Chapter 5).

Chapter 3 describes the synthesis and behavior in water of a photoresponsive PCCA functionalized with a water-soluble azobenzene derivative. Chapter 4 describes a PCCA

functionalized with a malemide derivative of azobenzene. In both systems, a gradual red-shift of the diffraction peak upon UV illumination is accompanied by a decrease in $\pi \rightarrow \pi^*$ absorption and an increase in $n \rightarrow \pi^*$ absorption, due to the trans $\rightarrow$ cis isomerization of azobenzene. Excitation with visible light results in the reverse cis $\rightarrow$ trans isomerization, and a gradual diffraction peak blue-shift resets the diffraction to the original position. This behavior allows information to be written using UV light and stored until visible light is used to erase it.

Chapter 5 includes an additional route for developing a photoresponsive PCCA by introducing photochemical crosslinks inside the hydrogel network around the CCA. For this purpose we used azophenyl-p-N,N'-dimaleimide. In contrast to the previously described PCCA, this PCCA shows the opposite photochemical switching behavior. UV light induces a diffraction blue-shift, and visible light induces a red-shift.

Chapter 6 describes the synthesis and properties of a photoresponsive material based on spirobenzopyrans using two different methods of attachment. A spirobenzopyran derivative was attached to a hydrogel network via a maleimide-sulfhydryl reaction, and to the colloidal particles via nucleophilic substitution. In both systems, UV irradiation results in formation of a merocyanine form, which causes the spiropyran-modified PCCA to swell, red-shifting the diffraction. This process can be reversed with visible light. The photochemical responses of these hydrogels were studied in dimethylsulfoxide. Due to the difference in the microenvironment around the spirobenzopyran molecules, the PCCA made by functionalizing the hydrogel with spirobenzopyran showed positive photochromism, whereas the PCCA with spirobenzopyran fuinctionalized CCA showed negative photochromism.

This thesis shows that the material with pendant azobenzene groups in DMSO shows the largest photoresponse (60 nm diffraction shift) of all the photoresponsive PCCAs fabricated.

The spirobenzopyran-based system is interesting because the alternative ways of attachment provide the ability to control the photochemistry of the spirobenzopyrans, resulting in different PCCA photoswitching behaviors.

For all photoresponsive PCCAs, the volume change is controlled by the free energy of mixing of the hydrogel with the solvent as the PCCA is exposed to different wavelengths of light. In the future, this will enable us to improve the theory behind the hydrogel swelling and estimate the Flory-Huggins parameter, χ, for the free energy of mixing.

In the future, it will be useful to develop additional methods for creating photoresponsive PCCAs with even larger diffraction shifts. Currently, we are relying on instrumentation to detect 10-60 nm diffraction shifts, but larger shifts may be more readily observed by the human eye. Systems containing triphenylmethane leuconitrile groups could be explored, since they are known to change the polymer volume more pronouncedly than the azobenzene chromophore by the ionic photodissociation of C-CN bonds.

Our newly developed photoresponsive PCCA functions as a slow display device, and may be used as a novel recordable and erasable memory material. We know that smaller hydrogels will improve the kinetics and allow us to change the response under light from 10-30 sec (measured in this work for 3 cm X 3 cm X 76 μm hydrogels) to microseconds for 200 nm hydrogel spheres. In the future, we could try to make monodisperse hydrogel spheres containing azobenzene units. The irradiation of this type of crystalline colloidal array would change the size of the colloidal particles and consequently the intensity of the diffraction peak, making a very fast optical switch.

The spirobenzopyran-based PCCA can be directly used from this work and evaluated as a photoionic molecular device. It is known that the open merocyanine form exhibits a high

sensitivity to particular metal cations. The presence of this form which can be created by UV irradiation, will result in effective ion complexation. Irradiation of the complex with visible light would result in a reverse isomerization followed by ion release.

The short time kinetics for the 135 nm poly-(styrene-chloromethylstyrene) colloidal particles functionalized with spirobenzopyran described in this work was not measured due to the small diffraction shift from the CCA. In the future, greater diffraction shifts can be achieved by including a higher % of chlorine in the surface of the colloidal particles, resulting in a higher concentration of attached photochromic units, making the short time kinetic measurements possible. In addition, it is possible to substitute chlorine on the colloidal particle surface with iodine, which would result in a weaker C-I bond (compared to C-Cl) and make the substitution reaction easier, providing a higher concentration of photochromic molecules.

In addition, a PCCA functionalized with some recognition element (crown ethers, cyclodextrins, enzymes, etc.) could be coupled with azobenzene, resulting in a photocontrolled analyte recognition system. For example, photoresponsive crown ethers could bind alkali cations, and photoresponsive ethylenediamines could be used to bind transition metal ions. As the azobenzene in the trans configuration binds cations, it would introduce charged groups inside the hydrogel, resulting in a diffraction red-shift due to the osmotic pressure difference. Then, under UV irradiation, a change in the azobenzene's geometrical configuration to the cis isomer would lead to a significant change of the complexation constant for the cations. If there is a decrease in the cation complexation constant, the PCCA would shrink, the diffraction would blue-shift, and ions would be released from the hydrogel. Consequently, this system would find use in recoverable sensor applications, with multiple uses of the same sensor for analyte extraction.